

GEOLOGY AND GEOCHRONOMETRY OF THE COGBURN CREEK-SETTLER CREEK
AREA, NORTHEAST OF HARRISON LAKE, B.C.

by

JANET ELIZABETH GABITES

B.Sc., Victoria University Of Wellington, New Zealand, 1973,
B.Sc.(Honours), Victoria University Of Wellington, New Zealand,
1975

A THESIS SUBMITTED IN PARTIAL FULFILMENT OF
THE REQUIREMENTS FOR THE DEGREE OF
MASTER OF SCIENCE

in

THE FACULTY OF GRADUATE STUDIES
Department Of Geological Sciences

We accept this thesis as conforming
to the required standard

THE UNIVERSITY OF BRITISH COLUMBIA

September 1985

© Janet Elizabeth Gabites, 1985

In presenting this thesis in partial fulfilment of the requirements for an advanced degree at the University of British Columbia, I agree that the Library shall make it freely available for reference and study. I further agree that permission for extensive copying of this thesis for scholarly purposes may be granted by the head of my department or by his or her representatives. It is understood that copying or publication of this thesis for financial gain shall not be allowed without my written permission.

Department of Geological Sciences

The University of British Columbia
1956 Main Mall
Vancouver, Canada
V6T 1Y3

Date 8 October 1985

Abstract

Metamorphic supracrustal rocks in the Cogburn Creek area belong to the Cogburn Creek Group and the Settler Schist. These are separated by a melange zone, which has been correlated with the Shuksan thrust zone and contains Baird Metadiorite and ultramafic rocks, and intruded by the Spuzzum batholith and minor younger granodiorite. Three phases of folding are recognised in the schist units: f_1 is associated with contact metamorphism that preceded regional metamorphism, f_2 produced pervasive mica foliation and tight folds, and kinks and broad warps are associated with f_3 , which was locally pervasive approaching pluton margins. Mineral assemblages indicate increasing metamorphic grade from west to east from garnet to garnet-staurolite, andesine-epidote amphibolite, staurolite-kyanite, fibrolite, and coarse sillimanite zones. Metamorphic conditions vary from 300 to 500 °C in Cogburn Creek Group rocks to 550 to 700 °C at 6 to 8 kbar for pelites in the Settler Schist. Conditions deduced for metamorphism of the ultramafic rocks are consistent with those for enclosing pelitic schists.

Geochronometry indicates that the Baird Metadiorite is probably Precambrian and equivalent to the Yellow Aster Complex of the North Cascade Mountains, Washington. The Cogburn Creek Group was dated as Late Paleozoic (296 ± 58 Ma, Rb-Sr WR isochron), and is provisionally correlated with the Bridge River Group. The protolith of the Settler Schist was deposited around 210 ± 27 Ma (Rb-Sr WR isochron), and it contains 2450 ± 230 Ma detrital zircon indicating partial ultimate derivation from

Precambrian basement rocks. The Spuzzum batholith was intruded at 95 to 110 Ma, before the culmination of regional metamorphism. Rb-Sr biotite dates from all units and K-Ar Hb isochron dates in the range 66 to 88 Ma are metamorphic cooling dates. The youngest intrusive rocks, granodiorite dated at 32 ± 2 Ma to 42 ± 14 Ma, postdate the regional metamorphic and intrusive event. Movement on the Shuksan Thrust is bracketed as Albian, after regional blueschist metamorphism of the Shuksan Suite in the North Cascade Mountains and before intrusion of Spuzzum batholith and regional metamorphism east of Harrison Lake.

Table of Contents

Abstract	ii
List of figures	vii
List of plates	xi
List of tables	xii
Acknowledgements	xiii
1 Introduction	1
1.1 Geographic location and access	1
1.2 Previous work	1
1.3 Regional geology	4
2 Geology of the Cogburn Creek area	9
2.1 Baird Metadiorite	12
2.2 Ultramafic rocks	14
2.3 Cogburn Creek Group	15
2.4 Settler Schist	18
2.5 Premetamorphic intrusive rocks	21
2.6 Foliated diorite in melange zone	22
2.7 Spuzzum Batholith	23
2.8 Younger Intrusives	24
2.9 Breakenridge Formation gneiss	25
3 Metamorphism	27
3.1 Baird Metadiorite	27
3.2 Ultramafic rocks	27
3.3 Cogburn Creek Group	28
3.4 Settler Schist	31
3.5 Premetamorphic intrusive rocks	35
3.6 Discussion	36

	Ultramafic rocks	36
	Contact metamorphism	36
	Regional metamorphism	39
4	Structure	50
5	Geochronometry	59
	5.1 Previous Geochronometry	59
	5.2 Baird Metadiorite	64
	5.3 Cogburn Creek Group	66
	5.4 Settler Schist	67
	5.5 Premetamorphic intrusive rocks	70
	5.6 Foliated diorite in fault zone	72
	5.7 Spuzzum batholith	72
	5.8 Agmatized quartz diorite	77
	5.9 Breakenridge Formation	77
	5.10 Discussion	78
6	Regional Synthesis	107
	Plates	115
	References	125
	Appendix A. Isotopic dating methods. K-Ar, Rb-Sr, zircon U-Pb	134
	Appendix B. Rb-Sr isotopic data	136
	Appendix C. Dating sample descriptions, locations	147
	Zircon descriptions	149
	Appendix D. Thin section location map	150
	Geochronometry sample location map	151
	Appendix E. Rb-Sr data and isochron for Chilliwack batholith in the North Cascades Mountains	152
	Maps	in pocket

List of Figures

Figure 1.1	Area Location Map	2
Figure 1.2	Regional Geology of the North Cascade Mountains and southern Coast Mountains	5
Figure 1.3	Geographical location of the Settler Schist and Chiwaukum Schist	8
Figure 2.1	Generalised geology of the Cogburn Creek Area ..	10
Figure 3.1a	Timing of mineral growth with respect to deformation, Cogburn Creek Group	29
Figure 3.1b	Timing of mineral growth with respect to deformation, Settler Schist	29
Figure 3.2	Schematic T-X(CO ₂) diagram for the system MgO- SiO ₂ -H ₂ O-CO ₂ at elevated pressures and temperatures, adapted from Johannes (1969)	37
Figure 3.3	Pressure-temperature conditions in the pelitic assemblages, from Pigage (1973)	38
Figure 3.4	Metamorphic mineral assemblages in pelites and greenschist from the Cogburn Creek Group ...	40
Figure 3.5	Metamorphic mineral assemblages in pelites from the Settler Schist	41
Figure 3.6	Equilibria calculated for P ₂ at a(H ₂ O)=0.81, plus the alumino-silicate equilibria, adapted from Bartholomew (1979)	44
Figure 3.7	Map of metamorphic mineral assemblages and isograds around Cogburn Creek	46
Figure 3.8	Regional isograds	47
Figure 4.1	Equal area projection for poles to compositional	

	layering in the Settler Schist	51
Figure 4.2	Equal area projection for poles to f_2 foliation for the Settler Schist south of Cogburn Creek ..	52
Figure 4.3	Equal area projection for poles to f_2 foliation in Settler Schist north of Cogburn Creek	54
Figure 4.4	Equal area projection for poles to f_2 foliation in Cogburn Creek Group	55
Figure 4.5	Equal area projection for poles to foliation and mineral lineations in Spuzzum batholith	58
Figure 5.1	Map showing geochronometry of the Harrison Lake - Fraser River region	63
Figure 5.2a	Rb-Sr isochron plot for Baird Metadiorite	88
Figure 5.2b	Rb-Sr isochron plot for Cogburn Creek Group	89
Figure 5.2c	Rb-Sr isochron plot for Settler Schist	90
Figure 5.2d	Settler Schist, expanded scale	91
Figure 5.2e	Rb-Sr isochron plot for premetamorphic intrusive rocks	92
Figure 5.2f	Rb-Sr isochron plot for small body of foliated granodiorite in imbricate zone (SD92)	93
Figure 5.2g	Rb-Sr isochron plot for Spuzzum batholith, Hut Creek body	94
Figure 5.2h	Rb-Sr isochron plot for Spuzzum batholith, Settler Creek body	94
Figure 5.2i	Rb-Sr isochron plot for agmatitic quartz diorite (SD14), marginal to Cogburn Granodiorite	96
Figure 5.2j	Rb-Sr isochron plot for Breakenridge Formation gneiss	97
Figure 5.2k	Rb-Sr isochron plot for Chilliwack Group	98

Figure 5.2l	Rb-Sr isochron plot for Bridge River Group	99
Figure 5.2m	Rb-Sr isochron plots for Shuksan Suite and Darrington Phyllite	100
Figure 5.3	U-Pb concordia diagram for zircon dating	101
Figure 5.4a	Plot of $^{40}\text{K}/^{36}\text{Ar}$ v. $^{40}\text{Ar}/^{36}\text{Ar}$ for hornblende separates from Spuzzum batholith	102
Figure 5.4b	Plot of %K v. ^{40}Ar nl/g for hornblende separates from Spuzzum batholith	102
Figure 5.5	U-Pb concordia diagram for Yellow Aster Complex, Skagit Gneiss and Swakane Gneiss, from Mattinson (1972)	103
Figure 5.6	Data-field diagram for Rb-Sr analyses from possible correlative stratigraphic units	104
Figure 5.7	Plot of %K v. ^{40}Ar nl/g for regional data from Spuzzum batholith	105
Figure 5.8	Graph of eastward younging trend of K-Ar dates from Spuzzum batholith, from Bartholomew (1979).106	
Figure 6.1	Tectono-stratigraphic terranes, modified from Monger and Berg (1984)	108
Figure 6.2	Reconstruction of Bridge River Group and Methow terrane, modified from Kleinspehn (1985) and Monger and Berg (1984)	109
Figure 6.3	Reconstructions of Settler Schist and Chiwaukum Schist, after Misch (1977) and Monger (1985) ...	111
Figure 6.4	Partial reconstruction of the Methow-Tyughton basin, modified from Kleinspehn (1985)	112
Figure D-1	Map of Cogburn Creek area showing locations of samples studied in thin section	150

Figure D-2	Map showing locations of geochronometry samples, Cogburn Creek area	151
Figure E-1	Rb-Sr isochron plot for Chilliwack Batholith ...	153
Map 1	Topographic map showing rock units	in pocket
Map 2	Map showing planar structures	in pocket
Map 3	Map showing linear structures	in pocket
Map 4	Topographic map showing station numbers	in pocket

List of Plates

Frontispiece:	Old Settler Mountain, looking south along Settler Creek	xiv
Plate 2.1	Imbricate zone: Baird Metadoirite, ultramafic rocks, Settler Schist	115
Plate 2.2	Mafic amphibolite pod in Settler Schist	115
Plate 2.3	Photomicrograph of sample SD101	116
Plate 2.4	Photomicrograph of sample SD66	116
Plate 3.1	Photomicrograph of sample HL30	117
Plate 3.2	Photomicrograph of sample HL16	117
Plate 3.3	Photomicrograph of sample HL15	118
Plate 3.4	Photomicrograph of sample HL80	118
Plate 3.5	Photomicrograph of sample HL142	119
Plate 3.6	Photomicrograph of sample SS110	119
Plate 3.7	Photomicrograph of sample SS135	120
Plate 3.8	Photomicrograph of sample SS66	120
Plate 3.9	Twinned staurolite in SS57, Settler Schist	121
Plate 3.10	Photomicrograph of sample SS114	121
Plate 3.11	Photomicrograph of sample SS53	122
Plate 3.12	Sillimanite porphyroblasts from ridge north of Cogburn Creek	122
Plate 3.13	Photomicrograph of sample SS182a	123
Plate 4.1	Fault contact at the base of the imbricate zone	124

List of Tables

Table 5.1	Table of dates and age estimates from previous studies between Harrison Lake and Fraser River .	60
Table 5.2	Summary of events in the Cogburn Creek area based on new analyses	79
Table B-1	Rb-Sr analytical data	136
Table B-2	Rb-Sr isochron dates	140
Table B-3	K-Ar analytical data, Spuzzum Diorite	142
Table B-4	Sample weights for U-Pb analyses	143
Table B-5	U-Pb analytical data including isotope ratios ...	144
Table B-6	Calculated U-Pb dates	146
Table C-1	Rock descriptions and sample locations	147
Table C-2	Description of zircon samples	149
Table E-1	Rb-Sr analytical data, Chilliwack batholith	152

Acknowledgements

I would like to thank Dr R.L. Armstrong for critical supervision of this project. Drs P.R. Bartholomew, J.S. Getsinger, L.C. Pigage, and J.W.H. Monger provided aid and discussions. Krista Scott and Joe Harakal provided instruction and analyses for the geochronometry. Nel Grond and Lenore Shapka each survived a summer as field assistant.

My housemates Cathy, Denise, Eddie, Gary, Ian, Joe and Nounou gave me support, encouragement, and assistance with babysitting. Margo McTaggart helped my daughter Charlotte through my last weeks of writing.

Field and laboratory expenses were funded through Dr Armstrong's National Research Council Grant 67-8841.



Old Settler Mountain

Looking south along Settler Creek. The front face is a dip slope representing the upper contact of the Shuksan thrust imbricate zone.

1. Introduction

1.1 Geographic Location and Access

The Cogburn Creek area, which was mapped (Maps 1 to 4, in pocket) during the summers of 1981 and 1982, lies 20 km north of Harrison Hot Springs on the east side of Harrison Lake, B.C. (Fig. 1.1). The lake is north of the Fraser valley, 150 km east of Vancouver, in the southeastern Coast Mountains of B.C.

Access is by logging roads along the eastern shore of Harrison Lake and in the valley of Cogburn Creek; however, the ridge tops at 1800 to 1900 m are reached only by difficult climbs up steep, wooded hillsides. The area mapped covers 90 km². The lake shore is 10 m above mean sea level and the highest peak, Old Settler Mountain (2152 m), is 8 km inland. A helicopter was used to place high camps during the 1982 field season.

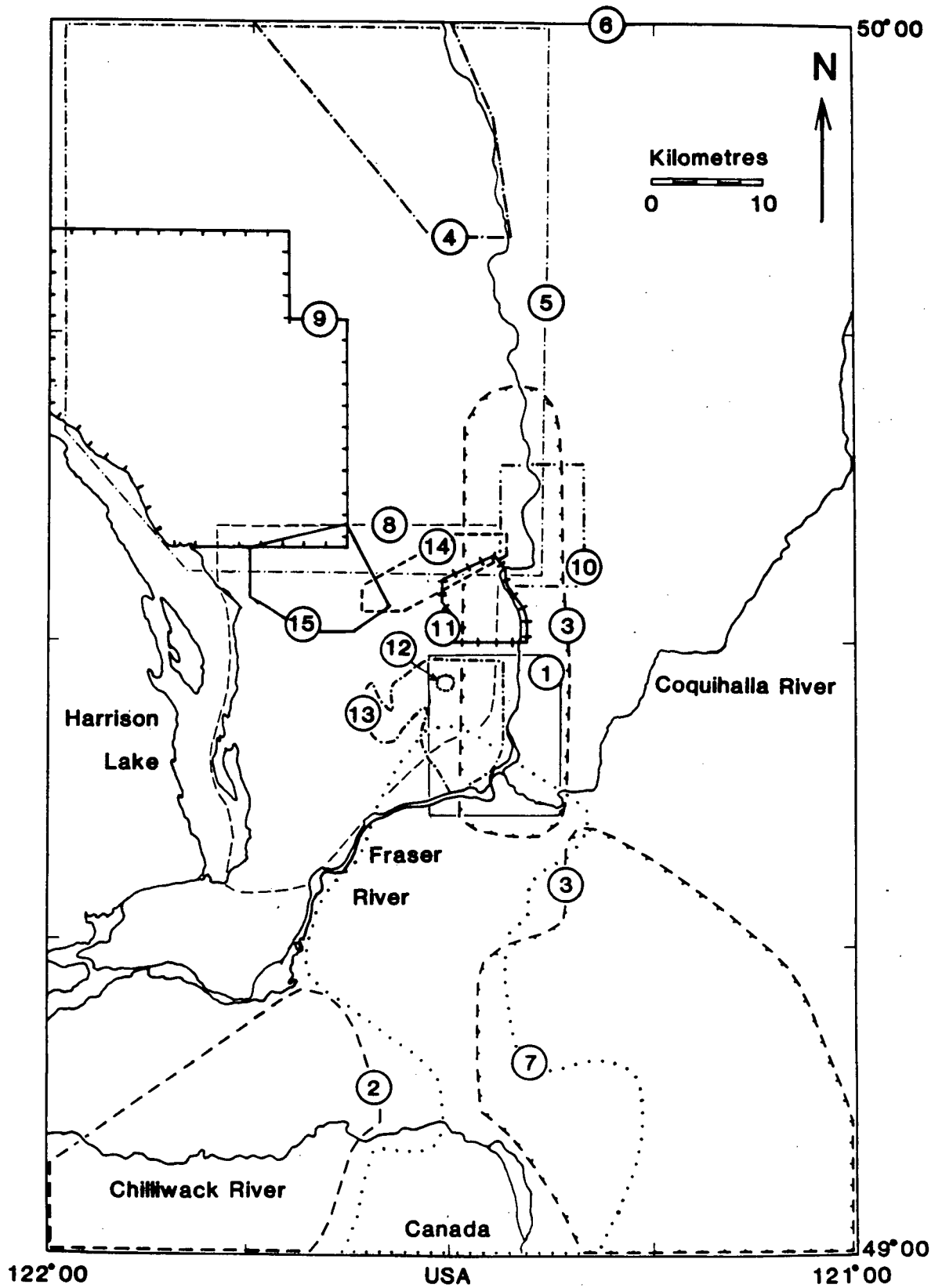
1.2 Previous Work

The area between Harrison Lake and the Fraser River has been studied by geologists since the 1920's. Monger (1970) compiled all work to 1969, including a review of the geology of the North Cascade Mountains by Misch (1966). Figure 1.1 shows areas mapped by some of the geologists mentioned below. Read (1960) studied schist similar to Settler Schist near the contact with batholithic rocks on Zofka Ridge and along Stulkawhits Creek, and concluded that the metamorphic isograds were not related to the intrusions. Monger (1966) mapped the Chilliwack

Figure 1.1 Area Location Map

Key to map areas

15. Gabites, this study
14. Bartholomew 1979
13. Vining 1977
12. McLeod 1975
11. Pigage 1973
10. Bremner 1973
9. Reamsbottom 1971, 1974
8. Lowes 1972
7. Richards 1971
6. Monger 1970
5. Roddick and Hutchison 1969
4. Hollister 1969
3. McTaggart and Thompson 1967
2. Monger 1966
1. Read 1960



Group in the type area in the Chilliwack valley. McTaggart and Thompson (1967) mapped the region along the Fraser River Canyon and southward from Hope. A regional summary of the tectonic relationship between the southern Coast Ranges and North Cascade Mountains was published by McTaggart (1970). Hollister (1969a,b) studied the relationships between metamorphic minerals in schists near Kwoiek Creek that are considered to be equivalent to Settler Schist. Roddick and Hutchison (1969) covered the northwestern part of the Hope map-area, including the Big Silver River area north of Cogburn Creek. Richards (1971) mapped the Chilliwack batholith and Spuzzum batholith north and south of the Fraser River; Vining (1977) mapped the Spuzzum batholith further north in the vicinity of the Giant Mascot Nickel Mine. Lowes (1972) mapped the area from Harrison Lake east and south to the Fraser River; the ridges north of Cogburn Creek were his northern boundary. His northern edge overlapped the area around Big Silver River mapped by Reamsbottom (1971 and 1974). Bremner (1973) studied metamorphism in a section of the Fraser Canyon north of Yale. Pigage (1973) mapped the Gordon Creek area south of Yale, with emphasis on metamorphism of the Settler Schist. Bartholomew (1975) extended the work of Pigage in the Yale Creek area, between Gordon Creek and Cogburn Creek. McLeod (1975) studied the geology of the Giant Mascot Nickel Mine in Stulkawits Creek.

Previous geochronometry is reviewed in Chapter 5.

1.3 Regional Geology

The study area lies in a zone of complex geology at the south end of the Coast Plutonic Complex and the north end of the Cascade Mountains. Many of the structures are continuous with those of the North Cascade Mountains. Geology of the region has been summarised in Figure 1.2, after Monger (1970), Pigage (1973), Bartholomew (1979), and Haugerud (1979).

The Coast Plutonic Complex consists of composite plutons of dominantly quartz diorite and granodiorite composition, mainly Cretaceous in age, in which lenticular bodies of metamorphosed sedimentary and volcanic rocks form pendants.

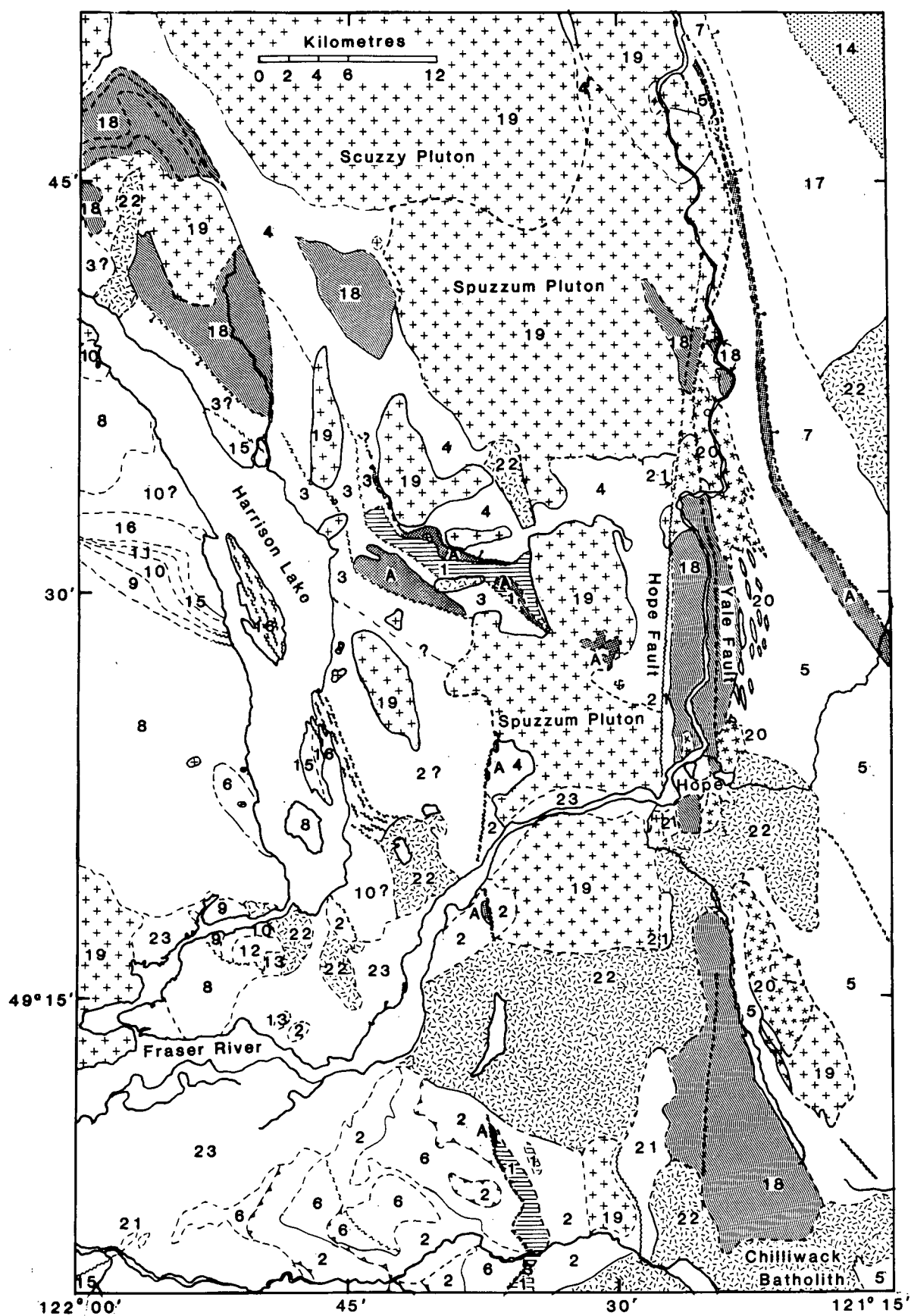
Supracrustal rocks in the study area have been divided into two lithologically and structurally distinct units, the Settler Schist (Lowes 1972) and the Cogburn Creek Group (this study). The rocks of the Cogburn Creek Group were previously mapped as part of the Pennsylvanian - Permian Chilliwack Group of the North Cascades (Monger 1970, Lowes 1972), but as this correlation is uncertain a new name has been applied in the Cogburn Creek area. Reamsbottom (1971 and 1974) included rocks of both Cogburn Creek Group and Settler Schist in his Cairn Needle Formation. Settler Schist was named and described by Lowes (1972) and dated as early Mesozoic (Bartholomew 1979).

The two stratigraphic units are separated by a steeply dipping belt of imbricated tectonic slices of ultramafic and dioritic rocks that has been interpreted as a northern extension of the root zone of the Shuksan thrust of the North Cascades (Lowes 1972). Some of the units in this zone resemble Yellow

Figure 1.2 Regional Geology of the North Cascade Mountains
and South Coast Mountains

Key for Regional Geology Map

Quaternary	23	Drift and alluvium
Miocene and Oligocene	22	Granodiorite, quartz diorite; Chilliwack Batholith, Cogburn Granodiorite, Needle Peak Pluton, Silver Peak Pluton,
Eocene	21	Conglomerate
Early Tertiary	20	Diorite, granodiorite; Yale Intrusions
-Late Cretaceous	19	Diorite; Spuzzum Pluton and outliers, Scuzzy Pluton
Cretaceous	18	Gneiss; Custer, Breakenridge Formation
	17	Jackass Mountain Group
	16	Brokenback Hill Formation
	15	Peninsula Formation
Late Jurassic	14	Granodiorite;
-Cretaceous	13	Agassiz Prairie Formation
Upper Jurassic	12	Kent Formation
	11	Billhook Creek Formation
Mid Jurassic	10	Mysterious Creek Formation
	9	Echo Island Formation
	8	Harrison Lake Formation
U-M-L Jurassic	7	Ladner Group
Triassic-Jr	6	Cultus Formation
Pm-Tr(?) - Jr	5	Hozameen Group Triassic or older
	4	Settler Schist
Tr or older	3	Cogburn Creek Group
Penn.-Permian	2	Chilliwack Group
Precambrian -	1	Yellow Aster Complex, Baird Metadiorite
Early Paleozoic	A	ultramafic rocks
Age unknown		thrust fault
		steep fault, downthrown side



Aster Complex (Misch 1966), which is partially of Precambrian age (Mattinson 1972).

Dioritic and granodioritic rocks of Cretaceous age have intruded the schists and gneisses. These are syn- to post-tectonic with respect to the regional metamorphism and deformation but predate movement on the Fraser Fault zone. Discordant mid- to late-Tertiary granodiorite bodies are the youngest intrusives.

The youngest stratigraphic units are Eocene conglomerates that have been deformed along the Fraser Fault zone (McTaggart and Thompson 1967), and Pleistocene glacial deposits.

McTaggart (1970) considered that the belt of crystalline gneisses north of the International Border was the deeply eroded axial zone of a Cretaceous orogen. The metamorphosed and deformed sediments of the North Cascade Mountains represented a shallower level. A lenticular body of gneiss (Custer Gneiss) bounded by faults of the Fraser Fault zone was interpreted as the core of this orogen. The Custer Gneiss was first described by McTaggart and Thompson (1967) as migmatitic gneiss with small areas of schist. They correlated it with gneisses mapped in the North Cascade Mountains by Misch (1966). Age estimates range from Early Paleozoic to Cretaceous (McTaggart 1970). McTaggart considers that the Custer Gneiss may be related to Spuzzum batholith. Reamsbottom (1971) correlated two domes of granodioritic gneiss in the Mount Breakenridge area with Custer Gneiss.

Movement on the Fraser Fault zone was once thought to have

started in the Mesozoic and continued until Eocene times (Monger 1970). New data now indicates that most of the movement is Tertiary, mostly Eocene (Monger 1985). The fault zone is sealed by the mid-Tertiary Chilliwack batholith (Appendix E) and related plutons. Major movement on the Straight Creek fault in Washington ended by 33 Ma (Miller and Vance 1981). Correlation of the Settler Schist with the Chiwaukum Schist of the Skagit Metamorphic Suite in the Stevens Pass area led Misch (1977) to postulate 150 to 200 km right lateral offset on the Fraser-Straight Creek fault system (Figure 1.3). Displacement of the Hozameen and Bridge River Groups and Bridge River Metamorphic zone (Monger 1978, 1985) and Tyaughton-Methow Basins (Kleinspehn 1985) support that inference and may bracket the fault movement to within the Eocene. Kleinspehn (1985) restores the Tyaughton-Methow basin to a reasonable depositional environment by reversing 110 km of dextral motion on the Fraser - Straight Creek Fault. This was preceded by 150 km of Cenomanian to Turonian motion on the Yalakom - Ross Lake Fault. A more detailed discussion of fault movements is in Chapter 6, with appropriate figures.

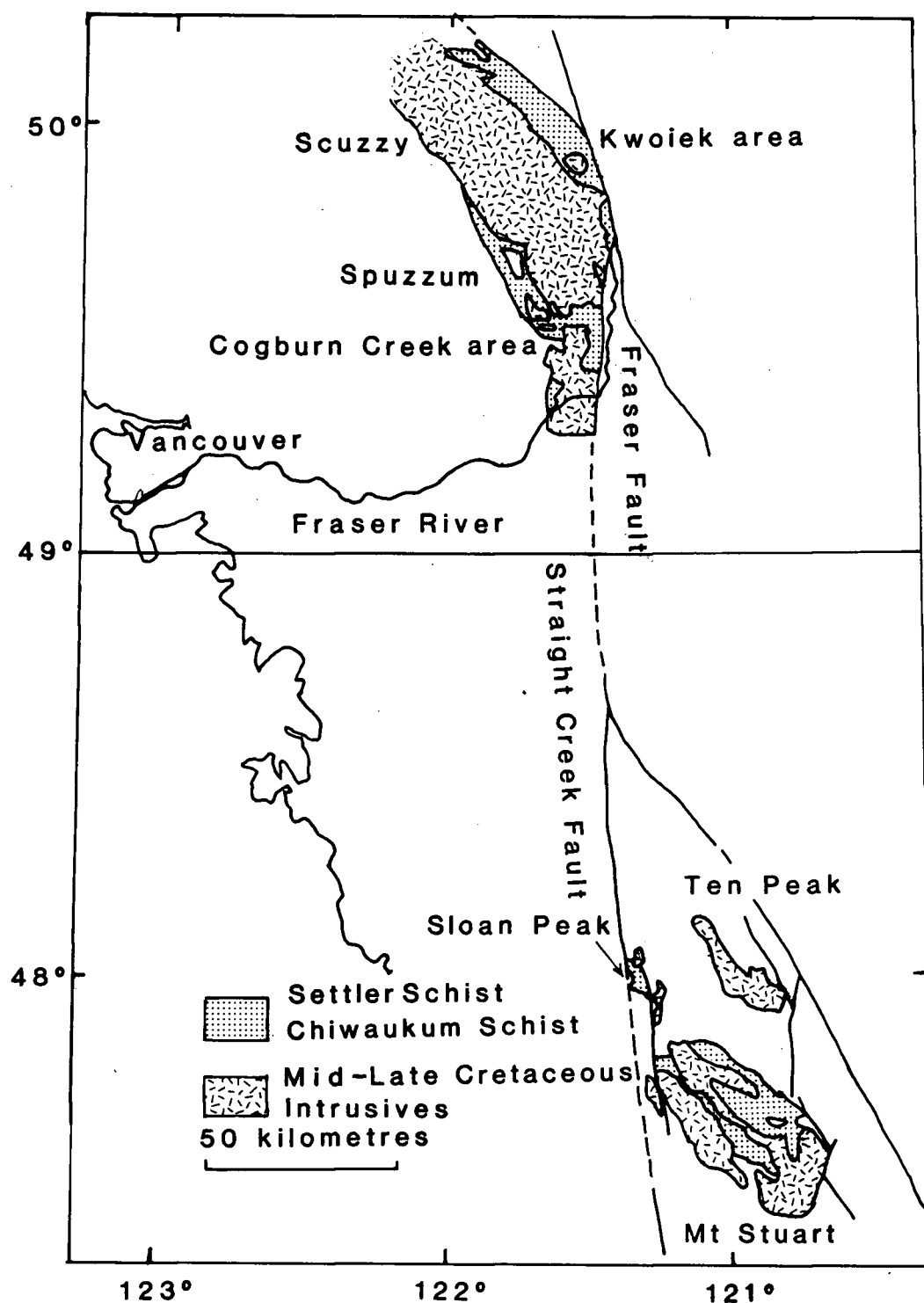


Figure 1.3 Geographical location of the Settler Schist and Chiwaukum Schist, modified from Evans and Berti (1985). Individual plutons intruding the two schist units are named. This map is used as a base for Figure 6.2.

2. Geology of the Cogburn Creek area

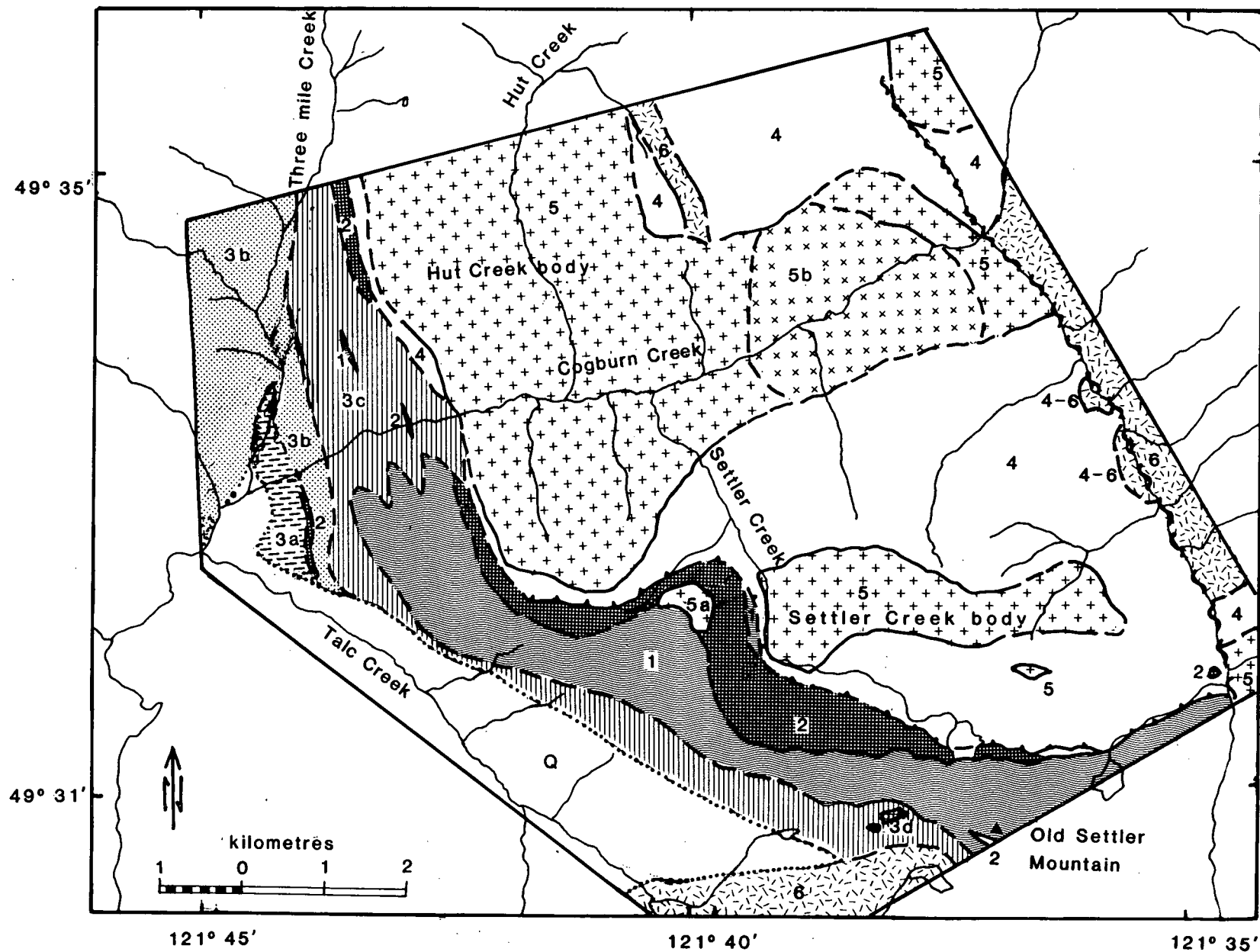
Rocks in the Cogburn Creek area are divided into five main units, with areal distribution as shown in Figure 2.1. The most extensive units are two lithologically and structurally distinct schists, the Cogburn Creek Group and the Settler Schist, and the Spuzzum batholith that intrudes them. The main structural feature of the area is a sinuous zone of almost vertical tectonic slices of metadiorite and ultramafic rocks (Plate 2.1) that separates the Cogburn Creek Group and Settler Schist. This zone strikes east-west in the south part of the area around Old Settler Mountain, and turns to strike north-northwest in the northwestern part of the area, with a deflection around the Spuzzum batholith, Hut Creek body. Lowes (1972) correlated this zone with the Shuksan thrust zone (Misch 1966) on the basis of structural position, lithological similarities of rocks in the zone, and general continuity of the belt along strike with similar rocks and structures to the south.

Both schists have undergone at least three phases of deformation, mostly related to the Cretaceous episode of metamorphism and diorite intrusion. The dominant structures in the Settler Schist were formed by the second recognisable deformation (Pigage 1973, Bartholomew 1979). Although Pigage found graded bedding in the Settler Schist in the Gordon Creek area, no convincing evidence of bedding was found around Cogburn Creek. In the Cogburn Creek Group, metamorphosed cherts exhibit what appears to be original bedding rather than metamorphic transposition. Schistosity is subvertical over most of the

Figure 2.1 Generalised geology of the Cogburn Creek Area

Key to map units.

- Q Pleistocene glacial debris
- 6 Granodiorite (Cogburn)
- 4-6 Agmatized diorite, mixture of Settler Schist and Cogburn Granodiorite
- 5 Diorite (Spuzzum)
- 5a Foliated diorite in melange zone
- 5b Hornblende-hypersthene gabbro
- 4 Settler Schist
Cogburn Creek Group
- 3a -grey pelite
- 3b -greenschist
- 3c -metachert
- 3d -marble
- 2 Ultramafic rocks
- 1 Baird Metadiorite
- Shuksan thrust
- Cogburn Fault



study area, but has variable strike.

Regional metamorphic grade changes across the area from greenschist grade in the west (on the shore of Harrison Lake), through garnet-staurolite, kyanite, fibrolite \pm kyanite, to sillimanite \pm fibrolite in the northeastern corner. The increase is consistent with proximity to the large mass of diorite that comprises the Spuzzum batholith. Within a kilometre of the two diorite bodies in the field area an earlier contact metamorphism is indicated in the Settler Schist by relict chiastolitic andalusites.

The latest event is post-metamorphic intrusion of small granodiorite plutons. An example is the Cogburn Granodiorite stock (Bartholomew 1979) which occurs east of the forks of Cogburn Creek.

Age relations among the non-intrusive rocks are not clear from lithologic, stratigraphic, or structural evidence. Both schists are bounded by faults and intrusive contacts, and the metamorphic grade and degree of deformation are high enough to make it unlikely that fossils would survive. The rock units are described below in order of decreasing age, as deduced from isotopic studies.

2.1 Unit 1. Baird Metadiorite

The name Baird Metadiorite is applied in this study to a unit of variably metamorphosed mafic igneous rocks. Occurrence is as lenses and tabular masses imbricated with ultramafic rocks, along the zone marking the northern extension of the Shuksan Thrust (Lowes 1972). The largest body forms the ridge which extends northwest from Old Settler Mountain to Cogburn Creek, and separates Talc and Settler Creeks (Figure 2.1).

The mafic rocks are variable in composition from gabbro to quartz diorite, and have been metamorphosed to amphibolite facies. They are grey-green in colour, hard, and form massive blocky outcrops and steep cliffs with sparse vegetation.

Texturally the rocks show weak to moderate foliation due to alignment of mafic minerals. Strain during metamorphism and deformation has been taken up along fine-grained, chloritic shear zones through the otherwise equigranular rock.

Compositionally the mafic rocks consist mainly of hornblende, plagioclase, quartz, clinozoisite, chlorite, and opaques, in varying proportions. Rutile is a common accessory. The hornblende occurs both as porphyroblastic, probably relict, large crystals and as small intergranular prisms. In the samples studied in thin section the plagioclase has been almost entirely converted to epidote, albite, sericite and calcite. Relict plagioclase compositions, measured by a-normal methods, were similar to those reported by Lowes (1972), and are in the range An₃₅ to An₄₂. Chlorite occurs mainly in fine-grained shear zones. Minor relict pyroxene now overgrown by hornblende

(sample MD1) may be part of the original mineral assemblage. Dynamothermal metamorphism to andesine - epidote amphibolite subfacies during the Cretaceous has reconstituted earlier mineral assemblages in the rocks, although there is only minor internal deformation. Lowes (1972) reported limited evidence here for a previous amphibolite facies metamorphism observed by Misch (1966) in the North Cascade Mountains.

Lowes (1972) correlated the rocks here called Baird Metadiorite with the Yellow Aster Complex (Misch 1966) in the North Cascade Mountains, on the basis of structural position with respect to the Shuksan Thrust. The Yellow Aster Complex occurs as tectonic slices with sheared ultramafic rocks in melange below the sole of the Shuksan thrust; in places it is imbricated with the underlying Chilliwack Group. Misch (1966) considered the Yellow Aster Complex to be "basement", and mapped it in the type area as schistose and directionless metamorphic hornblendites and amphibolites, gneissose and directionless metagabbros, metadiorites, meta-quartz diorites and metatrandhjemites, and migmatites of varied composition. He speculated that the schistose hornblendites and amphibolites are remnants of primary oceanic crust that was later converted to predominantly hornblende quartz dioritic continental crust. Zircons dated by Mattinson (1972) showed two age groups in the Yellow Aster Complex. Pyroxene gneiss was dated at 1400 to 1600 Ma and quartz diorite gneiss and pegmatite gneiss at 410 ± 85 Ma.

Rock types in the Baird Metadiorite are similar to those

comprising the Yellow Aster Complex. Rb-Sr and zircon U-Pb dating (Chapter 5) on the Baird Metadiorite suggest an old age similar to that measured by Mattinson on Yellow Aster pyroxene gneiss. Thus new isotopic evidence supports the correlation made by Misch (pers. comm. to Lowes 1972) based on lithologies and other field aspects of the rocks.

2.2 Unit 2. Ultramafic Rocks

Ultramafic rocks in the study area mainly occur as pods and elongate bodies of peridotite imbricated with the Baird Metadiorite along the root zone of the Shuksan thrust. The scale of imbrication varies from metres to kilometres. Some small bodies of pyroxenite and hornblendite are associated with the Spuzzum batholith, and occur within both the diorite and the surrounding schists. Outcrops of ultramafic rock are almost devoid of vegetation and weather orange, so they are recognisable from a distance. The largest body of ultramafic rock (mapped by Lowes 1972, outside the present study area) is faulted into the Cogburn Creek Group along the west side of Talc Creek, giving the drainage its name.

The peridotite composition is variable, from serpentinite to unaltered dunite. The most common is serpentinite, but metamorphic reconstitution of the original dunite, harzburgite and pyroxenite is quite variable within the rocks. Some of the serpentinite has been recrystallised by metamorphism back to olivine and talc.

2.3 Unit 3. Cogburn Creek Group

Pelitic schist, chert and metavolcanic rocks cropping out along the eastern shore of Harrison Lake and west of the Shuksan thrust zone have been given the informal name Cogburn Creek Group in this study. Because of their similarity in structural position beneath the Shuksan thrust, Lowes (1972) had previously assigned them to the Chilliwack Group of Monger (1966); however, because of lithological dissimilarity and lack of fossils I have chosen to designate them as the Cogburn Creek Group. Crickmay (1930) used the name Slollicum Group for metavolcanic rocks and low grade pelites around Slollicum Peak that may be part of the same unit. Reamsbottom (1971 and 1974) mapped rocks in the same structural position in the Big Silver River area to the north of Cogburn Creek as part of the Cairn Needle Formation, along with what is herein called Settler Schist. Monger (pers. comm. 1985) has followed the unit north at least as far as between the two gneiss domes in the Mount Breakenridge area.

The stratigraphic top and bottom of the Cogburn Creek Group are not seen. The unit is truncated on the northeast against Baird Metadiorite and ultramafic rocks in the melange zone below the Shuksan thrust. Since the rocks dip to the east, this is the structural top. The southwest contact has not been studied; Lowes (1972) did not recognise any subdivision of his Chilliwack Group. Monger (pers. comm. 1985) has found Chilliwack Group north of the Fraser River, but considers that most of the rock along the eastern side of Harrison Lake does not belong to the Chilliwack Group.

Three main rock types of the Cogburn Creek Group have been mapped. They are, from west to east: grey pelite, chlorite-actinolite greenschist, metamorphosed ribbon chert. All have been metamorphosed up to at least garnet grade during Cretaceous regional metamorphism. Grade increases eastward across strike.

Rock Types

1) Grey Pelite

The westernmost part of the Cogburn Creek Group at Cogburn Creek consists of light to dark grey pelite. These rocks are very fine grained, micaceous, and may contain porphyroblasts, usually embayed garnet or skeletal ilmenite. The colour of the rock depends on graphite content, which may be up to 50% as in a black shale with magnetite porphyroblasts.

Quartz and plagioclase are the main constituents. Plagioclase composition varies from oligoclase to andesine. Biotite or muscovite are common primary metamorphic minerals, with later alteration to chlorite. Minor alteration and accessory minerals include calcite, orthoclase, epidote, ilmenite and tourmaline.

2) Chlorite-actinolite greenschist

Greenschist occurs both as layers in the ribbon chert and as a massive unit which contains bands of chert. Present mineralogy is quartz, plagioclase (An₈ to An₂₈), green hornblende or actinolite, chlorite, calcite, epidote, sphene, and accessory mafics. Chlorite replaces hornblende in most of the thin sections studied. Calcite is common in parts of the unit. Grain size is generally fine, although coarser, knobbly

greenschists were found.

Mineralogy and association with ribbon cherts suggest that the greenschists were originally submarine volcanic rocks. Lowes (1972) found evidence of pillows south of Cogburn Creek. Calcareous rocks were probably marls interlayered with the volcanic rocks.

3) Metamorphosed ribbon chert

A rock containing bands of finely to coarsely crystalline quartz separated by fine grained biotite-rich layers has been interpreted as metamorphosed dirty ribbon chert. Opaques and accessory tourmaline and zircon are present in the biotite layers, and plagioclase is found with quartz. The bands have been contorted into numerous minor folds. Chert on the ridge west of Old Settler Mountain is interlayered and tightly folded with a 20 m thick band of marble. The marble is coarsely crystalline, and is dark grey with white patches.

The unit of ribbon chert contains layers of greenschist that become thinner and less numerous eastwards, away from the chlorite-actinolite greenschist. The association suggests a deep marine environment, mostly below the carbonate compensation depth and isolated from clastic input.

2.4 Unit 4. Settler Schist

The Settler Schist crops out east of the imbricate zone correlated with the Shuksan Thrust. The unit is dominated by metasedimentary pelitic schists, with minor amphibolite and quartzite. In the Gordon Creek area Pigage (1973) mapped four distinct rock types within the pelitic schist: layered pelitic schist, graphitic pelitic schist, quartzofeldspathic schist, and micaceous quartzite. A similar subdivision was attempted in this study, but although different lithologies could be identified they did not form mappable units.

Two main episodes of metamorphism have recrystallised the Settler Schist. Contact metamorphism by the Spuzzum batholith produced andalusite in rocks of suitable composition within a kilometre of the contact. Later regional (amphibolite facies) metamorphism caused an increase in grade up to sillimanite zone in the northeast corner of the study area. The grade increases from south to north across the Settler Schist in the study area, with garnet-staurolite grade rocks in the south and east along the Shuksan thrust, through kyanite grade to fibrolite ± kyanite to sillimanite ± fibrolite (Bartholomew 1979). This increase correlates with proximity to the main body of the Spuzzum batholith, although intrusion was before the peak of metamorphism (Bartholomew 1979). A general increase in grain size and the appearance of gneissic banding and thin leucocratic veinlets accompany the increase in grade.

Chemical compositions of staurolite-bearing rocks are typically restricted to low Mg:Fe ratios, high Al content, low

alkali and Ca content (Hoschek 1967). Mineral assemblages in the Settler Schist suggest a stratigraphic sequence of dominantly Fe- and Al-rich shales with lesser amounts of volcanic and calcareous rocks (Pigage 1973).

Rock Types

1) The pelitic part of the Settler Schist is fine-grained, and colour varies from black to medium grey depending on graphite content. The black argillite is massive with poor cleavage, while more micaceous pelite has good cleavage and variable metamorphic compositional layering. Some slate on the northern ridge and near diorite bodies has a spotted appearance due to porphyroblasts. The dominant mineral assemblage is quartz \pm plagioclase, biotite, graphite, garnet, staurolite, with minor and accessory muscovite, andalusite, kyanite, sillimanite, fibrolite, chlorite, magnetite, rutile, epidote, tourmaline, or zircon (detrital). Garnet, staurolite, andalusite, kyanite and sillimanite occur as porphyroblasts in rocks with appropriate bulk compositions and metamorphic grade. Andalusite is pseudomorphed by quartz and muscovite with kyanite or sillimanite. Both kyanite and sillimanite (and fibrolite) can be found with garnet and staurolite. Tourmaline is a common accessory. In rocks where it is present the biotite is a distinctive reddish brown.

2) The quartzofeldspathic rocks differ from the pelites mainly in grain size and graphite content. They are coarser than the pelites, and contain a lower percentage of graphite. Colour is medium to light bluish grey. Mineralogy is similar to the

pelitic schists, but in different proportions.

3) The micaceous quartzite has a sandy appearance and is pink in colour from biotite. Mineralogy is quartz, plagioclase (An₂₅ to An₄₀), biotite, muscovite, with varying amounts of graphite, magnetite, garnet, staurolite, alumino-silicates, chlorite, tourmaline, epidote, rutile, zircon and apatite. Two samples, SS66 and SS125, also contain pale green amphibole along the margins of quartz veins, indicating calc-silicate assemblages. In both these rocks the groundmass around the euhedral hornblendes is mylonitised. Large relict poikilitic plagioclase phenocrysts were found in two samples, SS134 and SS143.

4) Amphibolites are a minor constituent in the Settler Schist, and have been divided into two types as in Pigage (1973) and Bartholomew (1979). Speckled amphibolites were found interlayered with other rock types. They contain plagioclase, blue-green hornblende, quartz, and biotite, with accessory magnetite, chlorite, calcite, rutile, clinozoisite and apatite. The original rock was probably marl or calcareous mudstone.

The second type of amphibolite is found in small pods and lenses within the schist. These pods contain large crystals of dark green hornblende, and commonly have a very mafic rim around a lighter core (Plate 2.2). They are considered to have been mafic igneous rocks, perhaps dykes that were boudinaged during metamorphism and deformation.

Age relations of the Settler Schist within the regional stratigraphy have not been deciphered as the unit is bounded on all sides by faults and intrusive contacts. Earlier workers

have based correlations on lithological and chemical similarities. The Settler Schist has been correlated previously with the Chiwaukum Schist of the Skagit Suite in the North Cascade Mountains (Lowes 1972). Lithologies and metamorphic history are remarkably similar, and the two units can be brought together by removing 150 to 200 km of right lateral offset along the Straight Creek - Fraser fault system. Geochronometry (Chapter 5) indicates an old, possibly Precambrian provenance for at least part of the unit, which is similar to results of Mattinson (1972) for the Skagit Metamorphic Suite in Washington. Thus the lithological correlation is strengthened by isotopic evidence. The Rb-Sr whole rock isochron date of 210 ± 27 Ma (Bartholomew, 1979, and this study) indicates that the time of deposition of the the protolith of the Settler Schist was probably early Mesozoic.

2.5 Premetamorphic intrusive rocks

Some foliated rocks are interpreted as pre-metamorphic intrusive rocks, for example, a large foliated felsic dyke on the ridge north of Cogburn Creek. HL 111 is a light grey felsite, which is flecked with black biotite, and is foliated parallel to surrounding chert. Mineralogy is plagioclase (oligoclase), quartz, muscovite, sillimanite, biotite, garnet, with minor zircon. Igneous textures are preserved in patches of large myrmekitic plagioclase grains, but most of the rock is recrystallised. Muscovite and sillimanite are aligned along the foliation.

Garnet-cluster Dykes

Metamorphosed felsic dykes and sills are common in the Settler Schist. The most common type contains distinctive knobbly clusters of pink garnets up to 0.5 cm across with white depletion haloes. Pigage (1973) named them garnet-cluster dykes. The dated sample SS85 falls in this category. The rock is light pinkish grey, fine grained quartz-biotite schist with garnet clusters. Mineralogy is quartz, plagioclase (andesine), biotite or muscovite, garnet and opaques, with minor apatite, zircon, and/or diopside. Relict zoned plagioclase porphyroblasts indicate an igneous origin. Depletion haloes around the garnets contain only quartz and plagioclase. These are not necessarily post-crystalline reaction textures but may be a result of original metamorphic growth of garnet. The growing garnet uses the mafic constituents within the surrounding area, leaving felsic components behind.

Two cleavages are present in the dykes, as in the surrounding schist, and are marked by alignment of biotite. The f_2 foliation is deflected around both plagioclase porphyroblasts and garnet clusters, indicating a pre-deformation timing for the halo reaction.

2.6 Foliated diorite in melange zone

SD 92 was collected from a plug of foliated diorite that lies within the thrust fault zone, on the western side of Settler Creek. The composition of this body is biotite, quartz, plagioclase, garnet, and epidote, with minor rutile, and white

mica. Chlorite is a late alteration of biotite. Plagioclase can be separated into two generations based on texture and composition: 1) poikilitic igneous andesine, An₃₀, and 2) well-twinned metamorphic andesine, An₃₅. Geochronometry suggests that it is part of the Spuzzum batholith; however, the presence of metamorphic plagioclase and foliation means that the body must be older than the Spuzzum batholith, or one of the earliest phases.

2.7 Unit 5. Spuzzum Batholith

Intrusive rocks belonging to the Spuzzum batholith form two discrete bodies called Settler Creek body and Hut Creek body. The Hut Creek body is near to but not continuous with the body of diorite to the north and east of Cogburn Creek. The Settler Creek body is Unit 3d of Bartholomew (1979). Several small bodies of similar composition have been mapped as part of the same intrusive suite. Both large bodies intrude the Settler Schist and not the Cogburn Creek Group. Crosscutting relationships or otherwise with the thrust fault zone have not been determined, as critical areas are covered with glacial debris and/or thick vegetation. The fault zone appears to have been distorted during intrusion, implying that it is older than the Spuzzum batholith.

Because the diorite is more resistant to erosion than the supracrustal rocks, it forms high ridges with steep cliffs into deeply incised valleys. The Settler Creek body forms part of the ridge north of Old Settler Mountain. The Hut Creek body

spans the Cogburn Creek valley, up to 1000 m on either side. Hut Creek bisects a tongue of diorite that continues north into the area mapped by Reamsbottom (1971 and 1974).

Most of the intrusive rocks are hornblende-quartz-diorite. Accessory biotite and garnet occur locally either together or separately. Hornblende is generally brown, or has brown cores with green metamorphic overgrowths (Plate 2.3). Gabbro has been mapped west of the Cogburn Creek forks. The composition is hypersthene - hornblende or clinopyroxene with minor plagioclase and mafics, forming an equigranular rock that is extremely hard, resulting in the distinctively steep, blocky cliffs described above. Plate 2.4 shows replacement textures in hornblende in the gabbro. Fine grained opaque inclusions along cleavage planes are common in the relict hornblende cores.

2.8 Unit 6. Younger Intrusive Bodies

1) Cogburn Granodiorite is a medium grained, leucocratic granodiorite containing biotite, plagioclase (zoned from An₃₅ to An₆₀), quartz, with minor hornblende. The boundaries of the pluton crosscut both Settler Schist foliation and margins of the Spuzzum batholith (Bartholomew 1979).

2) SD 14 comes from a small area of agmatized diorite in the south fork of Cogburn Creek. The composition suggests assimilation of a graphitic member of the Settler Schist that it intruded. The rock can be divided into two types by difference in grain size and texture. The coarser part is medium grey diorite, speckled by biotite and garnets; the finer is darker

grey and foliated, and looks like Settler Schist. The grain size transition is sharp but the major mineralogy does not change. It is quartz, plagioclase (oligoclase), biotite, garnet, with minor magnetite, apatite and zircon. The finer part also contains minor graphite and green hornblende. The geochronometry indicates that this rock is younger than Cretaceous, (see Chapter 5), and is one of the younger intrusives rather than Spuzzum batholith.

3) A small body of granodiorite intrudes the Cogburn Creek Group southwest of Old Settler Mountain. The rock is light grey, fine grained biotite-hornblende granodiorite. Mineralogy is quartz, plagioclase, biotite, and hornblende. Igneous textures are preserved, and there is no foliation.

4) Basaltic dykes crosscut all units older than and including Spuzzum batholith. They are fine grained, grey to greenish grey, and undeformed. Mineralogy is quartz, plagioclase, hornblende, and opaques, with minor late chlorite alteration.

2.9 Breakenridge Formation Gneiss

Grey gneiss from the Breakenridge Formation mapped by Reamsbottom (1971,74) in the Big Silver River valley was sampled for geochronometry, so a description is included here. Roddick and Hutchison (1967) and Reamsbottom considered the grey gneiss coring the anticlinal dome centred on Mount Breakenridge to be the oldest rock in the region. Dating carried out in this study yields conflicting results (Chapter 5). The following description is from Reamsbottom (1974).

The Breakenridge Formation is composed mainly of homogeneous grey gneiss and amphibolite. Migmatitic, banded to irregularly banded gneiss, pelitic schist and skarn form heterogeneous zones between the grey gneisses and amphibolites.

The grey gneisses are medium-grained with an allotriomorphic granular texture. They consist of biotite, quartz and plagioclase (An10 to An34) locally with muscovite, garnet or microcline. Myrmekite commonly develops between grains of microcline and plagioclase.

3. Metamorphism

Schists in the Cogburn Creek area have been subjected to contact metamorphism from the Spuzzum batholith followed by regional metamorphism during the Cretaceous. Lowes (1972) recognised an earlier metamorphism in the Precambrian or Paleozoic Baird Metadiorite.

3.1 Unit 1. Baird Metadiorite

The present mineral assemblage of hornblende, plagioclase, quartz, clinozoisite, chlorite and opaques represents metamorphism of mafic intrusive rocks to andesine-epidote amphibolite subfacies. Hornblende is pale green and actinolitic, and occurs as large ragged porphyroblasts. These appear to have been left essentially undeformed while surrounding felsic minerals were fragmented. Rare brown cores may be of primary igneous origin. In sample MD1 rare relict augite cores may be of primary igneous origin. They are now rimmed by pale green hornblende. Plagioclase compositions in cores of large porphyroblasts in MD1 reach An₄₂, while rims and smaller grains have recrystallised at around An₃₅. Epidote and albite have replaced the plagioclase.

3.2 Unit 2. Ultramafic Rocks

Both the original composition of the ultramafic rocks and their degree of metamorphic reconstitution is variable. Several samples of dunite were found, for example HL30, containing olivine and chromite with later alteration to calcite and

tremolite (Plate 3.1). HL33 consists almost entirely of talc; HL31 and HL99 contain tremolite with minor late serpentine alteration. The other rocks all contain varying proportions of olivine, chromite or magnetite, enstatite or clinopyroxene, calcite or magnesite, with later alteration to talc, serpentine and chlorite. In HL54, consisting of calcite, serpentine, opaques and late chlorite in veins, some of the calcite exhibits deformed twin lamellae. This suggests that the rock was strained after it recrystallised. Its location, in the western tributary to Settler Creek (Appendix D), is very close to a visible fault plane separating Settler Schist from ultramafic rock and Baird Metadiorite. Thus there may have been some continued movement on this fault after metamorphism.

3.3 Unit 3. Cogburn Creek Group

Lack of suitable lithologies in the Cogburn Creek Group makes recognition of the metamorphic grade difficult. Mineral textures record three phases of deformation and folding, f_1 , f_2 and f_3 , with decreasing age. The timing of mineral growth with respect to these is shown in Figure 3.1a.

1) In the grey pelite, biotite \pm muscovite belong to the equilibrium assemblage. Mica foliation developed during f_2 , and individual flakes have recrystallised within this foliation to parallel f_3 . In sample HL16 (Plate 3.2) biotite is found as large brown porphyroblasts resulting from early contact metamorphism by Spuzzum batholith. These appear to have been

	Phase 1		Phase 2		Phase 3	Post-tectonic
Chlorite						
Biotite						
Muscovite						
Garnet						
Tourmaline						
Hornblende						

Figure 3.1a Relative ages of metamorphic mineral growth with respect to deformation, Cogburn Creek Group.

	Phase 1		Phase 2		Phase 3	Post-tectonic
Chlorite						
Biotite						
Muscovite						
Andalusite						
Garnet						
Staurolite						
Kyanite						
Fibrolite						
Sillimanite						
Tourmaline						

Figure 3.1b Relative ages of metamorphic mineral growth with respect to deformation, Settler Schist.

rotated during the formation of f_2 foliation, and are surrounded by quartz in pressure shadows. Large skeletal ilmenite porphyroblasts are also found in this sample.

Textures in garnet porphyroblasts indicate that they formed during and after f_1 and f_2 deformation. They contain inclusions and show evidence of rotation and synkinematic growth (e.g. HL15, Plate 3.3). A garnet in HL15 has a core with inclusions that mark f_1 and a solid rim that grew post-kinematically to f_1 . Small euhedral garnets in HL16 are synkinematic to f_2 (Plate 3.2).

Chlorite is part of the main equilibrium assemblage in HL16, but in HL103 it is a late replacement of biotite and garnet. Tourmaline where present appears to have crystallised during f_2 . Alumino-silicates were not found, but that may be a factor of bulk composition rather than metamorphic conditions. Lowes (1972) found staurolite porphyroblasts in pelitic schist in the upper part of Three Mile Creek, indicating that the higher range of epidote amphibolite facies was reached.

2) The main assemblage in the greenschist is plagioclase, quartz, hornblende, epidote, calcite, magnetite, biotite, and chlorite. Two generations of plagioclase are present. Early phenocrysts with graphic intergrowths are calcic oligoclase (An28), and igneous in origin. The later generation has albite composition (An8 to An10), and occurs aligned in felsic segregations. Hornblende is pale blue-green. Rare brown cores (HL77) are found as relicts from the original igneous assemblage. The grains are generally small, euhedral, and

aligned with the foliation around it, suggesting crystallisation after f_2 . In HL80 (Plate 3.4) large hornblende grains have crystallised parallel to an f_2 fold axial plane, while smaller grains are randomised by recrystallisation, suggesting crystallisation during and after f_2 . In this same sample calcite fills gashes that formed during late kink folding. HL142 (Plate 3.5) contains large porphyroblasts of dark brown-green to blue-green hornblende with inclusions of epidote, plagioclase and opaques. Although these porphyroblasts deflect the foliation, at least one contains it and a third phase fold, indicating growth late in the third phase. Garnets also formed at this time, and are now rounded. Epidote is found both as sieve-textured porphyroblasts (HL77) and as fine grained replacement of plagioclase (HL80). Chlorite occurs as a late replacement of biotite, hornblende and garnet.

3) The ribbon chert has been recrystallised during metamorphism to a coarse-grained aggregate of quartz and plagioclase. Biotite rich layers are finer grained and represent more argillic layers in the chert. A second cleavage is marked by biotite flakes oriented at an angle across the layers. No other metamorphic index minerals were recognised.

3.4 Unit 4, Settler Schist

Metamorphism of the Settler Schist was studied in detail by Pigage (1973) in the Gordon Creek area and by Bartholomew (1979) in the Yale Creek area. The metamorphic conditions in the Cogburn Creek area are similar, producing the same mineral

assemblages.

As in the Cogburn Creek Group, three phases of folding are recognised. Figure 3.1b gives mineral growth age relationships for Settler Schist. The earliest foliation is seen only in inclusion trails in early garnets (Bartholomew 1979).

Two episodes of metamorphism are recognised in these rocks. The first is high temperature contact metamorphism due to the Spuzzum batholith. It produced chiasmatic andalusite in schists of suitable composition up to a kilometre from the pluton margins. Both the Hut Creek body and Settler Creek body produced this effect. Later upgrading due to regional metamorphism has caused recrystallisation of the andalusite into aggregates of quartz, muscovite, staurolite, and kyanite or sillimanite. No andalusite remained in most of the specimens studied in thin section. Some small relict grains were found in SS43, SS80, SS96. Several chiasmatics were deformed during f_2 , before recrystallisation (SS110, Plate 3.6). The lack of orientation of the minerals in the pseudomorphs indicates that recrystallisation took place under static conditions. In SS110 staurolite that has grown across the boundary of a pseudochiasmatic contains graphitic inclusions of the external foliation where it is outside the pseudochiasmatic. This gives the timing of pseudomorphing and staurolite growth as after f_2 and before f_3 deformation.

Coexisting biotite and muscovite are ubiquitous throughout the schist. They define the f_2 foliation, and are recrystallised around small scale f_3 kink folds. In SS135

(Plate 3.7) biotite has crystallised along the axial plane of an f_2 fold.

Garnet textures are indicative of growth from synkinematic to f_1 to post f_2 . Early garnets are now rounded and may have quartz pressure shadows or haloes. Garnets found in association with sillimanite are rounded and surrounded by quartz, muscovite and fibrolite (SS66, Plate 3.8). Staurolite crystallised after f_2 ; it varies from synkinematic to f_3 to post-tectonic. Plate 3.9 shows post-tectonic twinned staurolite in pelite. Many are concentrically zoned (SS114, Plate 3.10) and contain graphite or quartz inclusions. The inclusion trains mark f_2 foliation and f_2 and f_3 folds within the mineral grains (SS53, Plate 3.11). In many of the rocks containing both minerals, garnet is usually earlier than staurolite.

Kyanite, where present, is in pseudochiastolite, having replaced andalusite during thermal and pressure upgrading of metamorphism. Most of the alumino-silicates in rocks in the study area are sillimanite or fibrolite. Crystalline sillimanite porphyroblasts reach 10 to 20 cm in length on the north ridge of the area (Plate 3.13), in close proximity to the Spuzzum batholith to the north. The grade of regional metamorphism increases towards this area. In thin section these crystals contain patches of fibrolite and inclusions of quartz, biotite and opaques, and have ragged outlines within a fairly regular halo of quartz and biotite (SS182a, Plate 3.14). Elsewhere, small crystals produce a spotted or streaky appearance in the pelites. Fibrolite occurs as mats with

biotite within the foliation but randomly oriented, and is therefore post-kinematic. It appears to have formed at the same time as and slightly before porphyroblastic sillimanite.

Tourmaline is a minor but common constituent of the Settler Schist. It appears to have formed during f_2 and continued to grow post-tectonically. Some larger grains show concentric zoning with graphite inclusions, similar to staurolite grains in the same rocks. Tourmaline-bearing rocks also contain distinctive reddish brown biotite.

On the basis of the mineral associations four metamorphic zones of Barrovian series have been recognised in the Settler Schist in the study area. They are as follows, in order of increasing grade:

- 1) Garnet-staurolite: biotite - garnet - muscovite - plagioclase - quartz - staurolite - (ilmenite - rutile)
- 2) Staurolite-kyanite: biotite - garnet - kyanite - muscovite - plagioclase - quartz - staurolite - (ilmenite - rutile)
- 3) Fibrolite: biotite - garnet - muscovite - plagioclase - quartz - fibrolite \pm kyanite \pm staurolite - (ilmenite - rutile)
- 4) Sillimanite: biotite - garnet - muscovite - plagioclase - quartz - fibrolite - sillimanite \pm staurolite

The first sillimanite (fibrolite) isograd is considered to represent equilibrium (Bartholomew 1979); it marks the first appearance of fibrolite. The coarse sillimanite isograd marks the appearance of porphyroblastic sillimanite recrystallising from fine grained sillimanite (fibrolite) and disappearance of kyanite. Bartholomew (1979) considers that it represents

overstepping of the kyanite to sillimanite reaction. Staurolite is found in sillimanite-bearing rocks but is not necessarily associated with the fibrolite-biotite masses or sillimanite porphyroblasts.

Although details of the relationships between metamorphic isograds and intrusive bodies are not clear, the grade increases towards the northeast. On a local scale, Bartholomew (1979) recognised a northwestern trend in Yale Creek, towards his Unit 3e, Fagervick body of the Spuzzum batholith. This was the last part of the Spuzzum batholith in his study area to intrude, and provided additional heat for the regional metamorphism to the northeast of Cogburn Creek. Metamorphic grade changes abruptly across Cogburn Creek, lending support to recognition of a fault along the south branch (Bartholomew 1979). The schist on the eastern side is in staurolite-kyanite zone, while rock directly west is in garnet-staurolite zone.

3.5 Premetamorphic intrusive rocks

The felsic sill HL111 that intrudes Cogburn Creek Group contains skeletal garnet porphyroblasts and fibrolite intergrown with biotite and muscovite. Large mica grains define f_2 foliation. The rock was collected from within 50 m of the contact with Spuzzum batholith Hut Creek body. The sillimanite is most probably the result of local increase in temperature in the country rock by heat from the diorite during regional metamorphism.

3.6 Discussion

Ultramafic rocks

Conditions of metamorphism in the ultramafic rocks appear consistent with those of the surrounding schist, indicating that the rocks were already juxtaposed before the culmination of regional metamorphism.

The mineral assemblages can be used to place broad limits on metamorphic conditions across the ultramafic belt. Pigage (1973) notes that coexisting serpentine and talc indicate a temperature below 500°C with less than 0.1 mole fraction CO₂ in the fluid phase (Greenwood 1967, Johannes 1969). The association, seen here in HL55, HL56, HL65, provides a lower temperature limit of 300°C (Figure 3.2). HL56 contains talc and magnesite, which is in the same stability field. Tabular crystals of olivine in HL30 (Plate 3.1) indicate metamorphic reconstitution of serpentinite back to olivine + talc, which requires a minimum temperature of 350°C.

Contact Metamorphism

Bartholomew (1979) considers that the andalusite formed under stable conditions at a pressure below the alumino-silicate triple point (Figure 3.3). Hollister (1969b) suggested metastable crystallisation of andalusite in the kyanite stability field for similar andalusite pseudomorphs in the Kwoiek area, with subsequent rapid conversion to kyanite and then sillimanite. However, this would require a steep

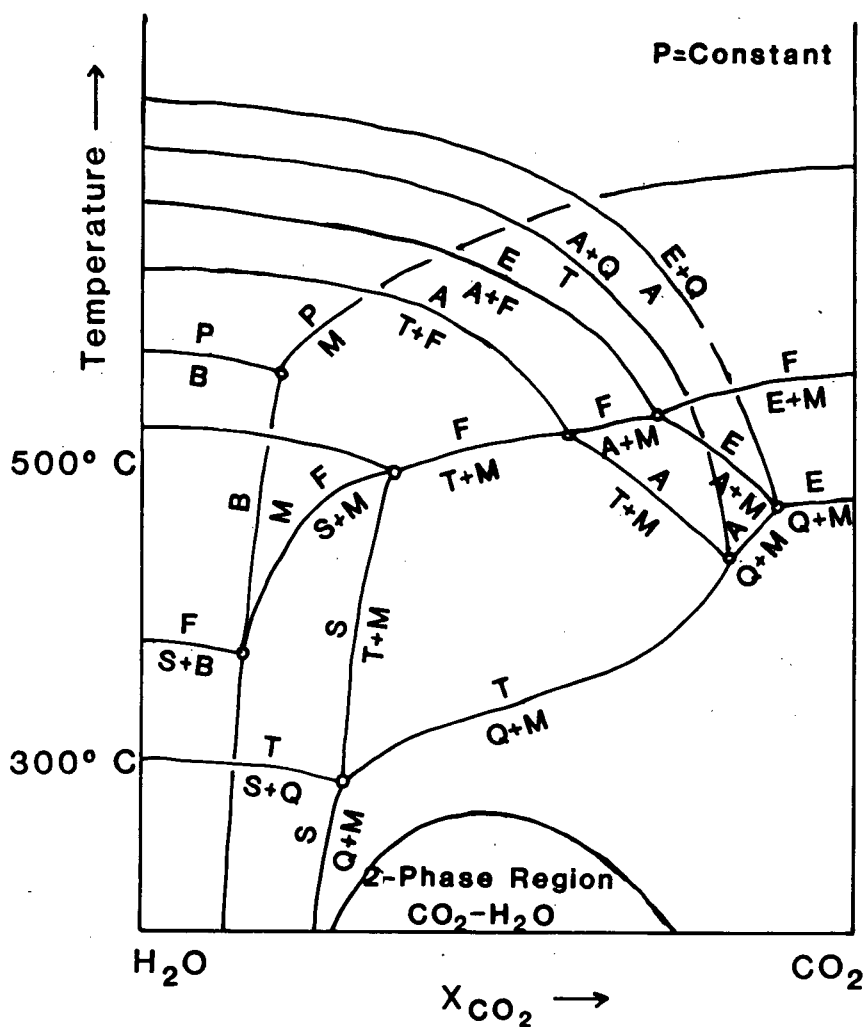
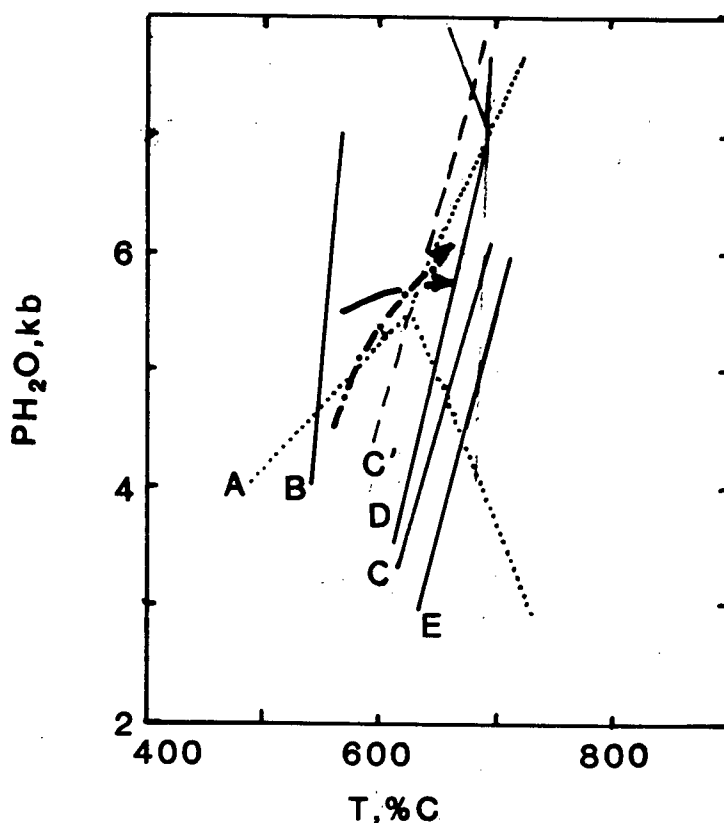


Figure 3.2 Schematic T- $X(\text{CO}_2)$ diagram for the system $\text{MgO-SiO}_2\text{-H}_2\text{O-CO}_2$ at elevated pressures and temperatures. Adapted from Johannes (1969).



- ↗ Pressure-Temperature gradient assuming
 / stable formation of andalusite
 ↗ Pressure-Temperature gradient assuming
 / metastable formation of andalusite in
 kyanite field (Hollister 1969b)

Figure 3.3 Pressure-temperature conditions in the pelitic assemblages, adapted from Pigage (1976).
 A Al_2SiO_5 System (Holdaway 1971)
 B Chlorite + Muscovite = Staurolite + Biotite + Quartz + vapour (Hoschek 1969)
 C Staurolite + Muscovite + Quartz = Al-silicate + Biotite + vapour (Hoschek 1969)
 C' Minimum temperature equilibrium position of curve C based on field evidence
 D Fe-staurolite + Quartz = Almandine + Sillimanite + Water (Pigage and Greenwood 1982)
 E Muscovite + Quartz = Sanidine + Sillimanite + Water (Chatterjee and Johannes 1974).

temperature gradient with little change in pressure associated with intrusion of diorite at depths of 17 to 21 km (Hollister 1969b). Subsequent studies have shown that Hollister's interpretation is unlikely. Bartholomew (1979) estimated pressure of regional metamorphism to be up to 3 kb above the alumino-silicate triple point, and noted that 14 km of burial would be required to produce the difference between contact and regional metamorphic conditions. He calculated that the Spuzzum batholith must have been emplaced at depths less than 14 km, and that a depth of burial of 27 ± 2 km (corresponding to a pressure of 7.6 ± 0.5 kb) must have been reached during regional metamorphism. Since andalusite formed before the most intense period of deformation, the time and pressure difference implied by stable formation is quite reasonable (Bartholomew 1979).

Regional Metamorphism

Pelites of the Cogburn Creek Group belong to the greenschist facies of regional metamorphism, grading from the chlorite subfacies in the west on the shore of Harrison Lake (outside the map area) to the biotite subfacies. Temperature conditions range between 300°C and 450°C. Lowes (1972) recognised staurolite grade rocks in upper Three Mile Creek. An AFM diagram representing the metamorphic mineral assemblage found in the Cogburn Creek Group pelite is in Figure 3.4.

Mineralogy in the greenschist suggests that the present metamorphic grade is upper greenschist facies to kyanite zone of amphibolite facies. An ACF-AKF diagram of the mineral

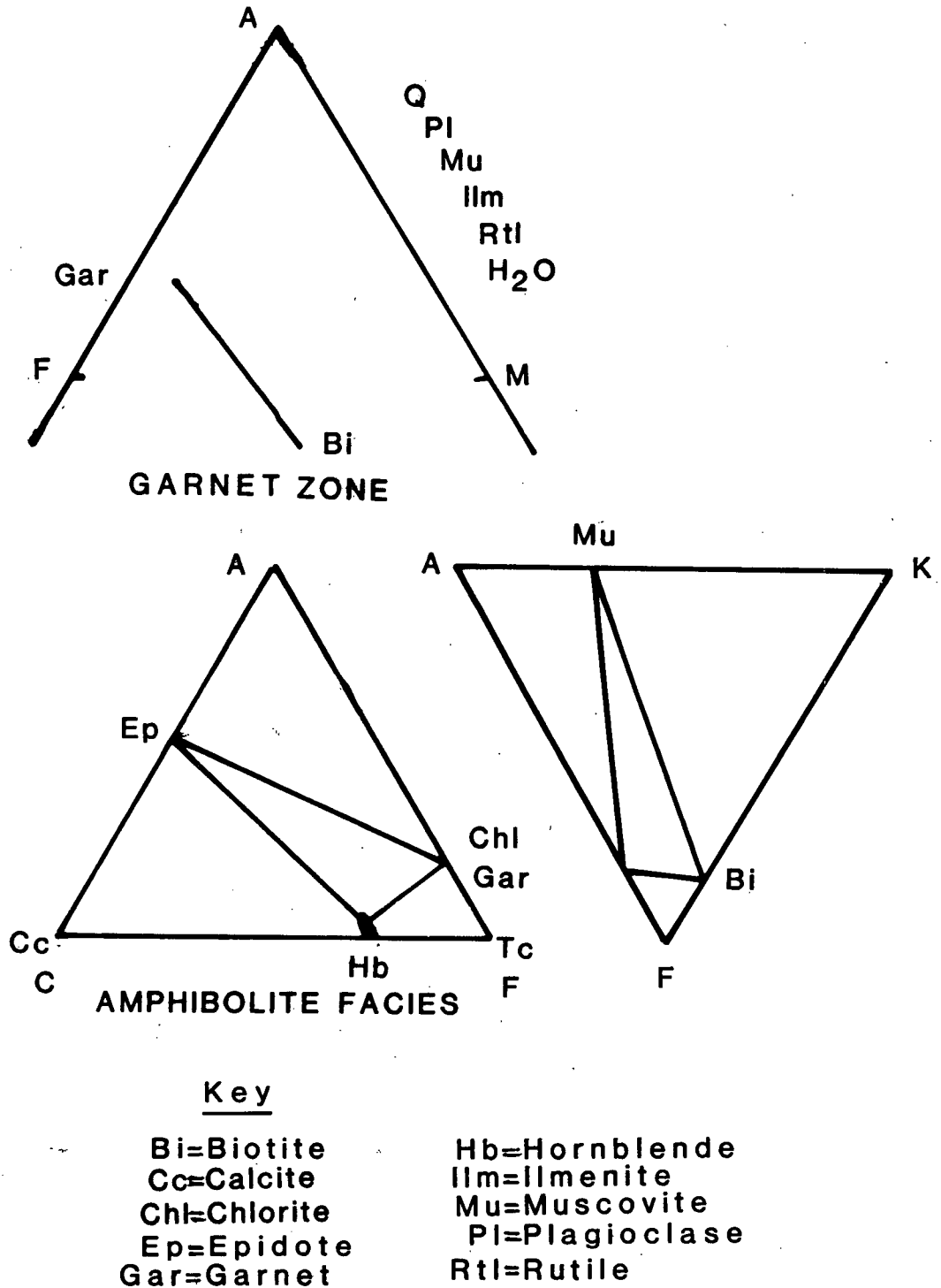


Figure 3.4 AFM projection of metamorphic mineral assemblages found in pelites from the garnet-staurolite zone, and ACF-AKF projection of assemblages in greenschist, from the Cogburn Creek Group.

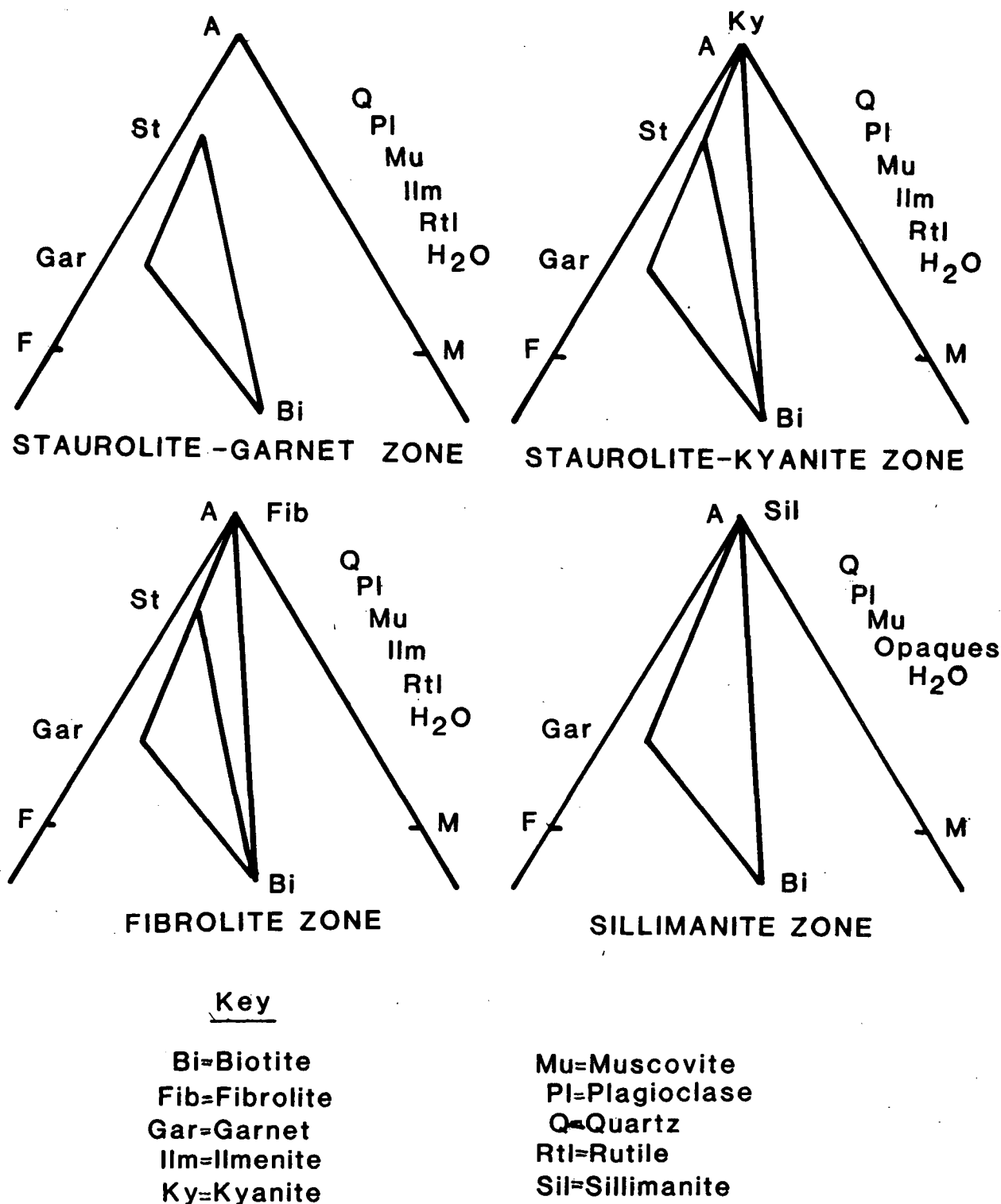


Figure 3.5 AFM projection of metamorphic mineral assemblages found in pelite from the garnet-stauroolite, stauroolite-kyanite, fibrolite, and sillimanite zones, from the Settler Schist.

assemblage found in the rocks is in Figure 3.4. The temperature of metamorphism must have been between 300 and 525°C, probably in the higher part of the range. Sampling was not detailed enough to enable recognition of discontinuities in metamorphic grade.

Mineral assemblages found in each of the metamorphic zones in the Settler Schist around Cogburn Creek are plotted on AFM diagrams in Figure 3.5. Pigage (1973) did regression analysis on pelitic mineral assemblages from the Settler Schist to provide information on possible reactions based on mineral compositions. He found several reactions with too many co-existing phases, resulting from disequilibrium or a univariant reaction relation. Co-existing kyanite - staurolite - garnet - biotite - muscovite - quartz is univariant on the AFM projection. This assemblage is found in a 3 km wide zone in Gordon Creek (Pigage 1973), and is recognised in Cogburn Creek (for example SS65, SS202).

Bartholomew (1979) found that two reactions were involved in the replacement of andalusite. Some took place via direct polymorphic transformation to kyanite or sillimanite. Pseudomorphs containing staurolite imply a replacement reaction of the type:

andalusite + biotite + H₂O = staurolite + muscovite + quartz.

Regression analyses by Pigage (1973) suggest two sillimanite - forming reactions of the form:

1) staurolite + muscovite + quartz + rutile = sillimanite +
biotite + ilmenite + H₂O

2) garnet + muscovite + rutile = sillimanite + quartz + biotite
+ ilmenite

Since there are 8 phases in each reaction and the minerals represent 8 components, these reactions must have been continuous rather than discontinuous (Bartholomew 1979). All the phases co-exist in the sillimanite zone in Cogburn Creek. Bartholomew (1979) interprets the fibrolite and sillimanite isograds as representing equilibrium and overstepped kyanite-sillimanite transitions respectively.

Estimates of metamorphic pressure and temperature for pelitic rocks in the Settler Schist were obtained by Pigage (1973, 1976) and Bartholomew (1979) by means of mutual intersection of several calculated equilibria (Figure 3.6). The accuracy of the estimate is based on the assumption of chemical equilibrium, accuracy and precision of microprobe analyses, validity of solid-solution models, and the quality of thermodynamic data (Pigage 1976). Pigage notes that the presence of ubiquitous staurolite in the lowest grade rocks in the Settler Schist defines a minimum temperature for metamorphism of approximately 540°C. He concludes that regional metamorphism of the Settler Schist took place under conditions between 550 and 700°C, and 6 to 8 kbar. Bartholomew (1979) estimated conditions in the vicinity of the fibrolite (fine grained sillimanite) isograd to have been 7.6 ± 0.5 kb and $705 \pm 45^\circ\text{C}$, with an activity of water between 0.81 and 0.86 and $\log f(\text{O}_2)$ between -18.1 and -17.3. He was not able to determine upper limits on conditions in the pelitic rocks of the highest,

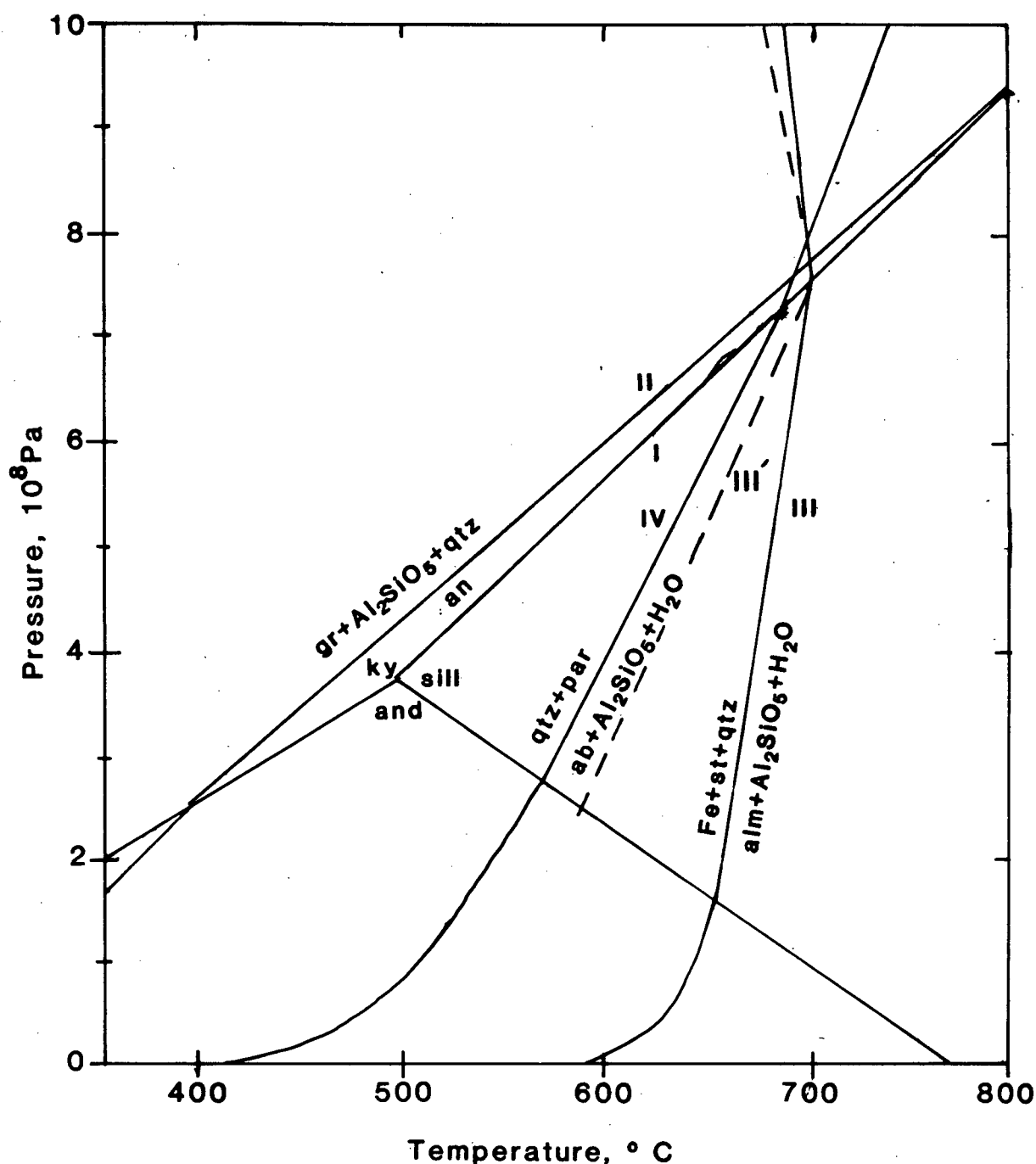


Figure 3.6 Equilibria calculated for P_2 at $a(\text{H}_2\text{O})=0.81$, plus the aluminosilicate equilibria, adapted from Bartholomew (1979). Intersections used to calculate metamorphic pressure and temperature conditions in the Settler Schist. Line III' is scaled off from Pigage and Greenwood (1982), a recent recalculation of the equilibrium of III.

coarse sillimanite grade.

Recent recalculation of the equation: staurolite + quartz = almandine + Al_2SiO_5 + H_2O (Pigage and Greenwood 1982), narrows down the stability field for staurolite + sillimanite, but does not significantly alter Bartholomew's (1979) estimate of metamorphic conditions (Figure 3.6).

Metamorphic conditions in the correlative Chiwaukum Schist (Lowes 1972) are similar. Getsinger (1978) found chiasolitic andalusite predating kyanite and sillimanite, in Chiwaukum Schist on Nason Ridge, Stevens Pass. Plummer (1969, 1980) had found the same mineral assemblages and textures but misinterpreted the age relationships of the alumino-silicates (Evans and Berti 1985). Getsinger (1978) was unable to map clear isograds in the Chiwaukum Schist, because of overlap in assemblages. In the Stevens Pass area Berti (pers. comm. 1983) calculated a temperature of 550°C from garnet-biotite pairs and a pressure of 4 to 6 kbar. At Wenatchee Ridge, McLaughlin (pers. comm. 1985) estimates 550°C and 6 to 8 kbar using garnet-plagioclase geobarometry, suggesting a pressure gradient associated with crustal thickening after intrusion of the Mount Stuart batholith (Evans and Berti 1985).

Isograds have been drawn for the Cogburn Creek area (Figure 3.7), based on mineral assemblages. The complex relationships between zones suggests post-metamorphic deformation, possibly related to the diorite bodies. In contrast to the relationships found by Bartholomew (1979) around Gordon Creek, the zone containing fibrolite only (no coarse sillimanite) appears to be

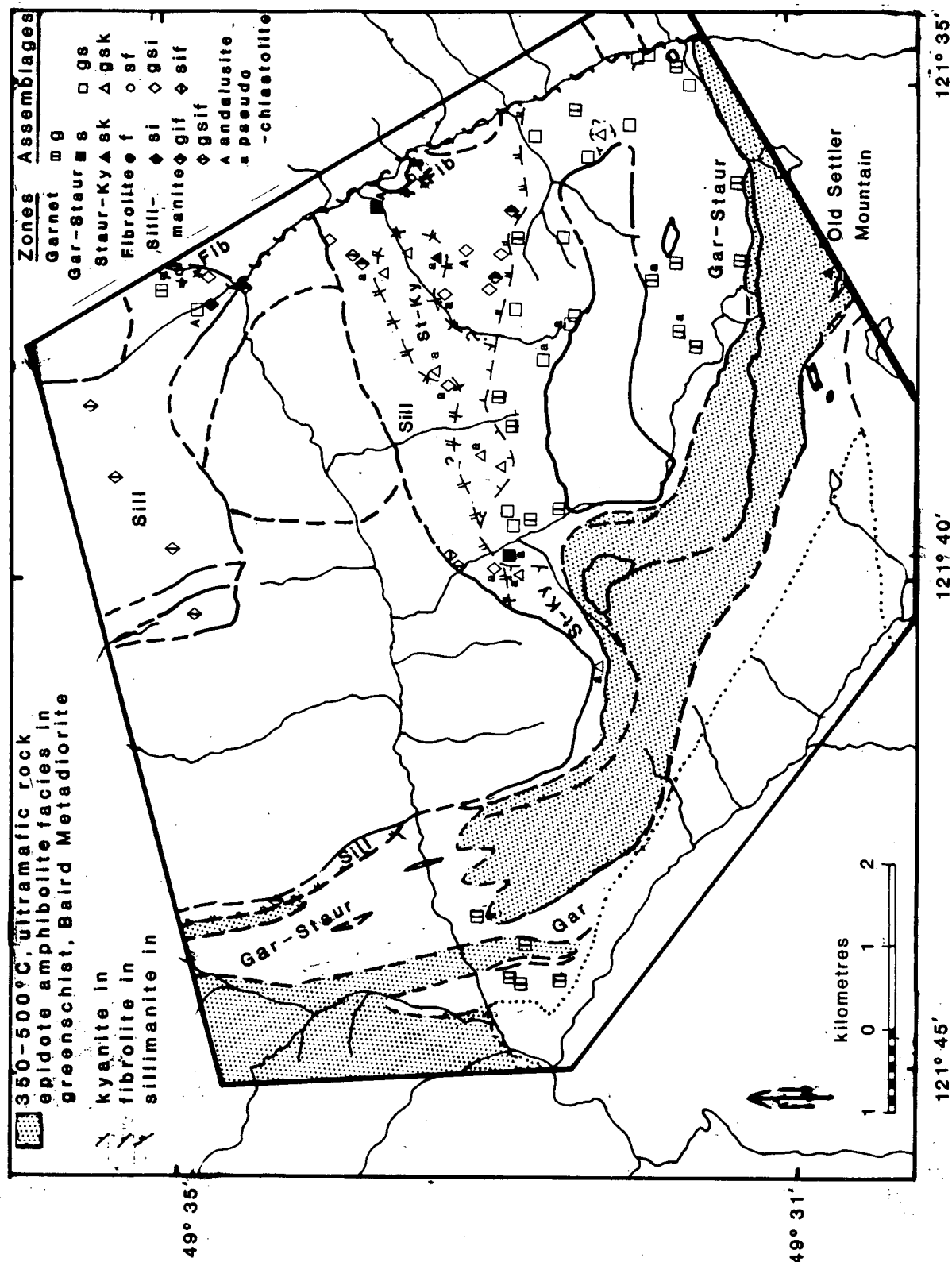


Figure 3.7 Map of metamorphic mineral assemblages and isograds for the Cogburn Creek area. See Figure 2.1 for key to rock units. Abbreviations of mineral names are: f=fibrolite, g=garnet, k=kyanite, i=sillimanite, s=staurolite.

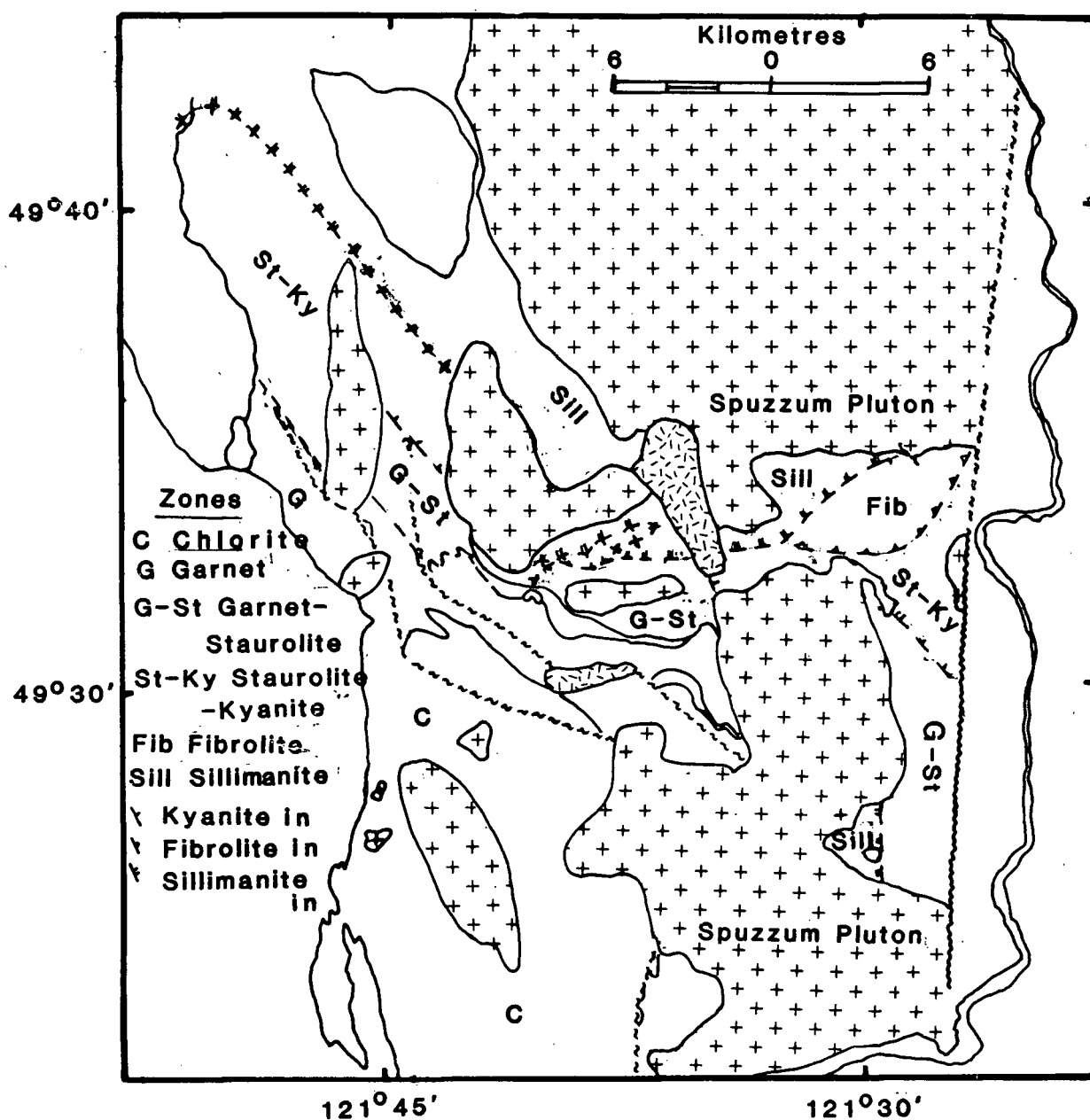


Figure 3.8 Regional isograds, modified from Bartholomew (1979), Lowes (1972), Pigage (1973), and Reamsbottom (1971, 1974). See Figure 1.2 for key to rock units.

directly related to contact metamorphism by the Cogburn Granodiorite. The presence of numerous small intrusive bodies throughout the region indicates large volumes of magma at fairly shallow depths (Pigage 1973), which could have supplied some of the heat for the regional metamorphism. For comparison with surrounding areas a regional synthesis of isograds is given in Figure 3.8. Information has been taken from Pigage (1973), Bartholomew (1979), Reamsbottom (1974) and Lowes (1972). Grade of regional metamorphism generally increases northeastward, toward the large northern pluton of Spuzzum batholith. However, the isograds are not parallel to the pluton margins, and in places are truncated by the intrusives. Evans and Berti (1985) account for regional metamorphism of the Chiwaukum Schist as relaxation of isotherms related to the Mount Stuart batholith, during an episode of crustal thickening soon after intrusion. They propose that after dynamic contact metamorphism heat flowed from the batholith into the surrounding rocks, levelling out to about 600 °C. This corresponds to a continental-crust geothermal gradient of 30 °C/km and pressure of 6 kbar. Thus they consider that the regional metamorphism of the Mount Stuart batholith and nearby contact-metamorphosed rocks was retrograde, and that of the Chiwaukum Schist distant from the batholith was prograde. Since the Chiwaukum Schist and the Settler Schist are correlative and probably formed a continuous belt at the time of intrusion and metamorphism, the same interpretation can be applied to the area east of Harrison Lake. The Spuzzum batholith and Scuzzy Diorite to the north form a much larger

body than the Mount Stuart batholith (Figure 2.2), so that the heat flow from it would have been greater. This would account for the higher-grade metamorphic assemblages seen in the Settler Schist than in the Chiwaukum Schist. The metamorphism of the Cogburn Creek Group rocks would be prograde. Beck et al. (1981) recognised a 30° tilt down to the southeast from paleomagnetic evidence from the Mount Stuart batholith. If this were applied to the Spuzzum batholith, it could also explain the northeastward increase of metamorphic grade in the surrounding schist. Recent paleomagnetic results of Irving et al. (1985) on the Spuzzum Diorite could be interpreted as indicating 28° tilt down to the southeast, rather than lateral displacement (they consider that their data are insufficient to prove either alternative).

4. Structure

Megascopic structure in the Cogburn creek area is expressed in the steep imbricate zone and deflections around intrusive bodies. Three outcrop-scale phases of folding have been recognised, consistent with observations of Lowes (1972) and Bartholomew (1979). The earliest deformation (f_1) is recognised only from inclusion trails in porphyroblastic garnet and re-orientation of biotite porphyroblasts (HL16). Strong mica foliation in both the Cogburn Creek Group and Settler Schist is assigned to f_2 , and is parallel to the axial planes of isoclinal folds up to 1 m in amplitude. Compositional layering, where present, is generally parallel or subparallel to the f_2 foliation (Figure 4.1, 4.2). Pigage (1973) considered that compositional layering in Settler Schist in the Gordon Creek area was original graded bedding and was able to determine a younging direction. However in the area I have mapped it may also be metamorphically transposed layering. Outcrops showing "bedding" were sparse around Cogburn Creek, and graded bedding or other facing criteria were not seen, making it impossible to specify a younging direction.

Fold style of minor folds associated with f_2 is isoclinal to tight, rounded to chevron. On the map scale foliation orientation parallels the trend of the map units and the margins of plutons. In the Settler Schist f_2 foliation dips steeply northeast (Figure 4.2), except for one small area in the southeast corner of the map area, where it dips steeply southwest. This may represent a fold hinge.

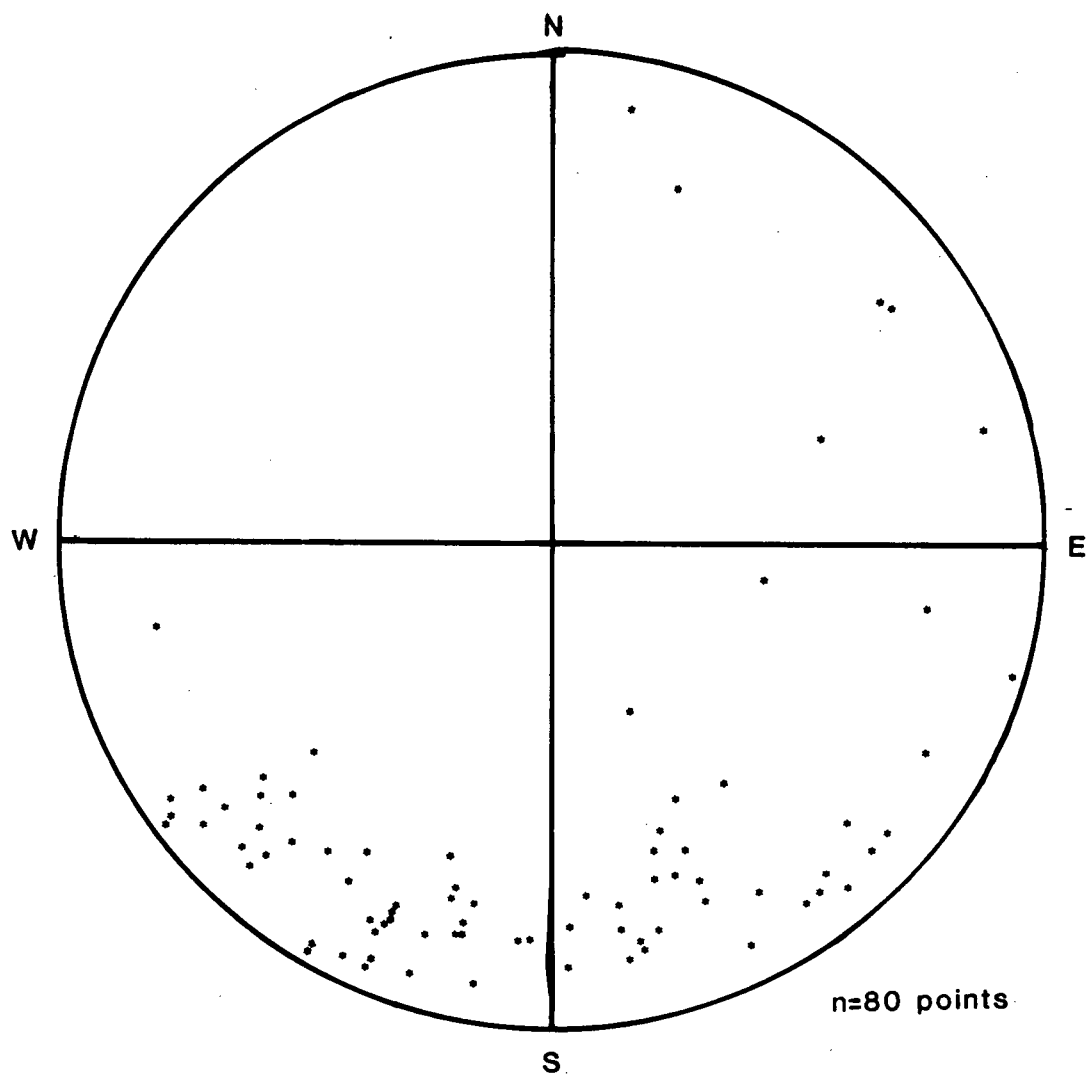


Figure 4.1 Equal area projection of poles to compositional layering in the Settler Schist.

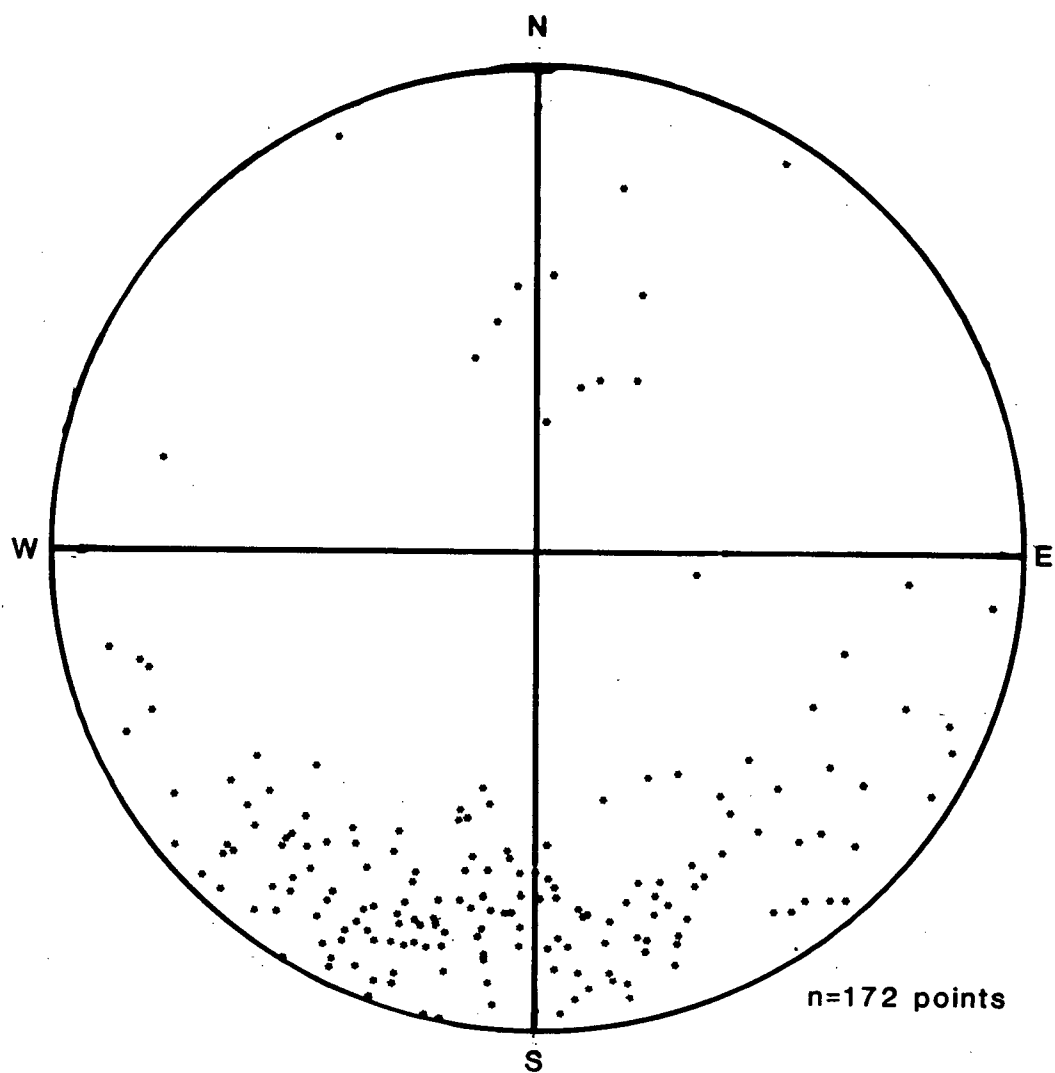


Figure 4.2 Equal area projection of poles to f_2 foliation for the Settler Schist south of Cogburn Creek.

The f_2 foliation has been rotated 40 to 50° westward on the north ridge (Figure 4.3). It may have been rotated by intrusion of the Spuzzum batholith, Hut Creek body.

In the Cogburn Creek Group rocks around Three Mile Creek, bedding in chert and foliation in greenschist and pelite is parallel to the melange zone. Dips are steep and to the northeast (Figure 4.4). Whereas the greenschist shows strong foliation, layering in the chert is inferred to be bedding that has survived because of resistance of competent quartzose layers to transposition.

The latest folding is a result of both f_3 regional folding and intrusive activity. Folds of this generation are characteristically broad warps and kinks. Close to pluton margins a penetrative foliation has developed with f_3 , producing mineral and cleavage-intersection lineations. The f_3 foliation is typically at an angle of 25° to 40° to the f_2 foliation. Orientations of fold axes to both f_2 and f_3 folds are scattered, probably due to ductility contrasts causing local variation (Bartholomew 1979).

The melange zone containing imbricated tabular bodies of ultramafic rocks and Baird Metadiorite curves sinuously across the study area from southeast to northwest (Figure 2.1). It appears to have been pushed aside by later intrusion of Spuzzum batholith. It could also have bent around an already emplaced resistant core of diorite. Fine stringers of diorite intruding the ultramafic rocks in the thrust zone, on the ridge south of Cogburn Creek appear to indicate the former interpretation.

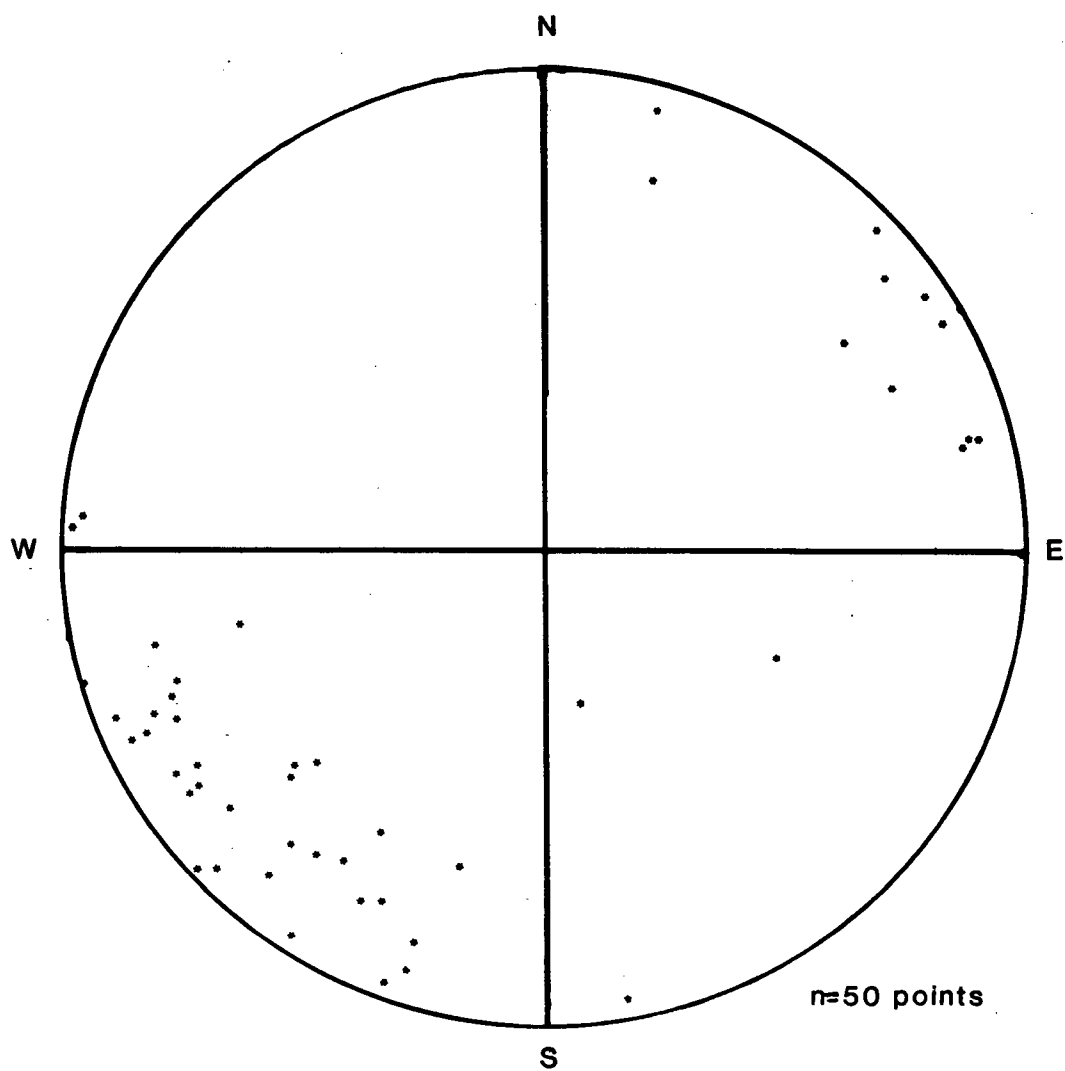


Figure 4.3 Equal area projection of poles to f_2 foliation in Settler Schist north of Cogburn Creek.

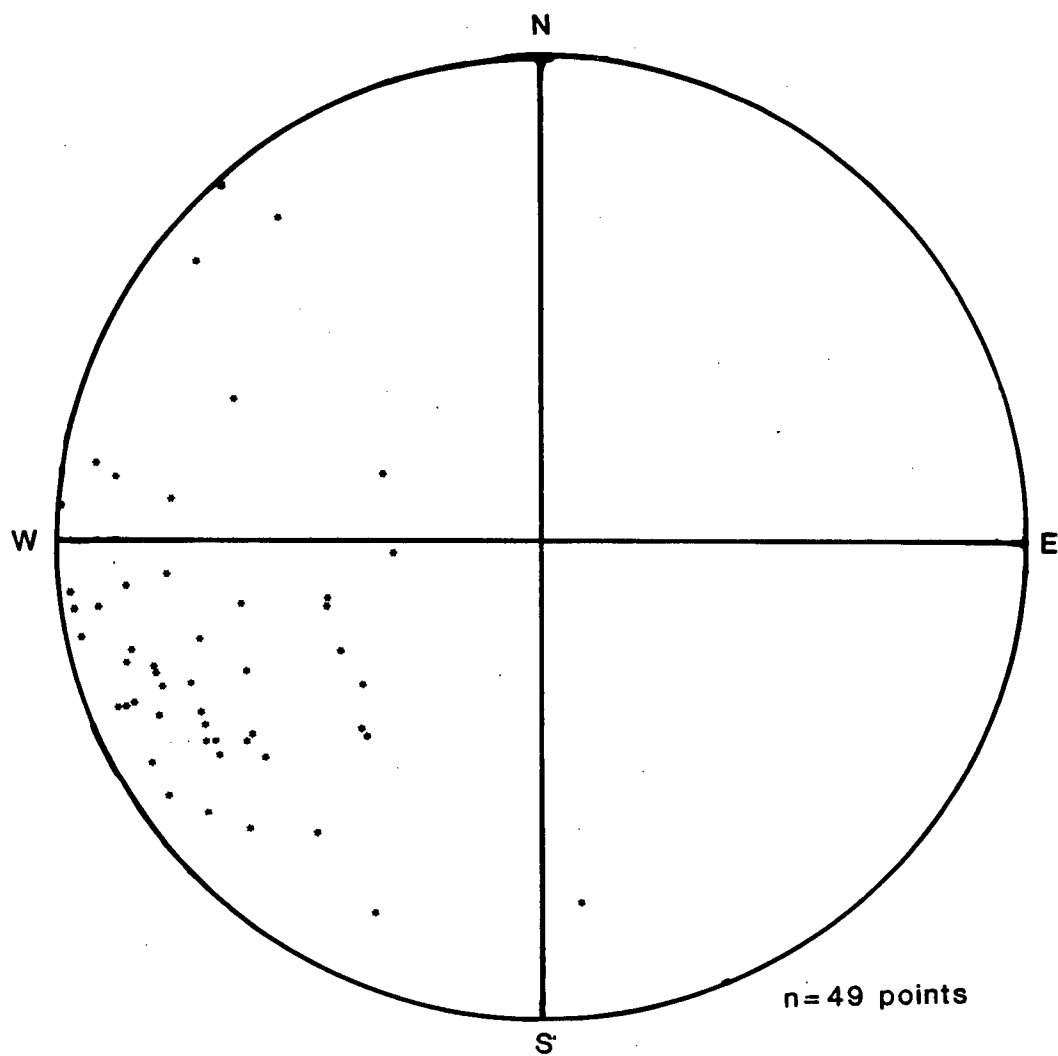


Figure 4.4 Equal area projection of poles to f_2 foliation in Cogburn Creek Group, for the area north of 1 km south of Cogburn Creek.

In contrast to the Shuksan thrust farther south, the imbricate zone here was active before the culmination of regional metamorphism. This does not preclude correlation of the melange zone with the Shuksan thrust, as regional metamorphism of the Shuksan Suite was earlier than metamorphism in the Cogburn Creek area (Brown et al. 1982).

Metamorphic foliation is found in places in the Spuzzum batholith. Poles to foliation and mineral lineations for the intrusions have been plotted in Figure 4.5. These appear to be randomly distributed. The main period of diorite intrusion postdates f_2 deformation and predates the culmination of regional metamorphism.

Settler Schist is structurally above the imbricate zone, which forms the northeast boundary of the Cogburn Creek Group. Lowes (1972) mapped in detail the structure of the imbricate zone around Old Settler Mountain. The upper contact of the zone with the Settler Schist is a steep (75°), north-dipping surface. The north face of Old Settler Mountain is a dip slope of Baird Metadiorite parallel to this fault, exposed by erosion of the narrow band of ultramafic rocks between that unit and the Settler Schist. Foliation in the Baird Metadiorite is generally parallel to this surface, which can be followed across the topography in both directions. The lower contact with the Cogburn Creek Group is as sharp as the upper contact, where it is exposed west of Old Settler Mountain (Plate 4.1). However, just south of the gorge in Cogburn Creek the 2 km wide zone of metadiorite and ultramafic rocks becomes no more than 100 m

wide, giving way to Cogburn Creek Group chert. The nature of the contact is unknown, as steep terrain precluded mapping. Macroscopic structure in the Cogburn Creek Group rocks in northern part of Three Mile Creek becomes complicated, but mapping was not continued far enough to unravel it. A series of minor north-easterly oriented faults may have disrupted the stratigraphy.

In spite of recent alluvial cover the Cogburn Fault was recognised by Bartholomew (1979) in the south branch of Cogburn Creek. He noted truncated geologic contacts (Figure 2.1) and contrasts in rock types, metamorphic grade, and structure across the valley. Alignment of the tributary stream to the north with the main valley of the south branch, and the occurrence of fault breccia on the ridge at its head, strengthen the evidence for the fault.

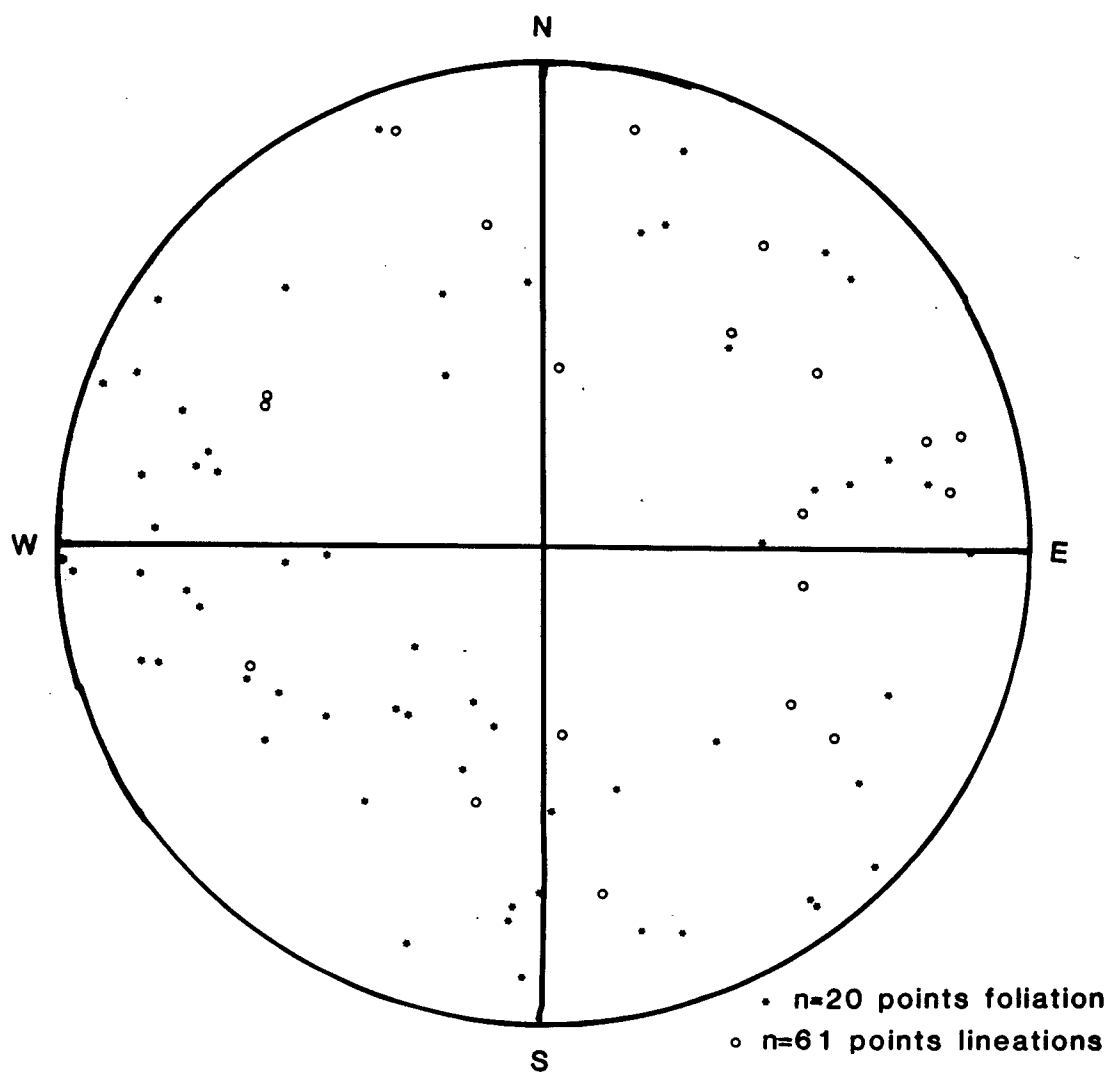


Figure 4.5 Equal area projection of poles to foliation and mineral lineations in Spuzzum batholith.

5. Geochronometry

Dating of rock units in the study area was carried out using Rb-Sr, K-Ar and U-Pb techniques. Analytical techniques are described in Appendix A; analytical data, isotope ratios and calculated dates are given in Appendix B; sample descriptions and locations in Appendix C, and locations plotted in Figure D-2.

Eighty-six whole rocks and mineral separates from 40 samples of Spuzzum batholith, Settler Schist, Cogburn Creek Group schist, Breakenridge Formation gneiss, Baird Metadiorite and several pre- and syn-tectonic intrusive bodies were analysed for Rb-Sr and Sr isotopic composition. The data have been used to calculate isochron dates for the different rock units. The isochron plots are shown in Figures 5.2 a to h. Five hornblende separates from Spuzzum batholith were dated by K-Ar. Data are plotted in Figure 5.4a and b. Zircons for U-Pb dating were separated from Baird Metadiorite, Breakenridge Formation gneiss, Settler Schist, Spuzzum batholith (Hut Creek and Settler Creek bodies), and one pre-metamorphic intrusive rock. The concordia diagram is Figure 5.3. All figures are at the end of the Chapter.

5.1 Previous Geochronometry

Although no one has undertaken an intensive dating study in the region between Harrison Lake and the Fraser Valley, a number of analyses have been carried out by previous workers. Most of these have been on intrusive rocks, particularly the Spuzzum

Table 5.1 Table of dates and age estimates from previous studies
between Harrison Lake and Fraser River

Reference	Rock	Date Ma			Method
<u>Baird Metadiorite (Unit 1)¹ and correlatives</u>					
Lowes (1972)		possibly Precambrian			correlation with Yellow Aster Complex
Mattinson (1972)	Yellow Aster				
	pyroxene gneiss	711	912	1452 ± 20	U-Pb zircon ^{2 3}
	pegmatite gneiss	64	75	427 ? 75	U-Pb zircon
	quartz diorite	368	375	411 ? 15	U-Pb zircon
	orthogneiss				
	Swakane gneiss				
	biotite gneiss	433	628	1419 ± 100	U-Pb zircon
	pegmatite gneiss	69			U-Pb zircon
<u>Cogburn Creek Group (Unit 3) and correlatives</u>					
Lowes (1972)		Permian-Pennsylv- anian			correlation with Chilliwack Group
Reamsbottom (1971)		L. Cret. and/or older			correlation with Chilliwack Group
Monger (1970)	Chilliwack Group	Permian-Pennsylvanian			fossils
Armstrong unpub.	Chilliwack Group	191 ± 16 @ 0.70510			Rb-Sr WR ^a n=14
Armstrong unpub.	Bridge River Group				
	high grade schists	104 ± 25 @ 0.70555			Rb-Sr WR n=14
	low grade schists	256 ± 35 @ 0.70394			Rb-Sr WR n=28
<u>Settler Schist (Unit 4) and correlatives</u>					
Pigage (1973)	Settler Schist	early-mid Paleozoic			correlation with Shuksan Suite
Bartholomew (1979)	Settler Schist	214 ± 32			Rb-Sr WR n=7
Mattinson (1972)	Skagit gneiss				
	biotite gneiss	98	112	428 ± 10	U-Pb zircon
	gneissic qtz di	66	67	79 ± 10	U-Pb zircon
	pegmatite gneiss	90			U-Pb zircon
		57			U-Pb zircon

Armstrong unpub.	Darrington Phyllite	132 ± 8 @ 0.70556	Rb-Sr WR n=22
	Shuksan blueschist	172 ± 18 @ 0.70387	Rb-Sr WR n=15
	and greenschist		
Brown et al.	Shuksan amphib.	148 ± 5	K-Ar Hb
(1982)	barroisite schist	164 ± 6	K-Ar Hb
	blueschists	128 ± 5	Rb-Sr Mu
		129 ± 5	K-Ar Mu

Spuzzum batholith (Unit 5) and correlatives

McTaggart and	tonalite	77 ± 4	K-Ar Bi
Thompson (1967)(6)	tonalite	77 ± 4	K-Ar Hb
Richards (1971)	foliated	80 ± 4	K-Ar Bi
(1)			
	diorite	82 ± 4	K-Ar Hb
	fol. diorite	84 ± 4	K-Ar Bi
	fol. diorite	105 ± 3	K-Ar Bi
Wanless (1973)(4)	quartz diorite	76 ± 4	K-Ar Bi, Hb
McLeod (1975)	tonalite	80.7 ± 2.5	K-Ar Bi
(5)	tonalite	86.6 ± 2.8	K-Ar Hb
	diorite	91.5 ± 2.8	K-Ar Hb
	diorite	91.2 ± 3.1	K-Ar WR
	hornblendite	96.4 ± 4	K-Ar Hb
	hornblendite	121.6 ± 4	K-Ar Hb
	fels. hbite	106 ± 4	K-Ar Hb
	hornblendite	112 ± 4	K-Ar Hb
Richards and	diorite	91.0 ± 2.8	K-Ar Hb
McTaggart (1976) (1)			
Bartholomew (1979) unit 3b		77.3 ± 2.6	K-Ar Hb
(2)			
	unit 3e	94.4 ± 3.2	K-Ar Hb
Armstrong unpub.	bi hb diorite	94.9 ± 7	K-Ar hb
(3)			
		101 ± 3	K-Ar Bi
	bi hb diorite	91.3 ± 2.2 @ 0.7038	Rb-Sr WR-
			Pl-Hb-Bi

Armstrong and bi hb diorite 112 122 331 U-Pb zircon
 Ryan unpub. (3)

Younger intrusives (Unit 6)

Bartholomew (1979) aplite	34.4 ± 1.4 @ 0.7041	Rb-Sr WR
(2) quartz diorite	30.7 ± 0.6 @ 0.7041	Rb-Sr Bi-WR
granodiorite	33.6 ± 1.1	K-Ar Bi
Woodsworth and granite(GEM-1)	35 ± 0.7	Rb-Sr WR
Armstrong unpub. (3)		

¹ Unit numbers are from this study

² All data recalculated with IUGS convention decay constants (Steiger and Jäger 1969), except U-Pb zircon from Mattinson (1972).

³ Zircon dates are reported as $^{206}\text{Pb}/^{238}\text{U}$, $^{207}\text{Pb}/^{235}\text{U}$, $^{207}\text{Pb}/^{206}\text{Pb}$

⁴ Initial $^{87}\text{Sr}/^{86}\text{Sr}$ ratios are reported with Rb-Sr isochron dates
 n= number of samples analysed for reported isochron date.

WR=whole rock, Hb=hornblende, Bi=biotite, Pl=plagioclase
 Numbers in brackets are references for symbols on Figure 5.1.

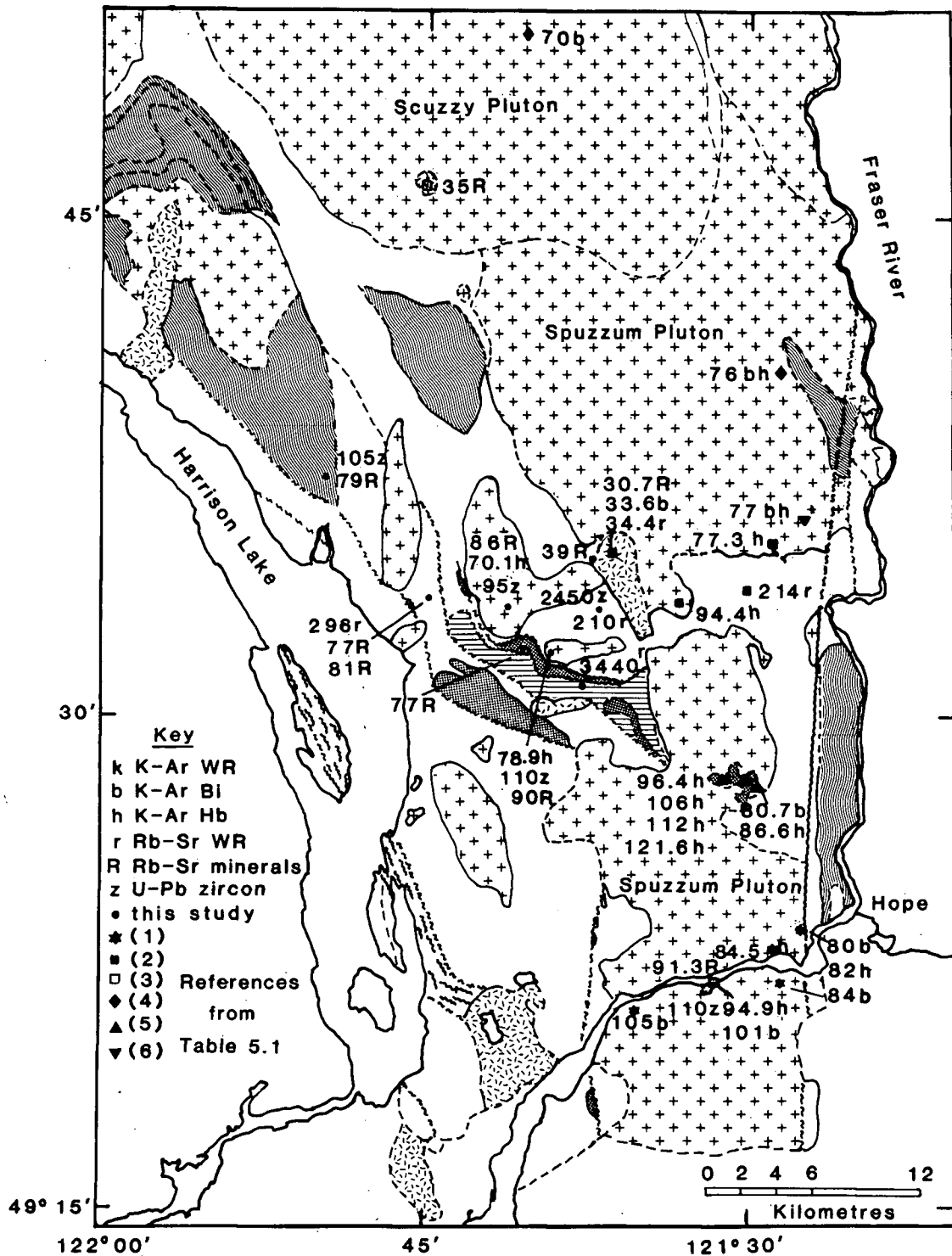


Figure 5.1 Map showing geochronometry of the Harrison Lake - Fraser River region
See Figure 1.2 for key to map units. Symbols indicate references listed in Table 5.1.

batholith. In the North Cascade Mountains, Washington, Mattinson (1972) dated by U-Pb zircons from units that are believed to be correlatives of rocks in the present study area. His results are tabulated in Table 5.1, along with other dating in the Harrison Lake - Fraser River region. The locations of these previously dated rocks have been plotted on a map (Figure 5.1).

5.2 Unit 1. Baird Metadiorite

This unit has been correlated previously with the Yellow Aster Complex of the North Cascades, Washington (Lowe 1972), because of its appearance, and structural relationships within the Shuksan thrust imbricate zone. Mattinson (1972) dated zircons from pyroxene gneiss of the Yellow Aster Complex from the North Cascades as 1452 to 2000 Ma, and from the younger orthogneiss as 430 Ma.

The Rb-Sr and U-Pb dating results reported here have large errors, but suggest a Precambrian age for the rocks. Figure 5.2a shows that $^{87}\text{Rb}/^{86}\text{Sr}$ ratios of the samples are extremely small, all are < 0.02 , and the differences hardly significant. The resulting isochron age has a large error (3.4 ± 2.4 Ga), because it is a least squares fit of a tight cluster of points. The cluster of points suggests that the strontium isotopic ratios may have been homogenised toward a value of approximately 0.7043 by Cretaceous metamorphism, from an initially lower value that would have defined a line with even greater slope. If this is the case, the calculated initial value of 0.7038 is only an

upper limit for the true initial ratio. The low rubidium values are consistent with a primitive ocean crust protolith.

Mattinson (1972) noted that Rb-Sr analyses of the older orthogneiss in the Yellow Aster Complex had failed to yield meaningful ages because although Sr concentrations are normal, the rocks are so depleted in Rb that Rb-Sr whole rock dating is precluded (J.C. Engels, 1968, pers. comm. to Mattinson). The same comment holds for the Yellow Aster-type rocks of the Baird Metadiorite of this study.

A highly discordant zircon U-Pb date (Table B-6) also suggests a pre-Mesozoic, perhaps Precambrian, age. Only one fraction was analysed (Table C-2), due to low zircon yield, and the analysis could not be repeated although it was of poor quality. The $^{207}\text{Pb}/^{206}\text{Pb}$ dates calculated for the natural and spiked runs are 704 ± 180 Ma and 1653 ± 175 Ma respectively, due to significant differences in the measured $^{207}\text{Pb}/^{206}\text{Pb}$ ratios. The averaged $^{207}\text{Pb}/^{206}\text{Pb}$ date is 1251 ± 180 Ma. When plotted on concordia (Figure 5.3) the averaged value lies away from concordia but close to the line defined by points from analyses of the Settler Schist. The single analysis for the metadiorite restricts the conclusions: either the rock is old and the U-Pb clock has been reset by amphibolite-facies metamorphism during the Mesozoic, or old lead has been incorporated into Mesozoic zircons. The first interpretation, which is reinforced by the Rb/Sr analyses, is compatible with Mattinson's (1972) interpretation for rocks of the Yellow Aster Complex in the Cascade Mountains of Washington, namely intrusion around 1400 to

1600 Ma followed by metamorphism at 415 Ma and 90 Ma. His concordia for Yellow Aster Complex is shown in Figure 5.5 for comparison with Baird Metadiorite.

5.3 Unit 3. Cogburn Creek Group

Rb-Sr data from this group of rocks clearly define two events, the earlier one is the approximate time of deposition and the later is the Cretaceous metamorphism. The calculated isochron date when biotite and chert analyses are not included is 296 ± 58 Ma (Table B-2, Figure 5.2b), which could represent either a late Paleozoic age for the sequence of chert, volcanic rocks and pelites, or a reset caused by Mesozoic metamorphism of even older rocks. The first alternative is favoured here, but no fossils have been found to define the stratigraphic age. A Rb-Sr whole rock isochron date for greenschist alone, 438 ± 68 Ma ($n=2$), is probably not sensible geologically, as no similar dates have been found in the region. Biotite dates from chert and greenschist are 81 ± 5 Ma and 77 ± 1.6 Ma respectively. These dates represent the waning stages of the Cretaceous metamorphic episode, and are similar to biotite dates from Settler Schist and Spuzzum batholith (see discussion below).

On the Rb-Sr isochron diagram (Figure 5.2b) the point representing chert (HL37a) whole rock has a higher $^{87}\text{Rb}/^{86}\text{Sr}$ and $^{87}\text{Sr}/^{86}\text{Sr}$ value than the other whole rocks. Similarly, the $^{87}\text{Sr}/^{86}\text{Sr}$ initial ratio, 0.7090, for the chert (HL37a)-Bi isochron is higher than those for other rock-biotite pairs. The date is, however, similar to other metamorphic dates. The

difference in $^{87}\text{Sr}/^{86}\text{Sr}$ may be due to incorporation of ^{87}Sr -rich seawater at the time the chert was deposited (Jäger 1979).

No zircons were dated from the chert and greenschist, although accessory zircon is present in sample HL37a.

5.4 Unit 4. Settler Schist

The Settler Schist is bounded by major faults and plutons, so stratigraphic relations with other units are unclear. On the basis of similarities in structural position with the Paleozoic (?) Shuksan Suite in the North Cascades, Pigage (1973) assigned an Early - Mid Paleozoic age to the Settler Schist. Reamsbottom (1971) suggested a late Paleozoic to Mesozoic age for similar schists in the Mount Breakenridge area north of this study area because granitoid clasts were found in conglomeratic horizons within the schists, and because there are no pre-Jurassic plutons in the area (see also Pigage 1973). Both these age estimates have been invalidated by subsequent studies in the region. Shuksan Suite blueschists have been dated as Mesozoic (Armstrong et al. 1982), and granite clasts have been found in Triassic rocks in the Bridge River area, indicating the presence of early Mesozoic plutons. Lithologically, the Settler Schist is like Chiwaukum Schist (Lowes 1972), which may be correlated with the Skagit Suite and is different from the Shuksan Suite. The Shuksan Suite contains blueschist and greenschist that are metamorphosed ocean floor (Dungan et al. 1981), and offshore sediments.

Bartholomew (1979) obtained an Rb-Sr isochron date from

Settler Schist in the Yale Creek area of 214 ± 32 Ma. He interpreted this as both the age of the source rock for the pre-metamorphic sediments and the time of their deposition because of the low initial $^{87}\text{Sr}/^{86}\text{Sr}$ ratio of 0.7043.

Eleven Rb-Sr whole rock analyses from this study combined with data from seven rocks from Bartholomew (1979) (all in Table B-1) produce an isochron age of 210 ± 27 Ma (Table B-2; Figure 5.2c and d). This reflects either Triassic - Jurassic deposition or partial to complete resetting by Mesozoic metamorphism of pre-Jurassic rocks. If it is the age of deposition, then it does not necessarily also represent the integrated age of the source rocks, as will be discussed later. The mineral isochron date from a biotite-bearing graphitic phyllite (SS82) indicates either a slightly later end to the metamorphism, at 66 ± 1.6 Ma, or a partial reset by the mid Tertiary Cogburn Granodiorite which crops out within a kilometre, on the east side of Cogburn Creek.

The youngest isochron drawn in Figure 5.2c and d is from a quartz-biotite-garnet schist (SS128) from near the contact with Cogburn Granodiorite. Bartholomew (1979) dated the granodiorite by Rb-Sr WR isochron, Rb-Sr Bi, and K-Ar Bi at 32 ± 4 Ma. The mineral isochron date for the schist SS128 of 39 ± 4 Ma is due to resetting by this young pluton. The initial $^{87}\text{Sr}/^{86}\text{Sr}$ ratio of 0.7066 for this schist sample has been pulled up from a value around 0.704 by re-equilibration of Sr between the biotite and feldspar components (Jäger 1979).

Zircon separated from two samples of Settler Schist is

small and subhedral, certainly detrital. They are unusual in that they contain small opaque (graphite ?) inclusions. This may indicate metamorphic overgrowths on the detrital cores, with inclusion of material from the sediments containing the zircons. The two samples yielded highly discordant U-Pb dates but similar $^{207}\text{Pb}/^{206}\text{Pb}$ ages, 1183 ± 12 Ma and 1279 ± 32 Ma (Table B-5). Plotted on concordia (Figure 5.3), the line joining the two points has a lower intercept of 211 ± 30 Ma, and an upper intercept of 2450 ± 230 Ma. The young lower intercept is consistent with the Rb-Sr isochron age for the schist. The old upper intercept indicates a Precambrian source for the zircons in these sediments. The age obtained is consistent with zircon ages obtained from schists and gneisses in the North Cascade Mountains of Washington by Mattinson (1972), as well as from the pyroxene gneisses of the Yellow Aster Complex. Zircons from the supracrustal Swakane Gneiss and Skagit Gneiss yielded highly discordant ages with $^{207}\text{Pb}/^{206}\text{Pb}$ ages in the range 1400 to 1650 Ma (Figure 5.5). The concordia for zircons from the two units (Mattinson 1972) is shown in Figure 5.5, for comparison with results from the Settler Schist. Mattinson considered those from the Swakane Gneiss to approximate stratigraphic age and those from the Skagit Gneiss to be detrital and derived from a Precambrian source. Thus the stratigraphic age for the Skagit Gneiss could be younger than Precambrian. Misch (1966) considered that the pre-metamorphic equivalent of much of the Skagit Gneiss was immature greywacke. The isotopic similarity between the Settler Schist and Skagit Gneiss is not surprising

since the Settler Schist is considered to be equivalent to the Chiwaukum Schist (Lowes 1972), which is part of the Skagit Metamorphic Suite defined by Misch (1966).

In summary, the zircon geochronometry suggests that the Settler Schist is at least in part derived from an old source. The Rb/Sr date of 210 ± 27 Ma does not reflect this old source; thus it represents only the approximate time of deposition of Settler Schist and, because of the low initial ratio, possibly the age of almost contemporaneous source rocks. From their lithologies and chemistry, Pigage (1973) and Bartholomew (1979) stated that the sediments forming the schist were eugeosynclinal and derived from a rising volcanic arc of approximately the same age as those sediments. However, there also must have been old basement exposed nearby to supply the old zircon and mature fine-grained sediments that now form the pelitic part of the Settler Schist. The time of deposition was most probably early Mesozoic, as indicated by the Rb-Sr whole rock isochron. Waning of the main Cretaceous metamorphic event is shown by the mineral (biotite) ages obtained from both a phyllite and a syn-tectonic felsic intrusive. The last intrusive event at 32 ± 4 Ma (Bartholomew 1979) reset biotite in the nearby schist.

5.5 Premetamorphic intrusive rocks

1) Zircon sample HL111, from a felsic body (Figure D-2, Table B-5), yielded U-Pb dates that are slightly discordant; the $^{207}\text{Pb}/^{206}\text{Pb}$ date is 376 ± 88 Ma. Because of the proximity of the sill to the Spuzzum batholith, Hut Creek body, and lack of

similar old dates from other intrusive rocks in the region the sill is probably Mesozoic. Sillimanite is intergrown with biotite and muscovite, indicating that the sill was in place before the height of regional metamorphism. The $^{206}\text{Pb}/^{238}\text{U}$ and $^{207}\text{Pb}/^{235}\text{U}$ ratios plot almost on concordia at 110 Ma (Figure 5.3). This Cretaceous date is a reasonable estimate for time of sill emplacement, based on local geology. I believe the sill was emplaced early enough during the Cretaceous intrusive and metamorphic event to have been deformed with the schists it intruded. The old $^{207}\text{Pb}/^{206}\text{Pb}$ date could be due to contamination by country rock lead or zircons. The Rb-Sr whole rock - mineral isochron date of 74 ± 10 Ma for the sill is similar to other dating that records the end of Cretaceous metamorphism. The felsic composition (biotite, no hornblende) and the high U and Pb contents compared with the Spuzzum batholith, Hut Creek body (Table B-4) suggests that this sill is not part of the main intrusive phase.

2) Mineral isochron dates from a foliated, felsic, garnet-cluster dyke (SS85) cutting the Settler Schist on the north ridge (Figure 5.2e), show the Cretaceous igneous and metamorphic event. Excluding Bi from the calculation yields a date of 105 ± 20 Ma, probably representing time of intrusion during the early part of the metamorphic cycle. The dyke became foliated parallel to the schist foliation, and cooled through the biotite blocking temperature of 300°C (Jäger 1979) at 80 ± 6 Ma.

5.6 Foliated diorite in fault zone

A small body of foliated diorite crops out on the west side of Settler Creek, intruding the metamorphosed ultramafic rocks in the imbricate zone of the Shuksan thrust. Foliation in the intrusive is parallel to the fault zone. A Rb-Sr mineral isochron was obtained from this rock in the hope that it might help date the thrusting event. The four point isochron gave a date of 77 ± 3 Ma (Figure 5.2f, Table 3-B). Since this is in the range of metamorphic ages, the thrusting either took place during metamorphism or before it so that all the rocks were equally affected. This small body was emplaced after the thrusting but before regional metamorphism, and the isotopic system has been reset.

5.7 Unit 5. Spuzzum batholith

Two discrete bodies of Spuzzum batholith in the area were mapped, and dated (Figures 1.2, 5.2). The small body intruding only Settler Schist north of Old Settler Mountain is called the Settler Creek body and is unit 3d of Bartholomew (1979). The Hut Creek body spans Cogburn Creek and extends north up Hut Creek (Figure 1.2).

Five K-Ar dates were obtained on hornblende separates from the two bodies (Table B-3). Hornblende from gabbro of the Hut Creek body (SD66) with very low %K ($0.046 \pm 0.002\%$) yielded a conventional date of 162 ± 7 Ma, and the other samples gave dates between 100 ± 3 Ma and 77.5 ± 3 Ma. The dates from the gabbro may have large analytical errors due to the very low K

content. The interpretation is further complicated by possible incorporation of initial radiogenic argon. The measured K content has a reproducibility of $\pm 4\%$ (1σ for 4 analyses), but such a low K means that the fraction of the total ^{40}Ar that is radiogenic is also low. For this sample, the radiogenic ^{40}Ar is only 38% of total ^{40}Ar , leading to possible error in the age calculation of up to 5 %. Apart from this sample, ages obtained from the Hut Creek body were slightly younger at 80.9 ± 3 and 77.5 ± 3 Ma than those from the Settler Creek body, 100 ± 3 and 94.5 ± 4 Ma. Figure 5.5a shows the data plotted on an isochron diagram of $^{40}\text{Ar}/^{36}\text{Ar}$ v. $^{40}\text{K}/^{36}\text{Ar}$. If no excess initial radiogenic argon were present the isochron lines would pass through an intercept of 295.5 on the argon axis, representing the atmospheric $^{40}\text{Ar}/^{36}\text{Ar}$ ratio. Whether the points are grouped together or split according to diorite body, the intercept is still >295.5 . The slopes of the lines through the plotted intercepts represent dates of 70.1 ± 5 Ma for the North body and 78.9 ± 2 Ma for the Settler Creek body. The actual amount of excess argon can be found from Figure 5.4b, a concentration-isochron plot of ^{40}Ar v. %K. Lines on this plot should pass through the origin; a positive intercept on the ^{40}Ar axis gives the amount of excess argon in nl/g. For these rocks the values are 0.19 ± 0.02 nl for the Hut Creek body and 0.14 ± 0.01 nl for the Settler Creek body. The slopes of the concentration-isochrons represent 65.7 ± 5 Ma and 79.7 ± 2 Ma respectively. The low date from the Hut Creek body reflects the effects of excess argon. The best minimum age estimates for the diorite

bodies are those calculated from the isochrons. Of the individual conventional dates, those for the Settler Creek body are closer to intrusive ages than those from the Hut Creek body, as the hornblendes contain less excess argon. Since the diorite was intruded before the peak of the high pressure and temperature regional metamorphism, all K-Ar dates must have been subject to some resetting. Pigage (1976) calculated the conditions of metamorphism of the Settler Schist to be 6 to 8 kbar and 550 to 700°C. The K-Ar blocking temperature for hornblende is 400°C. The diorite was subjected to temperatures high enough to reset the K-Ar clock of all the constituent minerals during metamorphism. In thin section, hornblendes in the diorite have brown cores and green rims that have recrystallised during metamorphism.

Rb-Sr dating of the Hut Creek body gives a WR-Pl-Hb isochron date of 127 ± 41 Ma and a biotite date of 88.3 ± 2 Ma (Figure 5.2g, Table B-2). One hornblende anomalously high in radiogenic strontium was not included in the WR-Pl-Hb isochron. The biotite date, similar to all other biotite dates from the area, indicates that the diorite cooled through the biotite blocking temperature of 300°C at the same time as the schists during the waning metamorphism. The WR-Pl-Hb isochron produces a date older than, but not in disagreement with, any date for diorites in the region reported by previous workers (e.g. Richards 1971, McLeod 1975). K-Ar, Rb-Sr and U-Pb dating along Highway 1 west of Hope has produced dates in the range 70 to 110 Ma, and further north in the range 70 to 90 Ma. The

older date obtained in this study may be due to movement of radiogenic strontium between mineral components during cooling (cf. Wasserburg et al. 1964), especially as the diorite was subjected to high grade regional metamorphism along with the schists it intrudes, or merely due to random analytical error.

Zircon from the Hut Creek body yielded a highly discordant date with large errors; the overlapping $^{207}\text{Pb}/^{206}\text{Pb}$ dates calculated independently from unspiked and spiked runs were 778 ± 360 Ma and 1235 ± 600 Ma. The averaged value is 1023 ± 500 Ma. This date, which contradicts local geology, indicates the presence of old lead or old zircon. There seems no likelihood of physical contamination from the schist, as this sample was collected well within the diorite body; however, the zircon yield was extremely low, 210 zircons from 35 kg of rock. Analytical errors may be high, because of the small amount of Pb and U available for measurement. When the $^{206}\text{Pb}/^{238}\text{U}$ and $^{207}\text{Pb}/^{235}\text{U}$ ratios are plotted the point lies off concordia. A mixing line through this point and those for Settler Schist intersects concordia at 110 ± 5 Ma. This is a plausible intrusive age, and indicates that the discordance might be due to the presence of old zircon picked up from the country rock, such as Settler Schist, at the time of intrusion (cf. Gebauer and Grunefelder 1979).

Rb-Sr and U-Pb isotopic analysis of the Settler Creek body shows a pronounced effect of either assimilation of schist in the magma during intrusion or mobilisation of Sr and Pb by fluids. Since the dating samples were collected unintentionally

close to margins of the body the former is quite likely. When an isochron is calculated for WR analyses of all samples except SD97 a date of 274 ± 179 Ma is obtained. This date is obviously too old, since it is greater than the isochron age obtained for the country rock, and most probably represents incorporation of Sr from the schists at the time of intrusion. A more realistic but still old date of 167 ± 46 Ma (Figure 5.2h) is obtained for Pl-Hb. The data for sample SD97 were left out of the isochron calculations above as they have lower $^{87}\text{Sr}/^{86}\text{Sr}$ values than the other samples for similar $^{87}\text{Rb}/^{86}\text{Sr}$ values. The diorite body is apparently isotopically heterogeneous, as SD97 was collected close to SD96 and is similar lithologically. The biotite-dominated mineral isochron date for sample SD97 is 89 ± 7 Ma. The WR-Pl-Hb date is 186 ± 49 Ma; this is probably too old because the hornblende analysis is abnormally high in $^{87}\text{Sr}/^{86}\text{Sr}$. All the hornblende samples analysed from the Settler Creek body are high in radiogenic strontium; since they were all collected near the margin of the pluton they may have been enriched with radiogenic strontium when they recrystallised during metamorphism.

Zircons from the Settler Creek body yielded $^{207}\text{Pb}/^{206}\text{Pb}$ dates of 242 ± 194 Ma, 629 ± 88 Ma and 217 ± 138 Ma for the natural and two spiked runs. The spread is due to the points lying on a chord very close to concordia (Figure 5.3). On the plot of $^{206}\text{Pb}/^{238}\text{U}$ v. $^{207}\text{Pb}/^{235}\text{U}$ the points lie near 95 ± 5 Ma on the concordia, so this is taken as a minimum estimate of the age of the Settler Creek body.

5.8 Agmatized quartz diorite

A diorite agmatite (SD 14), collected on the east side of the south branch of Cogburn Creek, gave a three point isochron date of 42 ± 14 Ma with a high initial $^{87}\text{Sr}/^{86}\text{Sr}$ ratio of 0.7048, which indicates resetting by the 32 ± 4 Ma Cogburn Granodiorite. The WR-Pl date of 182 ± 33 Ma (initial $^{87}\text{Sr}/^{86}\text{Sr}$ ratio of 0.7045) is close to the WR date obtained for the Settler Schist. Re-equilibration of radiogenic strontium between biotite and some other mineral phase during resetting by the Cogburn Granodiorite has pivoted the isochron line around the WR point to give a younger date. The data suggest that the body may have been intruded before the Spuzzum batholith, or they may be spurious due to ^{87}Sr redistribution during resetting.

5.9 Breakenridge Formation

Roddick and Hutchison (1967) and Reamsbottom (1971) thought that this unit contained the oldest rocks in the area based on structural position in the cores of the domes, and the amount of deformation the rocks had undergone.

Two samples of Breakenridge Formation gneiss were collected from the western dome of Reamsbottom (1971) and dated by Rb-Sr and U-Pb. The composite Rb-Sr mineral isochron gave an age of 79 ± 2 Ma, so the metamorphism of the granodiorite that was deformed into gneiss (Reamsbottom 1971) and presumably the Cairn Needle Formation schists surrounding it ended simultaneously with metamorphism of the schists and diorite 10-15 km south in

the Cogburn Creek area.

Zircon from CU2 was dated by U-Pb at 153 ± 87 Ma and 224 ± 180 Ma ($^{207}\text{Pb}/^{206}\text{Pb}$ ages). When the $^{206}\text{Pb}/^{238}\text{U}$ and $^{207}\text{Pb}/^{235}\text{U}$ ratios are plotted (Figure 5.3) the point lies very close to concordia at 105 ± 5 Ma. This is a reasonable age for either intrusion of the granodiorite or its metamorphism to gneiss, and as with the Rb-Sr date it is similar to dates in the Cogburn Creek area. If it represents metamorphism then the $^{207}\text{Pb}/^{206}\text{Pb}$ date of 166 ± 115 Ma could represent intrusion of the granodiorite. There is no supporting evidence for this possibility, but it is feasible as the date is younger than the Rb-Sr date for the Settler Schist surrounding the dome. The zircons are clear and euhedral and could have crystallised during either intrusion or high-grade regional metamorphism to staurolite - kyanite grade.

5.10 Discussion

A summary of the timing of events based on geochronometry (this study) are given in Table 5.2.

The oldest unit in the study area is the Baird Metadiorite, which is equivalent to the Yellow Aster Complex of the North Cascade Mountains. A conclusive date was not obtained but both the Rb-Sr and zircon U-Pb (Table 5.2) suggest a Precambrian protolith. The rocks have been metamorphosed twice to amphibolite grade (Lowes 1972), which probably scrambled the geochronological clocks. Possible interpretations include intrusion during the Precambrian followed by metamorphism

Table 5.2 Summary of events in the Cogburn Creek area based on
new analyses

Method	Date Ma ¹	Interpretation
<u>Baird Metadiorite (Unit 1)</u>		
Rb-Sr	3.4 ± 2.4 Ga	Intrusion during Precambrian
U-Pb ²	269 400 1251 ± 180	followed by amphibolite facies metamorphism at 415 and 90 Ma (Mattinson 1972)
<u>Cogburn Creek Group (Unit 3)</u>		
Rb-Sr	296 ± 58	Approx. time of deposition
Rb-Sr	81 ± 5, 76.6 ± 1.6	End of Cretaceous metamorphism
<u>Settler Schist (Unit 4)</u>		
U-Pb	2450 ± 230 upper intercept	Precambrian source for zircons in sediments
U-Pb	211 ± 30 lower intercept	Deposition of sediments
Rb-Sr	210 ± 27	" "
Rb-Sr	66 ± 1.6	Cretaceous metamorphism
Rb-Sr	39 ± 4	Reset by Cogburn Granodiorite
<u>Premetamorphic intrusive rocks</u>		
Rb-Sr	105 ± 20	Intrusion?
Rb-Sr	80 ± 6, 74 ± 10	Cretaceous metamorphism
U-Pb	111 ²⁰⁶ Pb/ ²³⁸ U date	Reset by Spuzzum batholith?

Spuzzum batholith (Unit 5)

a) Hut Creek body

K-Ar	70.1 ± 5 isochron	Minimum intrusive age, metamorphism
U-Pb	181 ± 7 $^{206}\text{Pb}/^{238}\text{U}$ date	Meaningless
Rb-Sr	86 ± 4	Minimum intrusive age, metamorphism

b) Settler Creek body

K-Ar	78.9 ± 2 isochron	Minimum intrusive age, metamorphism
U-Pb	91.8 ± 1 $^{206}\text{Pb}/^{238}\text{U}$ date	Intrusion?
Rb-Sr	90 ± 8, 89 ± 7	Minimum intrusive age, metamorphism

Breakenridge Formation Gneiss (Unit 7)

U-Pb	105 ± 1 $^{206}\text{Pb}/^{238}\text{U}$ date	Either intrusion of granodiorite or its metamorphism to gneiss
Rb-Sr	79 ± 1.6	Cooling after metamorphism to gneiss

¹ All analytical data and results are listed in Appendix B.

² U-Pb zircon dates reported as $^{206}\text{Pb}/^{238}\text{U}$, $^{207}\text{Pb}/^{235}\text{U}$, $^{207}\text{Pb}/^{206}\text{Pb}$

intrusion during the Precambrian followed by metamorphism at 415 and 90 Ma as proposed by Mattinson (1972) for rocks of the Yellow Aster Complex and Swakane Gneiss (see Table 5.1 for his dates).

Cogburn Creek Group has been mapped previously as Chilliwack Group, based on structural position. The rocks at Cogburn Creek bear little resemblance to the type section of the Chilliwack Group in the Chilliwack valley and are unfossiliferous. Lithological correlation with Bridge River and Hozameen Groups would be more logical but this would require major re-interpretation of the regional geology. The whole rock isochron date from the Cogburn Creek Group of 296 ± 58 Ma at 0.7039 initial $^{87}\text{Sr}/^{86}\text{Sr}$ ratio represents late Paleozoic deposition of chert and pelites and extrusion of volcanic rocks. Biotite ages of 74 to 89 Ma from all units represent the waning of the Cretaceous intrusive and metamorphic episode. The Chilliwack Group has been dated by Rb-Sr whole rock isochron at 191 ± 6 Ma at 0.7051 initial $^{87}\text{Sr}/^{86}\text{Sr}$ ratio. This probably reflects a metamorphic event, as fossils of Lower Pennsylvanian to Permian ages occur in all divisions of the Group (Monger 1970). A better correlation based on lithology would be with the Bridge River Group, which also consists of chert and greenschist in greater abundance than phyllite and other clastic rocks. This correlation is echoed isotopically, as can be seen from the isotope correlation diagrams in Figure 5.6. Armstrong and others have dated the Bridge River Group (Rb-Sr isochron) at 256 ± 35 Ma at 0.7037 initial $^{87}\text{Sr}/^{86}\text{Sr}$ ratio. This date is

lower than expected from the spread of points, because the proportional errors assigned to the low $^{87}\text{Sr}/^{86}\text{Sr}$ -ratio samples are high. Data boundaries have been drawn using the data points plotted in Figures 5.3b, d, j, k, and the different fields superimposed in Figure 5.6. The fields do overlap considerably, although isochrons for all three units have somewhat different initial $^{87}\text{Sr}/^{86}\text{Sr}$ ratios and slopes. The Cogburn Creek Group and Bridge River Group data are very similar and different from Chilliwack Group. Calculations for the Cogburn Creek Group are based on a relatively small number of samples, which may have biased the results. Since the date for the Chilliwack Group is most probably metamorphic, the results presented here do not rule out the correlation of this unit with the Cogburn Creek Group. Monger (1978) considers that the Bridge River Group is equivalent to the Hozameen Group on the east side of the Fraser Fault. No data are available from the Hozameen rocks to confirm this isotopically. I propose that the Cogburn Creek Group is correlative with the Bridge River Group, and therefore also the Hozameen Group (See Chapter 6).

Settler Schist contains at least some detritus of Precambrian age, zircon 2450 ± 230 Ma old. The time of deposition was most probably around 210 ± 27 Ma (Rb-Sr WR isochron). The schist has undergone contact and then regional metamorphism. Contact metamorphism was related to intrusion of two bodies of Spuzzum batholith at around 95 to 110 Ma. Biotite K-Ar and Rb-Sr dates from schists and diorite in the range 80-60 Ma indicate cooling after regional metamorphism. K-Ar isochron

dates from hornblende in the two diorite bodies, 70.1 ± 5 Ma and 78.9 ± 2 Ma, are minimum values for time of intrusion. Rb-Sr WR dates and zircon upper intercept dates for Spuzzum batholith are too old and not valid, probably due to assimilation of country rock during intrusion.

Settler Schist has been correlated with Chiwaukum Schist of the Skagit Metamorphic Complex, based on similarities in lithology and metamorphic history. Outcrops of Chiwaukum Schist that I have visited in the Stevens Pass area look very similar to the Settler Schist. The same unusual rock types and metamorphic mineral assemblages are present. Foliated felsic dykes and metatrandhjemites are common in both units, as are ultramafic pods. Both the Mount Stuart batholith and the Spuzzum batholith were intruded before the end of regional metamorphism. The Chiwaukum Schist and Shuksan Suite are not related, and are separated by faults and metamorphic facies differences. Figure 2.2 shows the present geographical locations of the Settler Schist and the Chiwaukum Schist. Chiwaukum Schist has not yet been dated. Babcock et al. (1985) have found that Rb-Sr isotopic systematics of the Skagit Gneiss and Cascade River Schist show broad dispersion of data with no clear age, but a very strong overprint of Mesozoic and Early Tertiary re-equilibration. Clear isotopic correlation is not possible.

Based on structural position with respect to the Shuksan thrust and comparison with the North Cascades in Washington, a possible alternative correlative of the Settler Schist is the

Darrington Phyllite of the Shuksan Metamorphic Suite. Where I have seen the Shuksan Suite in the North Cascade Mountains, the rock appears completely different from the Settler Schist. Their metamorphic history is also different. Evidence points to the possible correlation of the two units being unjustified. Geochronometry on the Darrington Phyllite gives 132 ± 8 Ma (Rb-Sr WR, Figure 5.2m, Armstrong unpub.), which is far younger than deposition of the protolith of the Settler Schist. Dates from blueschist and greenschist in the Shuksan Suite demonstrate a Late Jurassic to late Early Cretaceous metamorphic age (Figure 5.2m, Armstrong et al. 1983), also dissimilar.

The data-fields in the correlation diagram (Figure 5.6) show an isotopic similarity between the Settler Schist and Chilliwack Group, although that is probably quite coincidental. Sampling of the Chilliwack Group may not have been representative, and could have included Mesozoic pelite from a melange (Armstrong pers. comm. 1985).

The Cogburn Creek Group and Settler Schist were juxtaposed before intrusion of Spuzzum batholith. A small body of diorite intruded into the imbricate zone before the end of metamorphism gave a mineral isochron date of 77 ± 3 Ma, a metamorphic cooling age. The imbricate zone appears to have been folded and possibly pushed aside at the western margin of the Spuzzum batholith in the Cogburn Creek area. Some late strain is indicated by foliation of the small diorite body.

Lowes (1972) correlated the imbricate zone north of the Fraser River with the Shuksan thrust of the North Cascades,

Washington. Misch (1966) considered the Shuksan thrust to be post-metamorphic and mid-Cretaceous in age. In the Cogburn Creek area the imbricate zone pre-dates the peak of regional metamorphism. In the Mount Watson area Armstrong et al. (1980) dated metamorphism in blueschist facies rocks as 120 to 130 Ma, which is earlier than regional metamorphism in Cogburn Creek. If the imbricate zone in Cogburn Creek is the Shuksan thrust then the juxtaposition of the Cogburn Creek Group and Settler Schist can be bracketed between blueschist metamorphism of the Shuksan Suite at 120 to 130 Ma and diorite intrusion at 100 ± 10 Ma. Current studies in the North Cascades, Washington (Silverberg 1985, Leiggi and Brown 1985) show that the Shuksan thrust changes in style and amount of deformation along its length. Movement may die out northwards, as Reamsbottom (1974) recognised no major structural break across schists in the Mount Breakenridge area. The northern limit of movement may in fact be at Cogburn Creek. This would explain the sudden change in lithology across the Cogburn Creek valley, from ultramafic rocks to the south to Cogburn Creek Group chert to the north (Figure 2.1).

All valid dates from the Spuzzum batholith are Cretaceous (Table 5.2, Appendix B). The diorite intruded during regional metamorphism (Bartholomew 1979); thus the zircon U-Pb dates of 110 ± 5 Ma (Hut Creek body, lower intercept of chord through QDHC and Sett1, Sett2) and 91.8 ± 0.5 Ma (Settler Creek body, $^{206}\text{Pb}/^{238}\text{U}$ date) are minimum intrusive ages (Table 5.2). Rb-Sr and K-Ar isochron dates of 66 Ma to 88 Ma reflect cooling

through blocking temperatures during waning of regional metamorphism. On a regional scale, dates from the southern part of the Spuzzum batholith around the Fraser Valley are older than those from in and north of the study area (Table 5.1, Figure 5.1). A concentration-isochron for all available Hb-Bi data from Spuzzum batholith has been plotted in Figure 5.7. Slope dates range from 75 to 97 Ma for individual sample pairs, with a calculated mean of 83 ± 5 Ma. Bartholomew (1979) found a trend of dates younging eastward towards the Fraser Fault zone (Figure 5.7). He considered that it represented greater uplift, erosion and later cooling through the argon blocking temperature approaching the fault, due to vertical movement on the fault. However, this implies tilting in the opposite sense to that suggested by paleomagnetic measurements. Evidence from the North Cascade Mountains indicates regional tilting down to the southeast of around 30° (Beck 1982), and Irving et al. (1985) note that their data from the Spuzzum batholith could be interpreted as 28° tilt down to the southeast. This would give rise to the northward younging trend of dates from the Spuzzum batholith that can be seen in Figure 5.1, and to the increase in metamorphic grade northwards.

Breakenridge Formation granodioritic gneiss gave a zircon $^{206}\text{Pb}/^{238}\text{U}$ date of 105 ± 1 Ma and Rb-Sr mineral isochron date of 79 ± 1.6 Ma, similar to dates from the Spuzzum batholith. The granodiorite is highly deformed, so these dates may represent either intense metamorphism of an older rock or synkinematic intrusion.

The latest event was intrusion of small plutons of granodiorite. One of these, the Cogburn Granodiorite, has been dated at 32 ± 4 Ma (Bartholomew 1979) and locally has isotopically reset nearby schists.

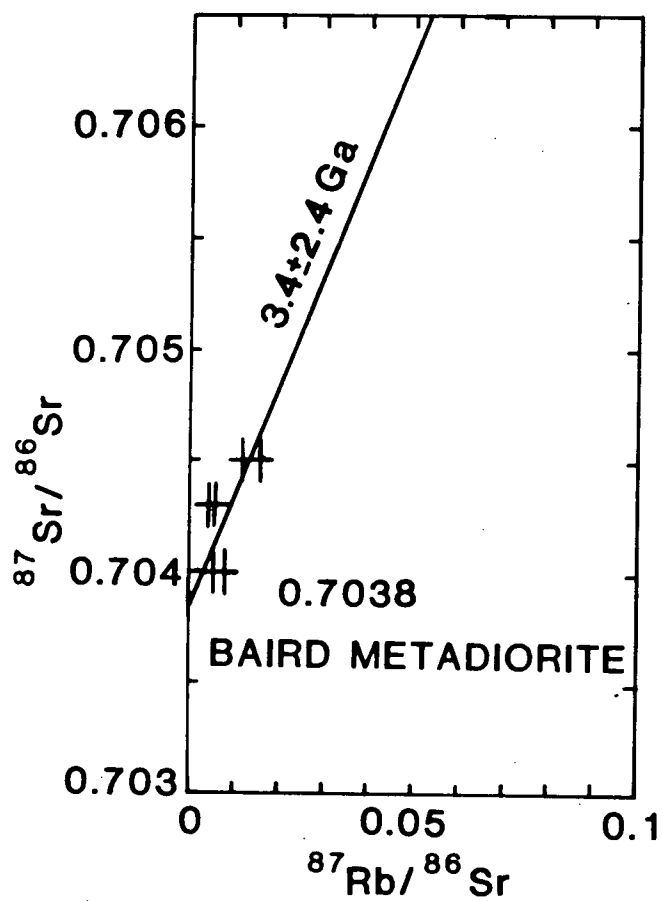


Figure 5.2a Rb-Sr isochron plot for Baird Metadiorite
All analyses are WR (whole rock).

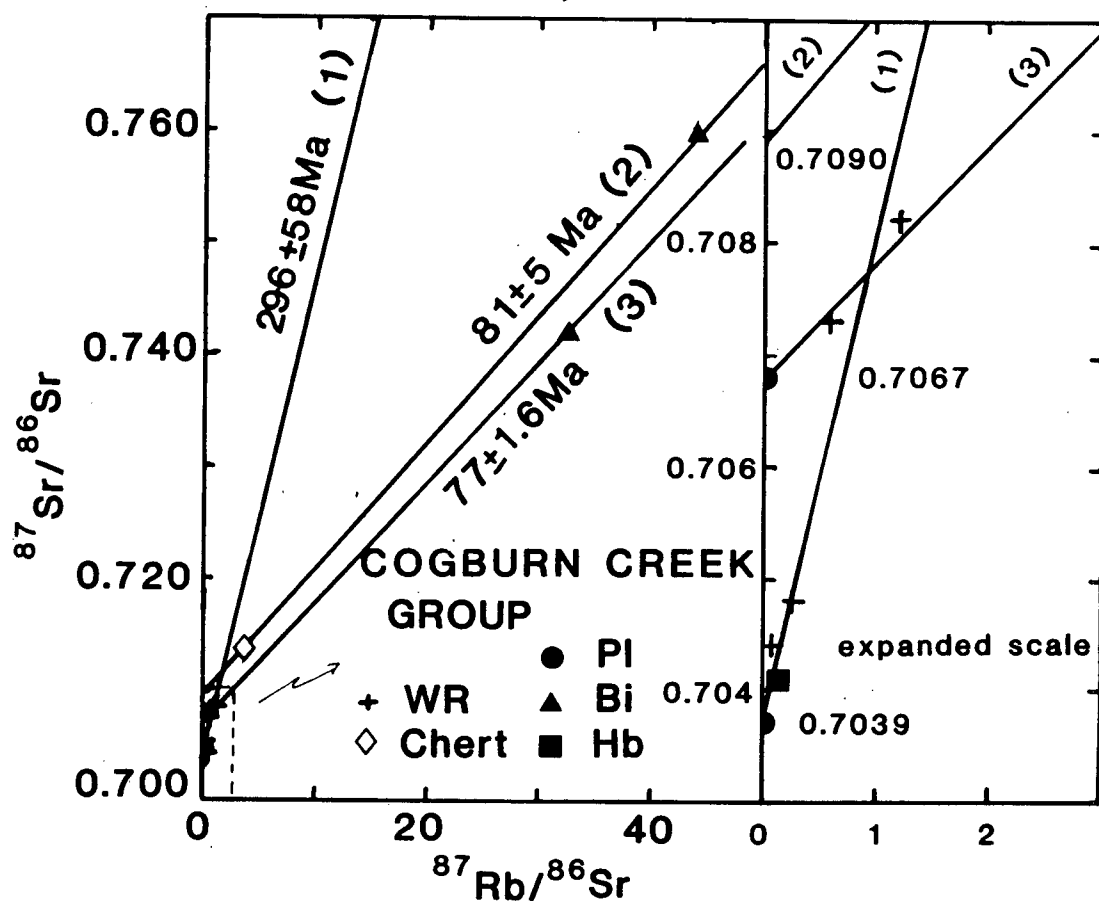


Figure 5.2b Rb-Sr isochron plot for Cogburn Creek Group
 Lines represent 1) WR and Pl data excluding chert
 2) chert HL37a WR-Bi pair
 3) metavolcanics and phyllite
 Inset shows points near the intercepts, expanded
 scale, also initial $^{87}\text{Sr}/^{86}\text{Sr}$ ratios.

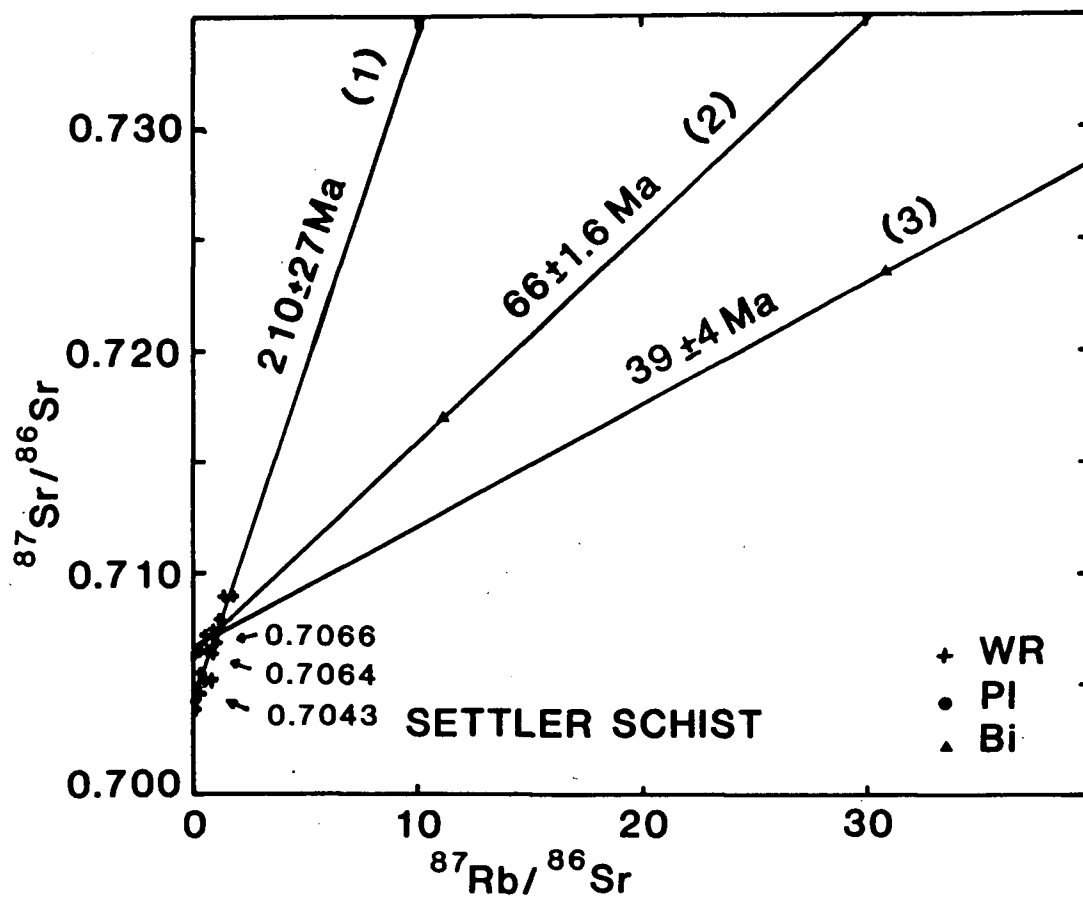


Figure 5.2c Rb-Sr isochron plot for Settler Schist
 Lines represent 1) all data, not including Bi and Mu
 2) WR-Pl-Bi isochron, phyllite SS82
 3) WR-Pl-Bi isochron for quartz-biotite-garnet schist marginal to Cogburn Granodiorite (SS128).

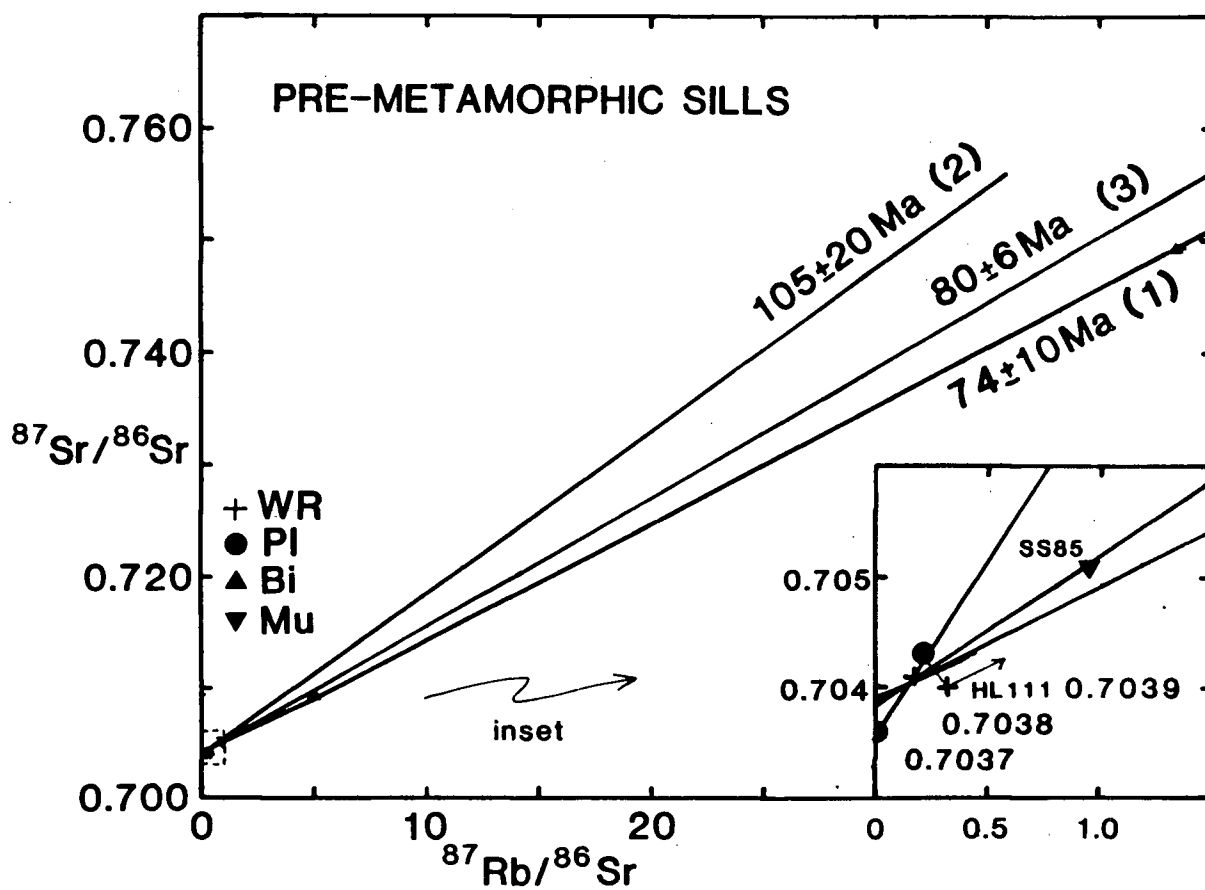


Figure 5.2e Rb-Sr isochron plot for premetamorphic intrusive rocks.
 Lines represent 1) WR-Pl-Bi, felsic sill HL111 intruding Cogburn Creek Group.
 2 + 3) foliated felsic garnet-cluster dyke, SS85, intruding Settler Schist.
 2) not including Bi
 3) including Bi

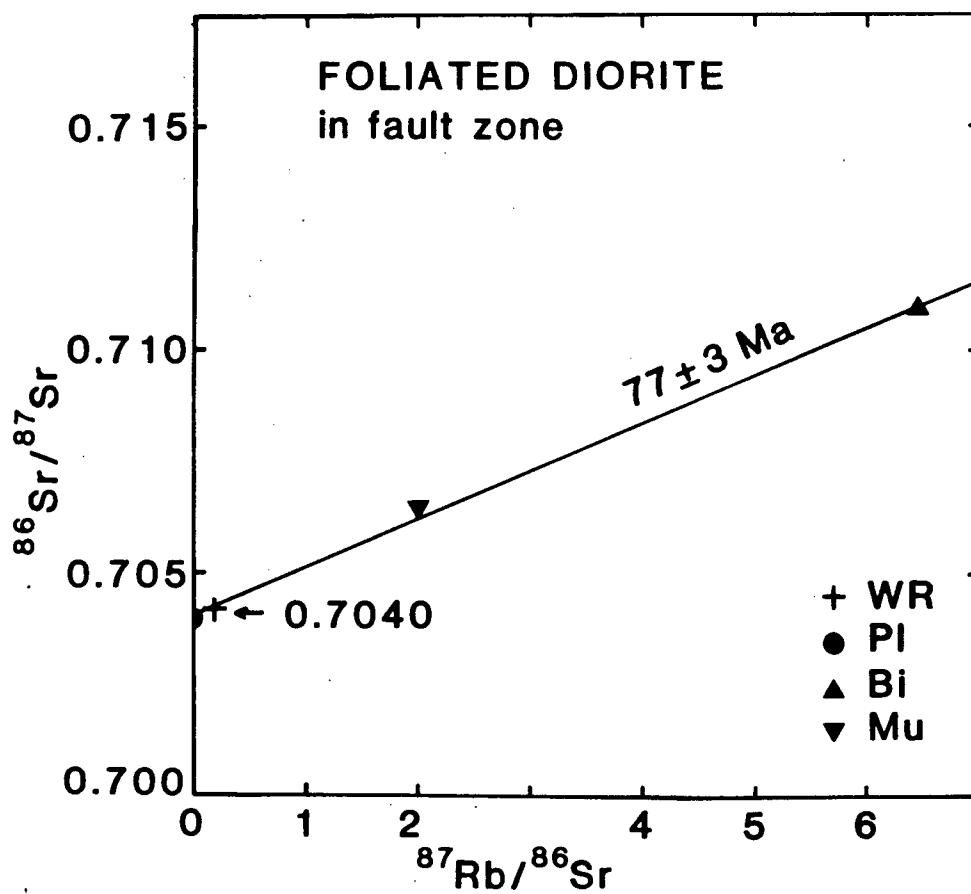


Figure 5.2f Rb-Sr isochron plot for small body of foliated granodiorite in imbricate zone (SD92).

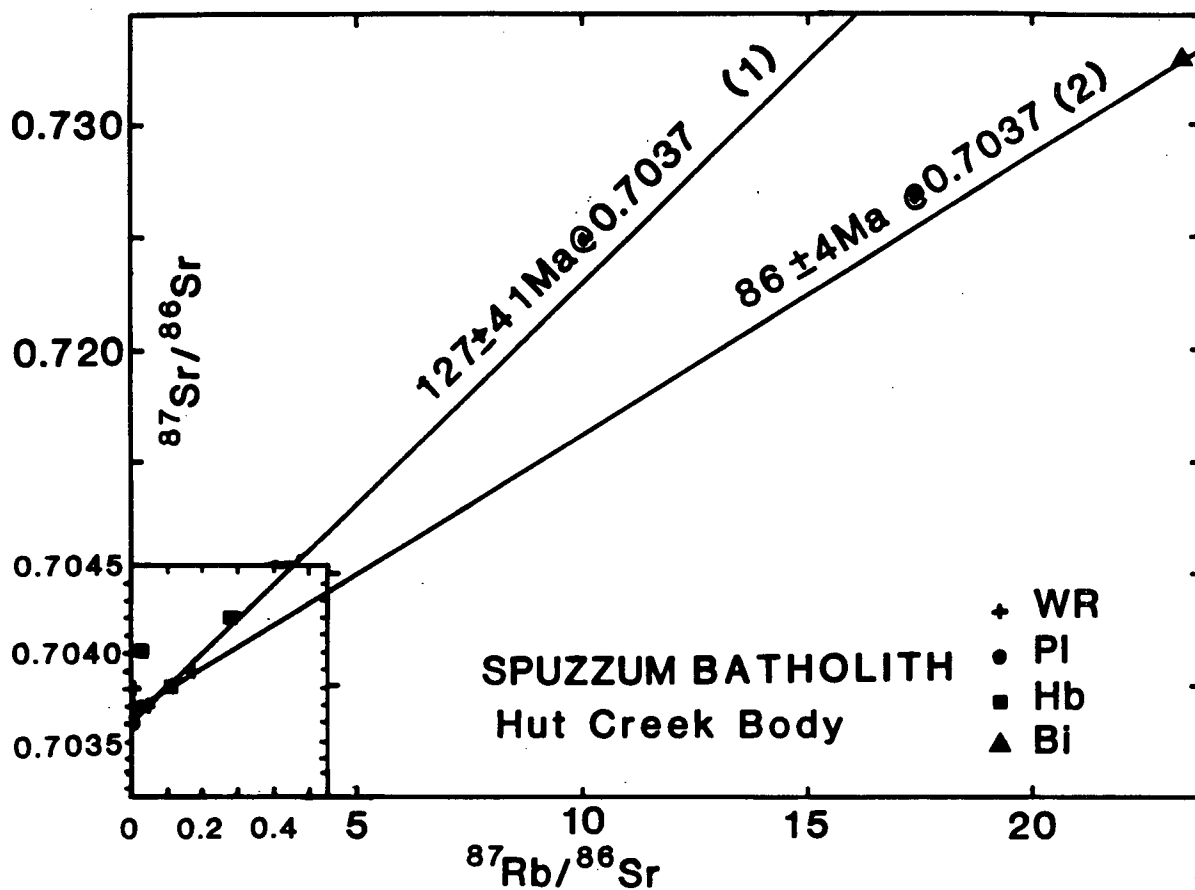


Figure 5.2g Rb-Sr isochron plot for Spuzzum batholith, Hut Creek body
 Lines represent 1) all data not including Bi
 2) all data including Bi

Inset shows points near intercepts on expanded scale.

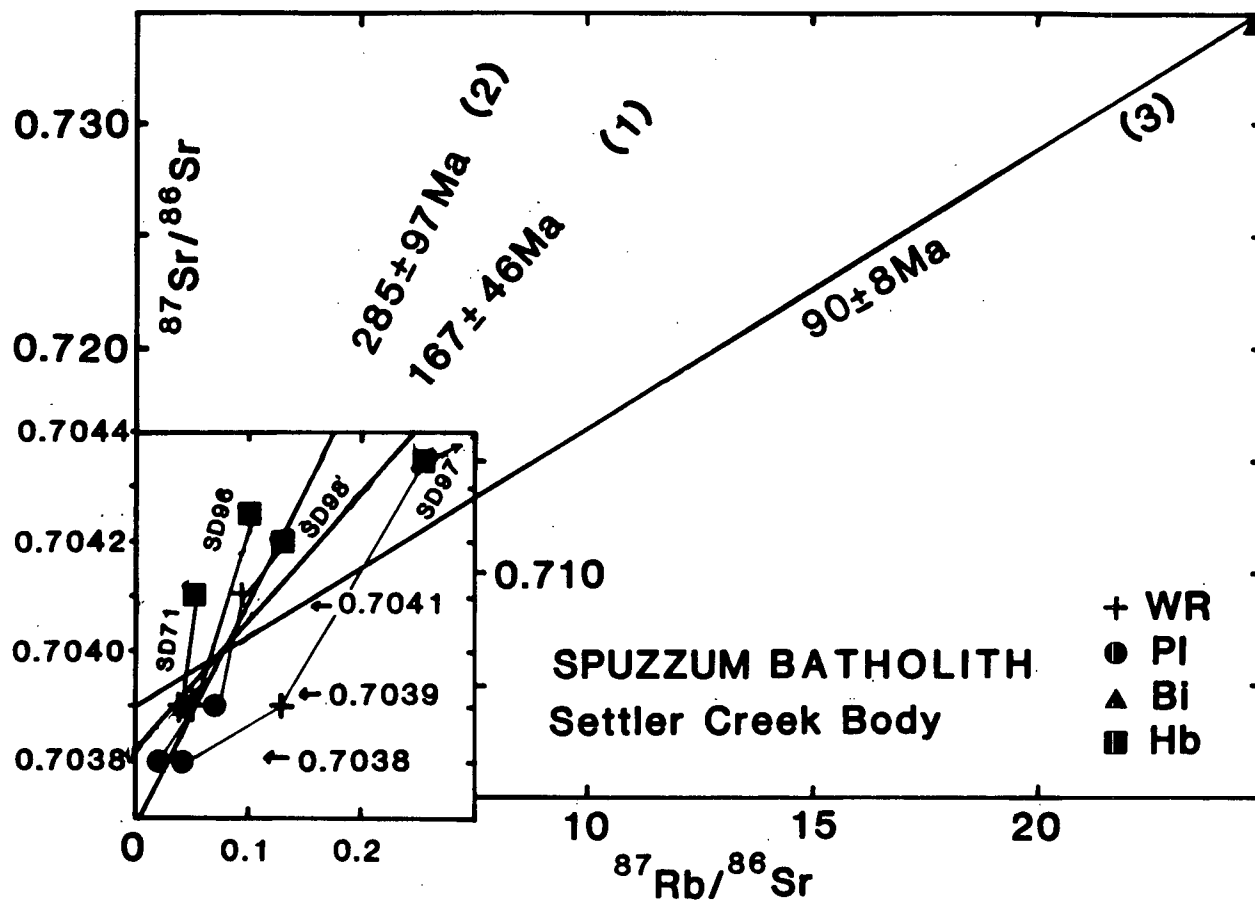


Figure 5.2h Rb-Sr isochron plot for Spuzzum batholith, Settler Creek body
 Lines represent 1) WR-P1 isochron for all samples except SD97
 2) WR-P1-Hb isochron for all samples including SD97
 3) isochron for all data including Bi
 Inset shows points near intercepts on expanded scale.

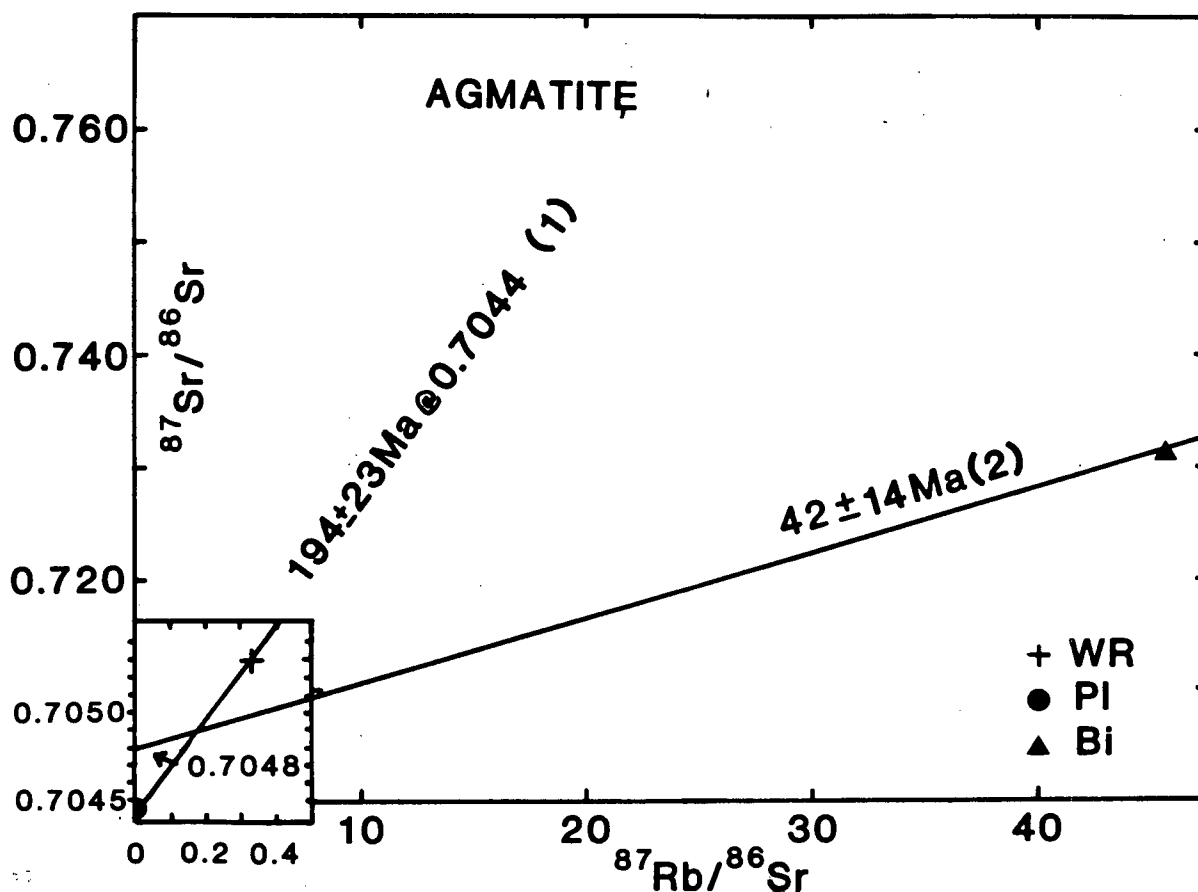


Figure 5.2i Rb-Sr isochron plot for agmatitic quartz diorite (SD14), marginal to Cogburn Granodiorite. Inset shows points near intercepts on expanded scale.

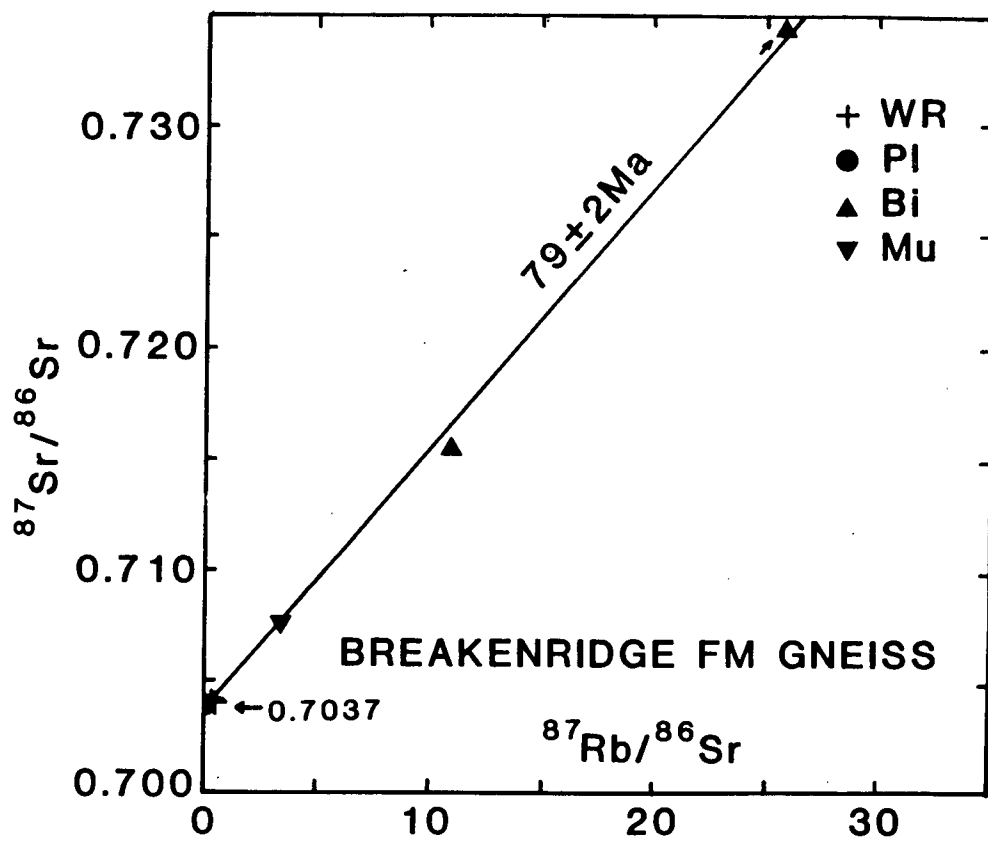


Figure 5.2j Rb-Sr isochron plot for Breakenridge Formation gneiss

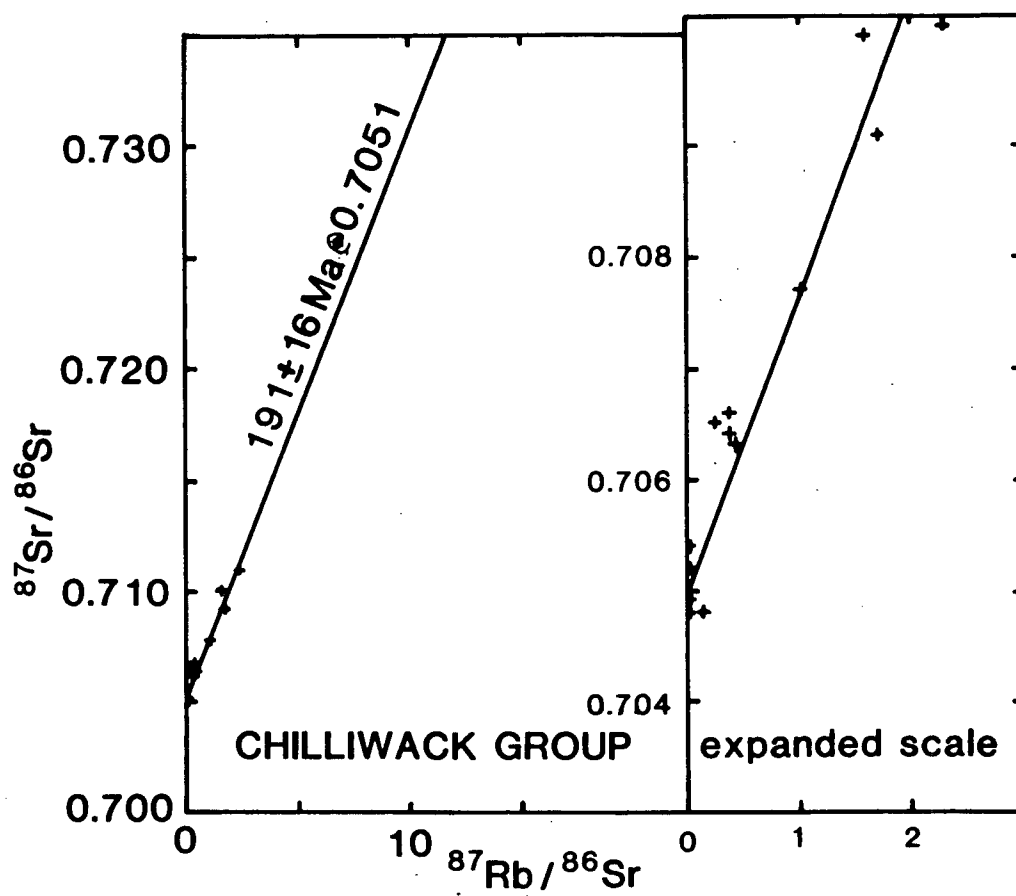


Figure 5.2k Rb-Sr isochron plot for Chilliwick Group sediments.
 Data from Armstrong and others (unpub.).
 All analyses are WR

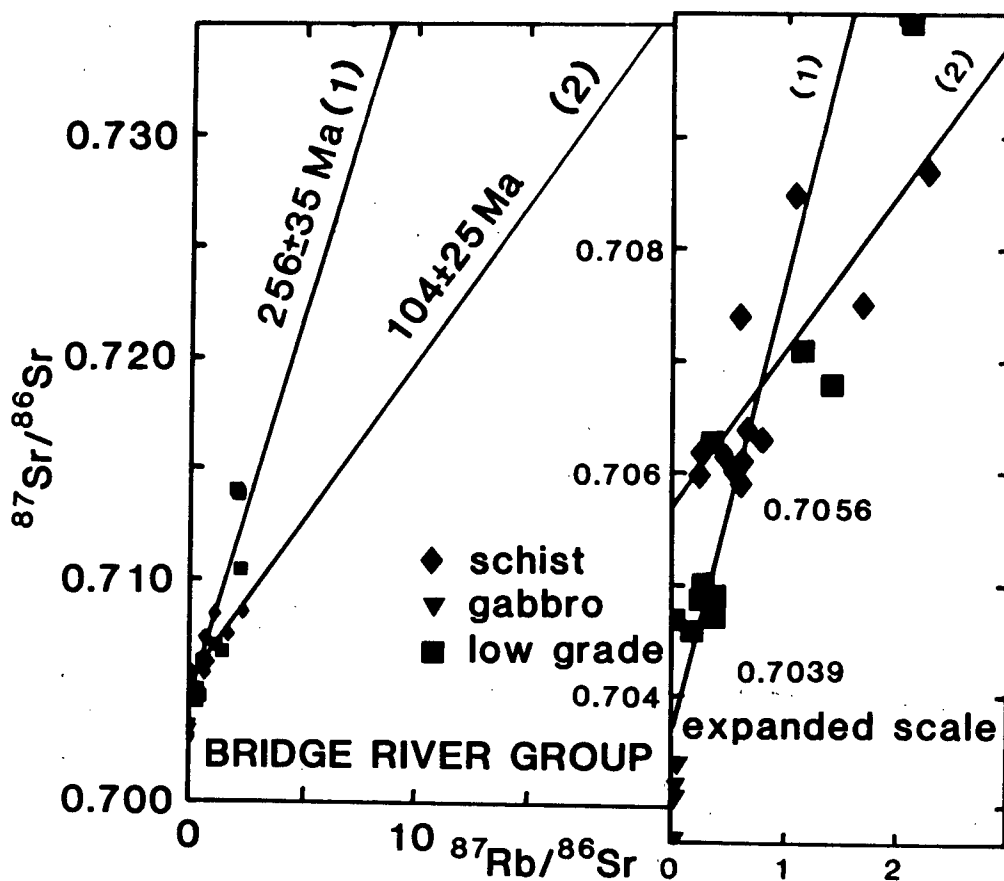


Figure 5.21 Rb-Sr isochron plot for Bridge River Group.
 Data from Armstrong and others (unpub.).
 Lines represent 1) all data
 2) high grade schists

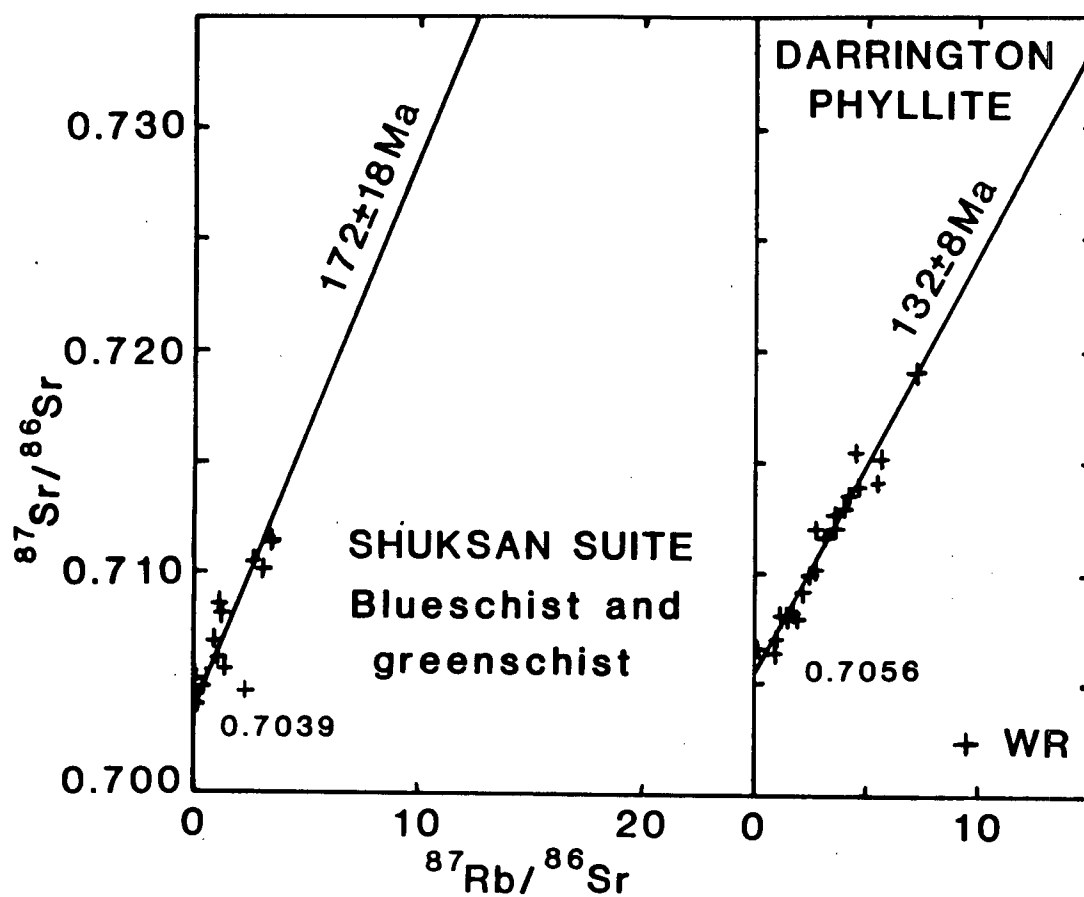


Figure 5.2m Rb-Sr isochron plot for Shuksan Suite blueschist and greenschist, and Darrington Phyllite. Data from Armstrong and others (unpub.).

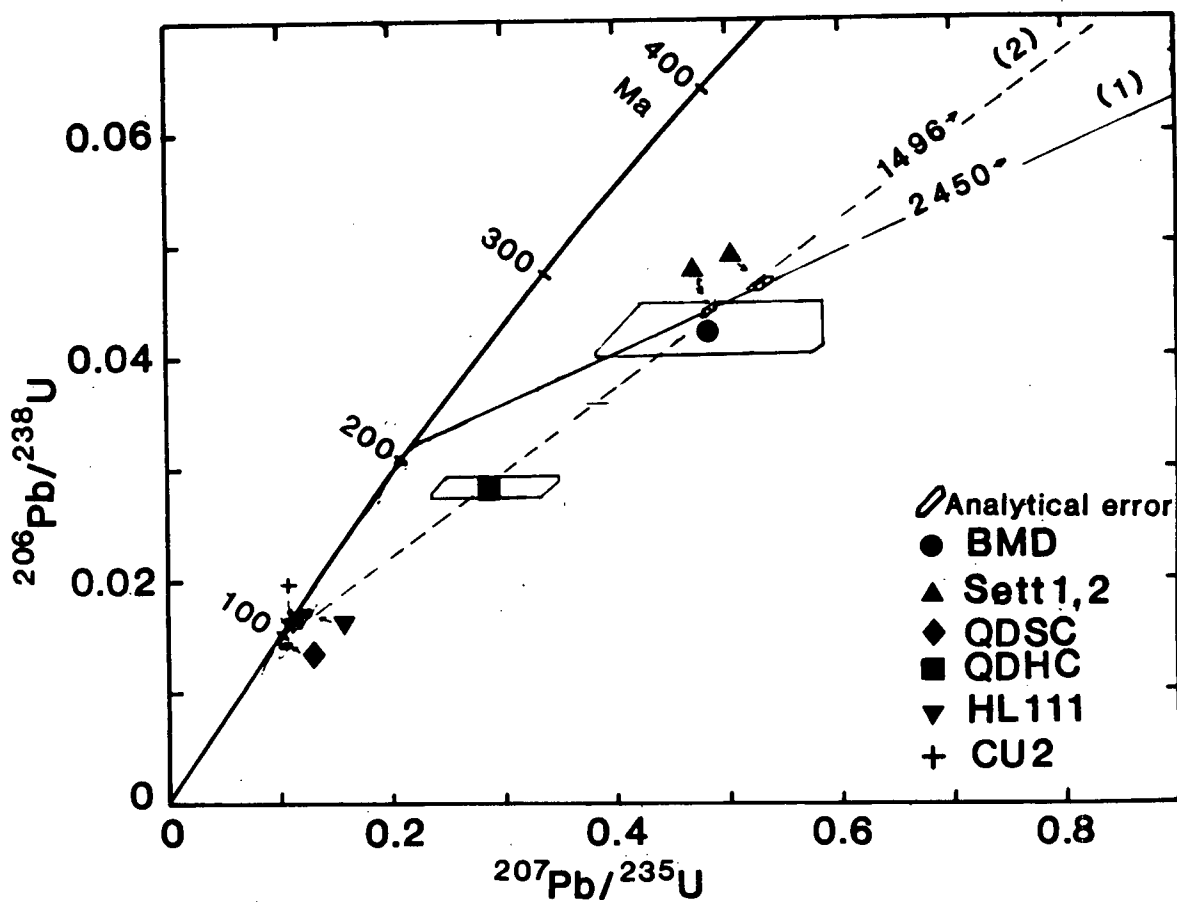


Figure 5.3 U-Pb concordia diagram for zircon dating. Plot of $^{206}\text{Pb}/^{238}\text{U}$ v. $^{207}\text{Pb}/^{235}\text{U}$ for all zircon samples. Line 1) is for Settler Schist, 2) is all samples combined. Sample numbers as listed in Appendix C.

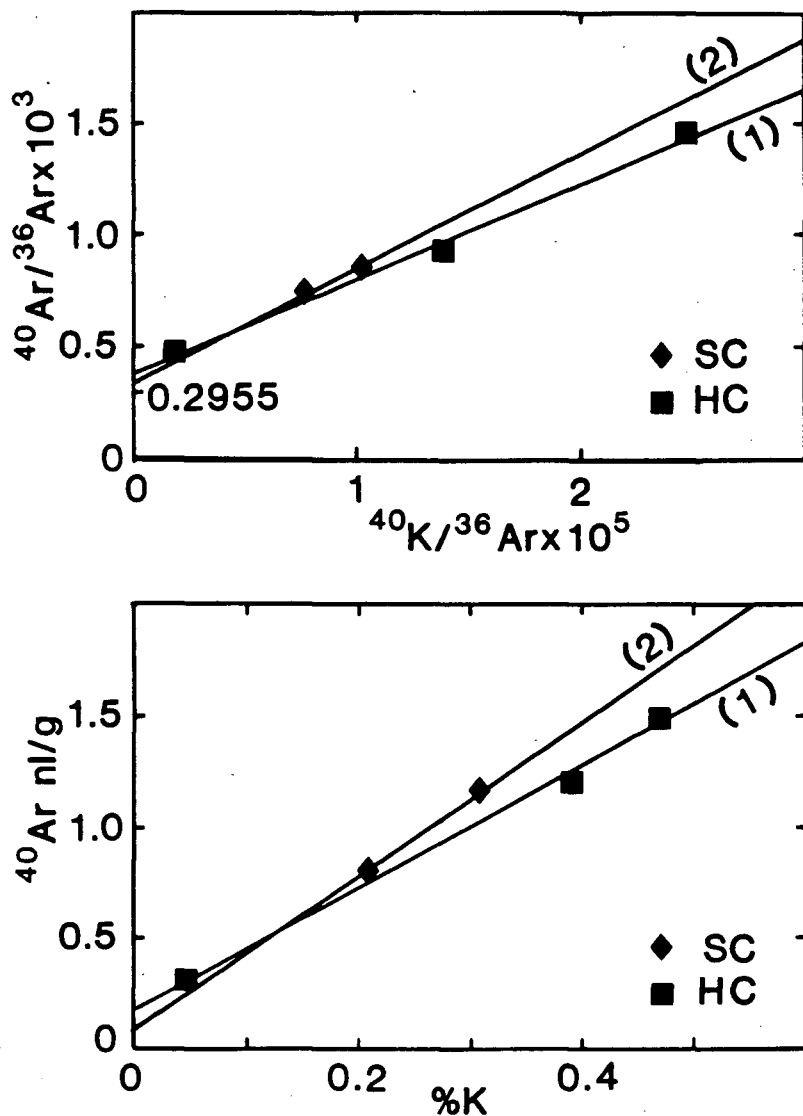


Figure 5.4a Plot of $^{40}\text{K}/^{36}\text{Ar}$ v. $^{40}\text{Ar}/^{36}\text{Ar}$ for hornblende separates from Spuzzum batholith.
Lines represent 1) Hut Creek body.

Slope gives 70.1 ± 5 Ma

Intercept 392 ± 25

2) Settler Creek body.

Slope gives 78.9 ± 2 Ma.

Intercept 388 ± 88

Figure 5.4b Plot of %K v. ^{40}Ar nl/g for hornblende separates from Spuzzum batholith.

Lines represent 1) Hut Creek body.

Slope gives 65.7 ± 5 Ma

Intercept initial ^{40}Ar 0.185 ± 0.016 nl/g

2) Settler Creek body.

Slope gives 79.7 ± 2 Ma

Intercept initial ^{40}Ar 0.139 ± 0.010 nl/g

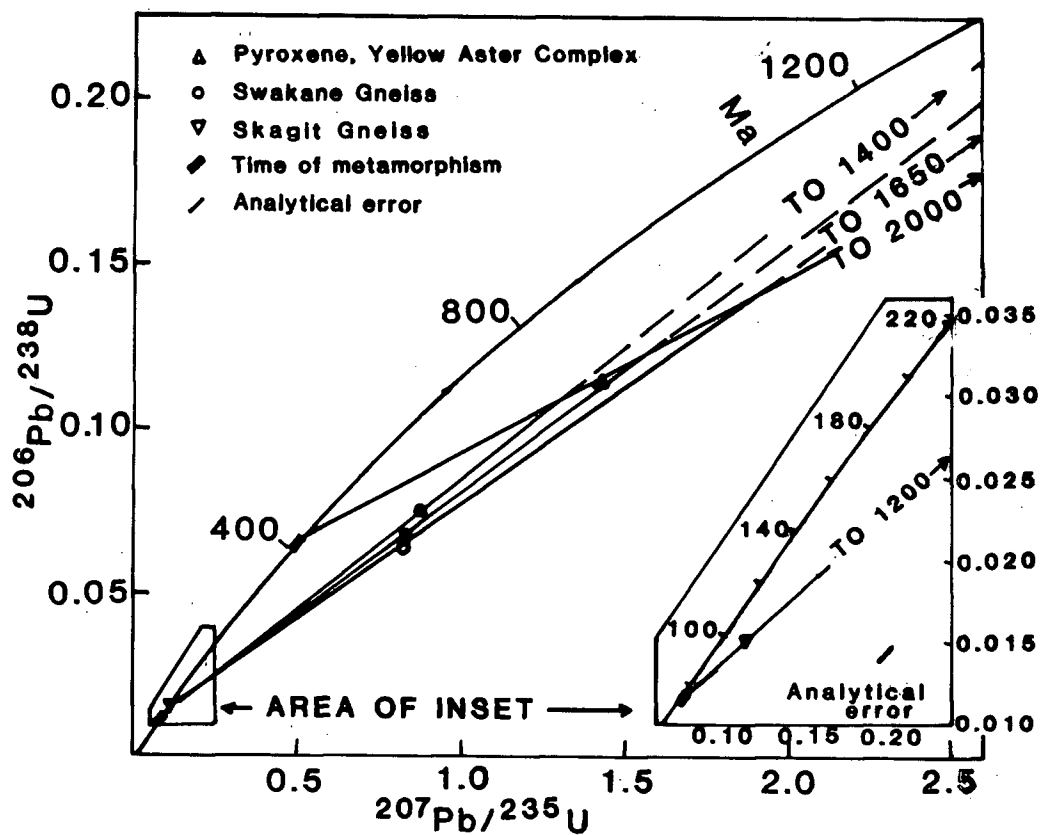


Figure 5.5 U-Pb concordia diagram for Yellow Aster Complex, Skagit Gneiss and Swakane Gneiss, from Mattinson (1972). Plot of $^{206}\text{Pb}/^{238}\text{U}$ v. $^{207}\text{Pb}/^{235}\text{U}$ for zircon samples.

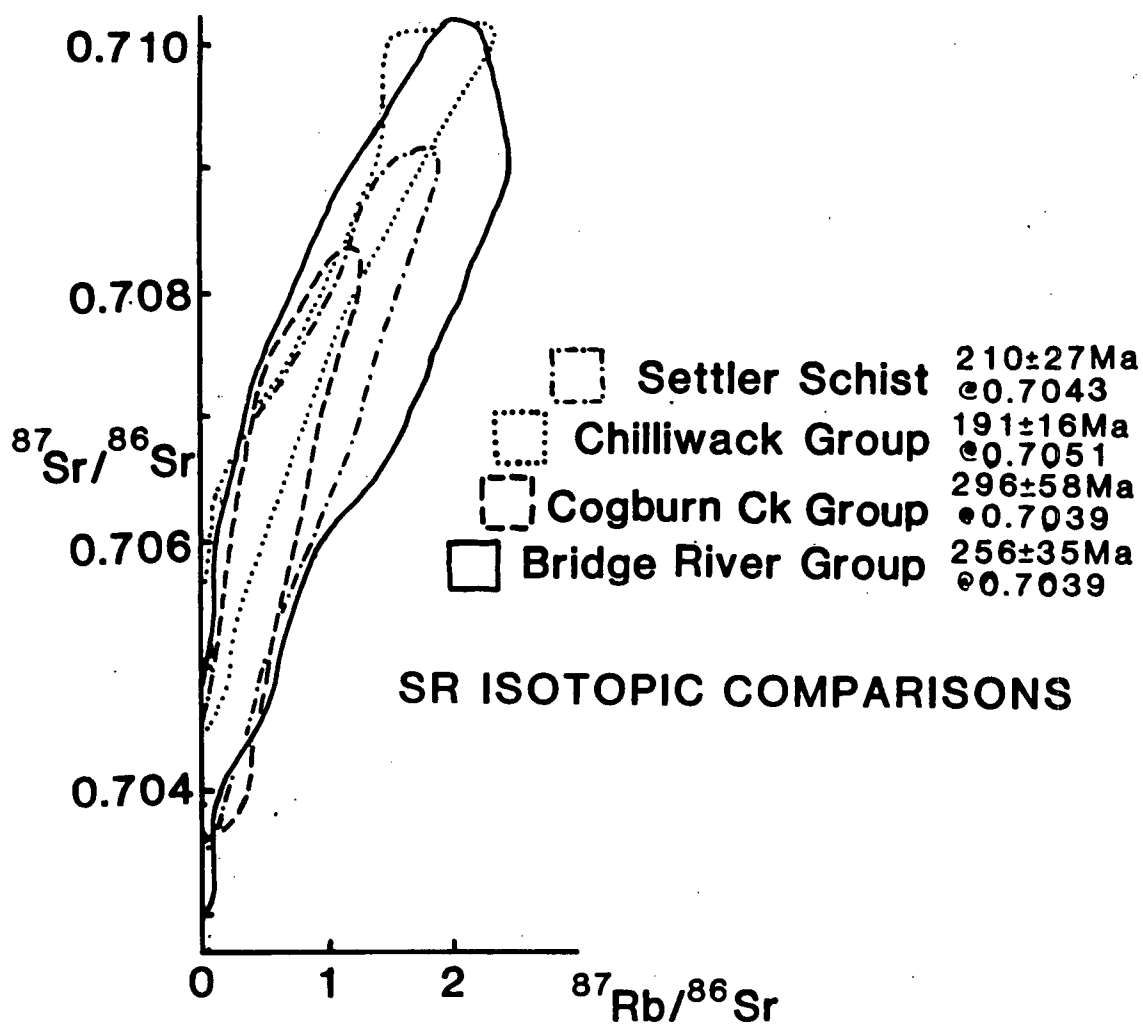


Figure 5.6 Data-field diagram for Rb-Sr analyses from possible correlative stratigraphic units.

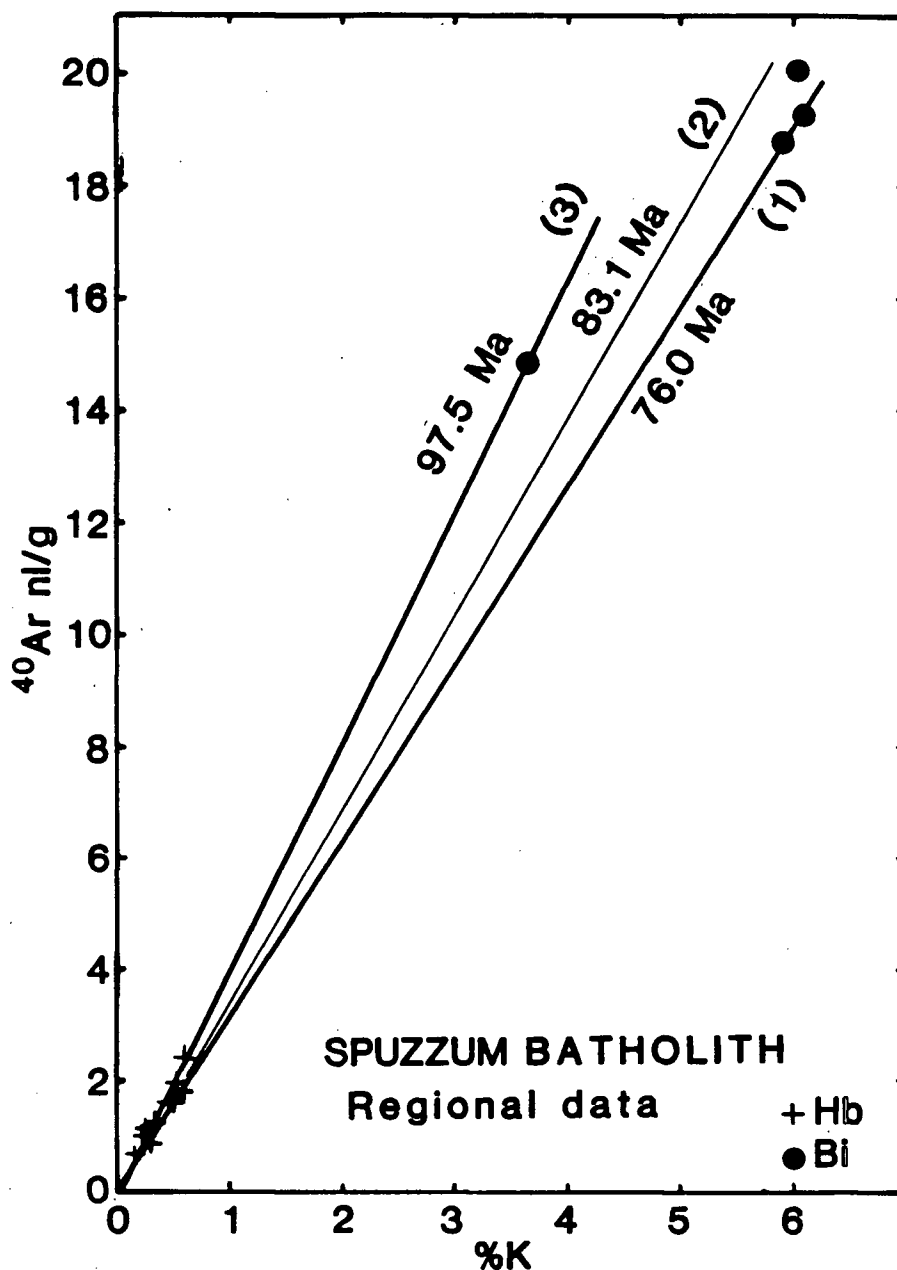


Figure 5.7 Plot of $\%K$ v. $^{40}\text{Ar nl/g}$ for regional data from Spuzzum batholith, not including this study. Lines represent 1) lower limit, slope gives 76.0 ± 5 Ma
 2) calculated mean, slope gives 83.1 ± 5 Ma
 3) upper limit, slope gives 97.5 ± 5 Ma

Lower and upper limit isochron dates represent Hb-Bi pairs from single samples; mean is for all data. Conventional K-Ar dates are listed in Table 5.1.

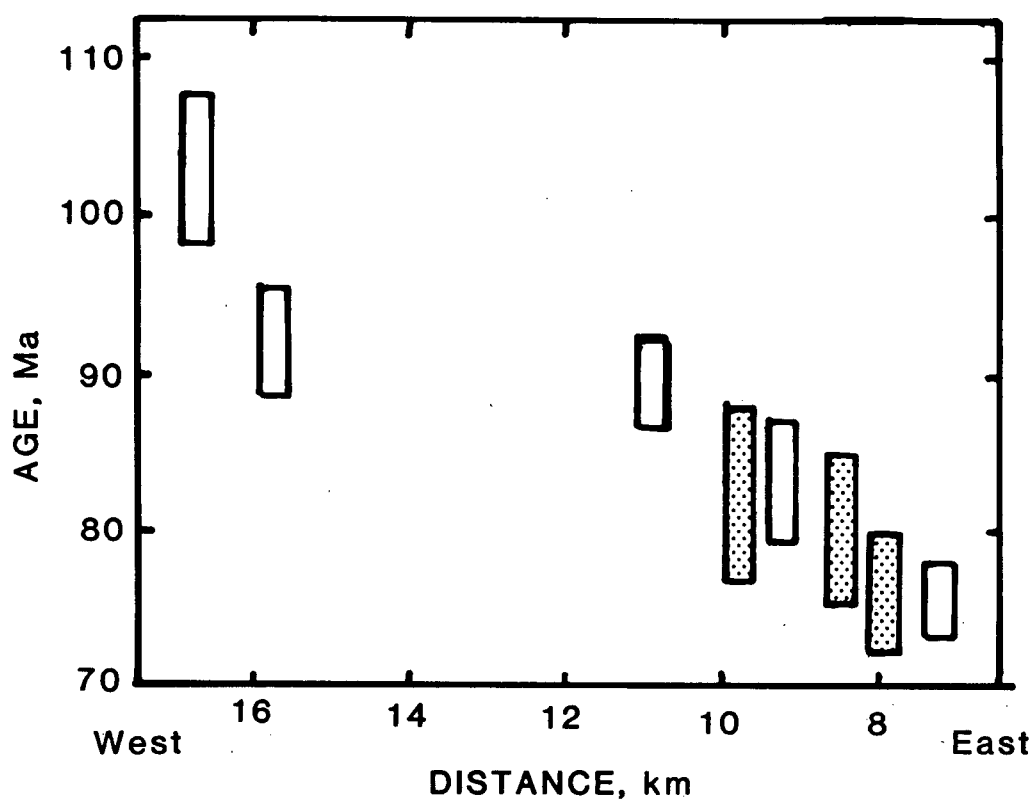


Figure 5.8 Graph of eastward younging trend of K-Ar dates from Spuzzum batholith, from Bartholomew (1979). K-Ar date versus perpendicular distance from a N-S grid line on NTS 92/H, approximately $121^{\circ} 20'$. Boxes indicate age and distance error margins. Stippled boxes are averaged hornblende-biotite pairs.

6. Regional Synthesis

The region between the Fraser River, Harrison Lake, and the Canada-United States Border is geologically complex. Monger and Berg (1984) separate the Intermontane superterrane (comprising Quesnel, Cache Creek and Stikine terranes) and the Insular superterrane (Wrangellia and Alexander terranes) with five small terranes (Figure 6.1). They are (from Monger 1985):

- 1) Methow; Triassic(?) basalt overlain by Jurassic and Cretaceous clastic sediments,
- 2) Bridge River-Hozomeen; Permian to mid-Jurassic disrupted basalt, chert, clastic and ultramafic rocks,
- 3) Cadwallader; Triassic basalt, clastic and carbonate rocks, Jurassic and Cretaceous clastic rocks,
- 4) Shuksan; Jurassic(?) basalt and clastic rocks,
- 5) Chilliwack-Nooksack; late Paleozoic volcanic, clastic and carbonate rocks, Mesozoic clastic and volcanic rocks.

He has restored these terranes to their pre-Tertiary configuration by removing 80 km of dextral motion on the Fraser-Straight Creek fault zone (Figure 6.2a). Timing of movement on these faults has been bracketed between Cretaceous and around 35 Ma (Monger 1985), and possibly all within the Eocene.

Monger considers that the Skagit Metamorphic Suite may be derived largely from rocks of the Methow, Bridge River and Cadwallader terranes. This may be true for the Custer Gneiss but it is not for the Settler Schist and Chiwaukum Schist, which are lithologically different from the rocks in those terranes.

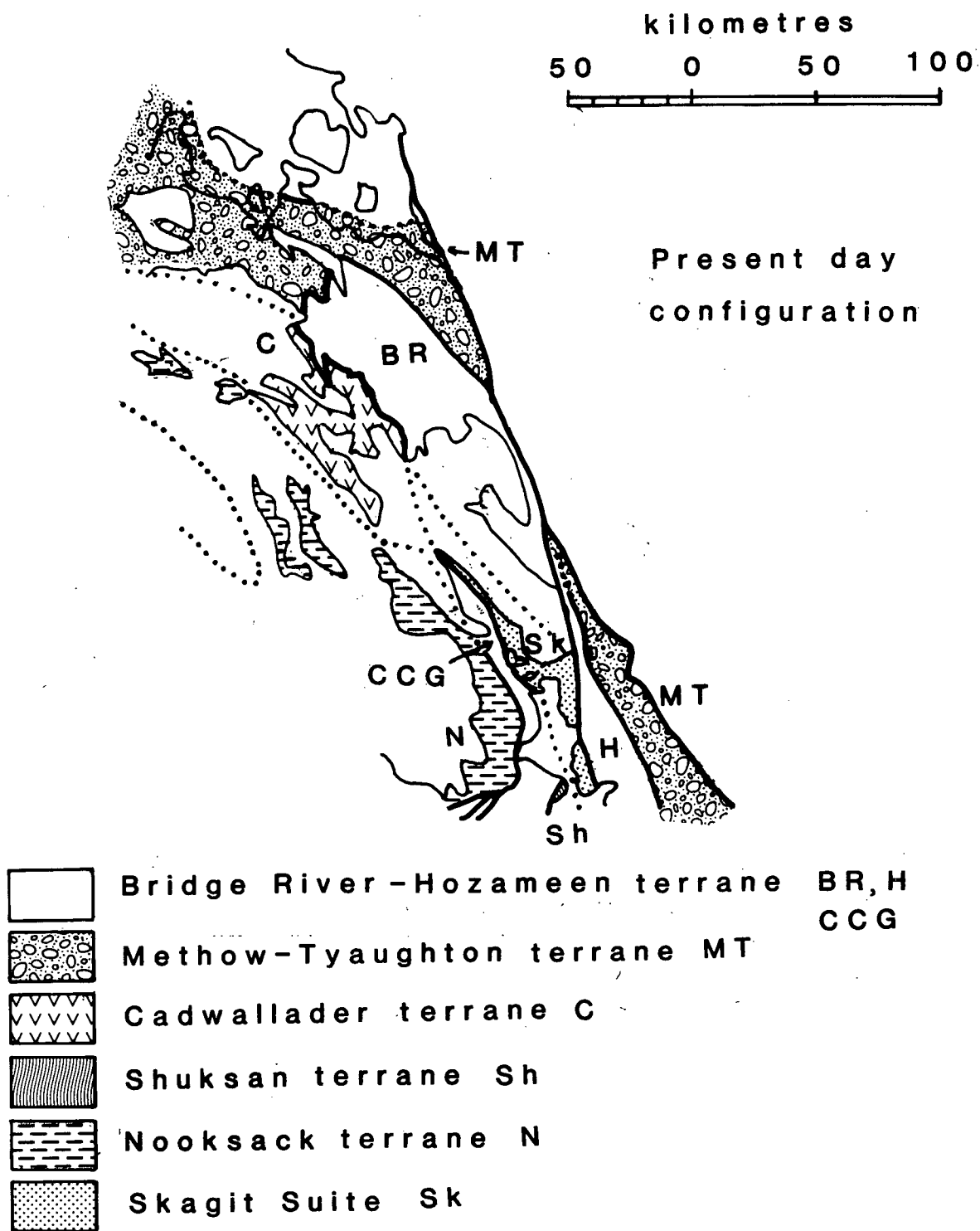
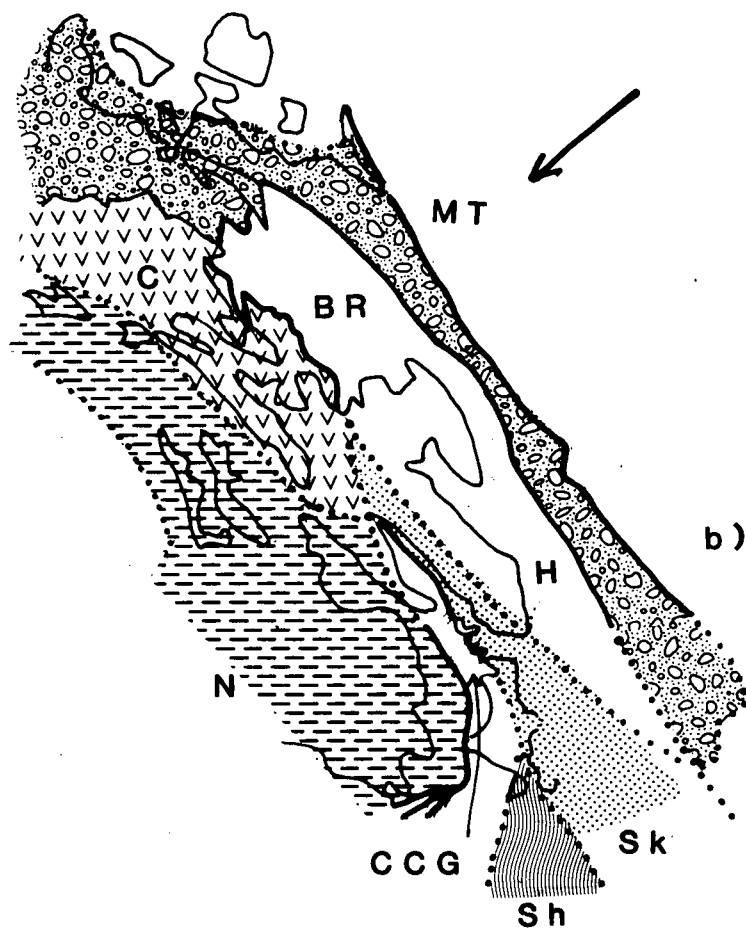


Figure 6.1 Present day configuration of tectono-stratigraphic terranes, modified from Monger and Berg (1984).

a) 100 km right-lateral
displacement,
Yalakom fault



b) 80 km right-lateral
displacement,
Fraser fault

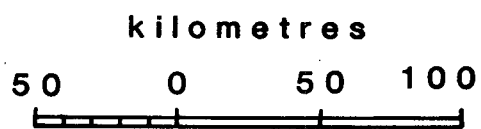


Figure 6.2 Reconstruction of Bridge River and Methow terranes,
using Monger and Berg (1984) and Monger (1985).

It is also difficult to put them in a suitable time and space configuration for the derivation. Figures 6.3a and b show post-Cretaceous, pre-Eocene, restoration of the Settler Schist and Chiwaukum Schist based on a) 150 km offset on the Fraser-Straight Creek faults, from Misch (1977), and b) 80 km offset, from Monger (1985). Figure 6.3a restores the two units to a reasonable configuration, but Bridge River and Methow terranes are disrupted (Figure 6.4a). Figure 6.3b leaves the schists separated by about 80 km. If the 80 km offset is correct, then there must have been at least 80 km of dextral movement on another, parallel, fault system in order to separate the Settler Schist and Chiwaukum Schist by a total of 150 km.

There is a dilemma here, as the fault reversal displacements proposed by Kleinspehn (1985) for the Tyaughton-Methow basin appear to be too great when applied to the most recent terrane map (Monger and Berg 1985). She proposed 110 km of offset on the Fraser-Straight Creek faults (Figure 6.4b) preceded by 150 km of movement on the Yalakom-Ross Lake Fault. More reasonable values for reconstruction of the Bridge River Group and Tyaughton-Methow basin are 80 km on the Fraser fault and around 100 km on the Yalakom-Ross Lake fault. Movement on the Ross Lake fault probably had a fairly large orthogonal component as well as dextral slip, allowing for greater total displacement, but this does not affect the relative positions of the Settler Schist and Chiwaukum Schist. Monger (pers. comm. 1985) surmises that the dilemma can be solved by having a stack of horizontal plates involved in the right-lateral

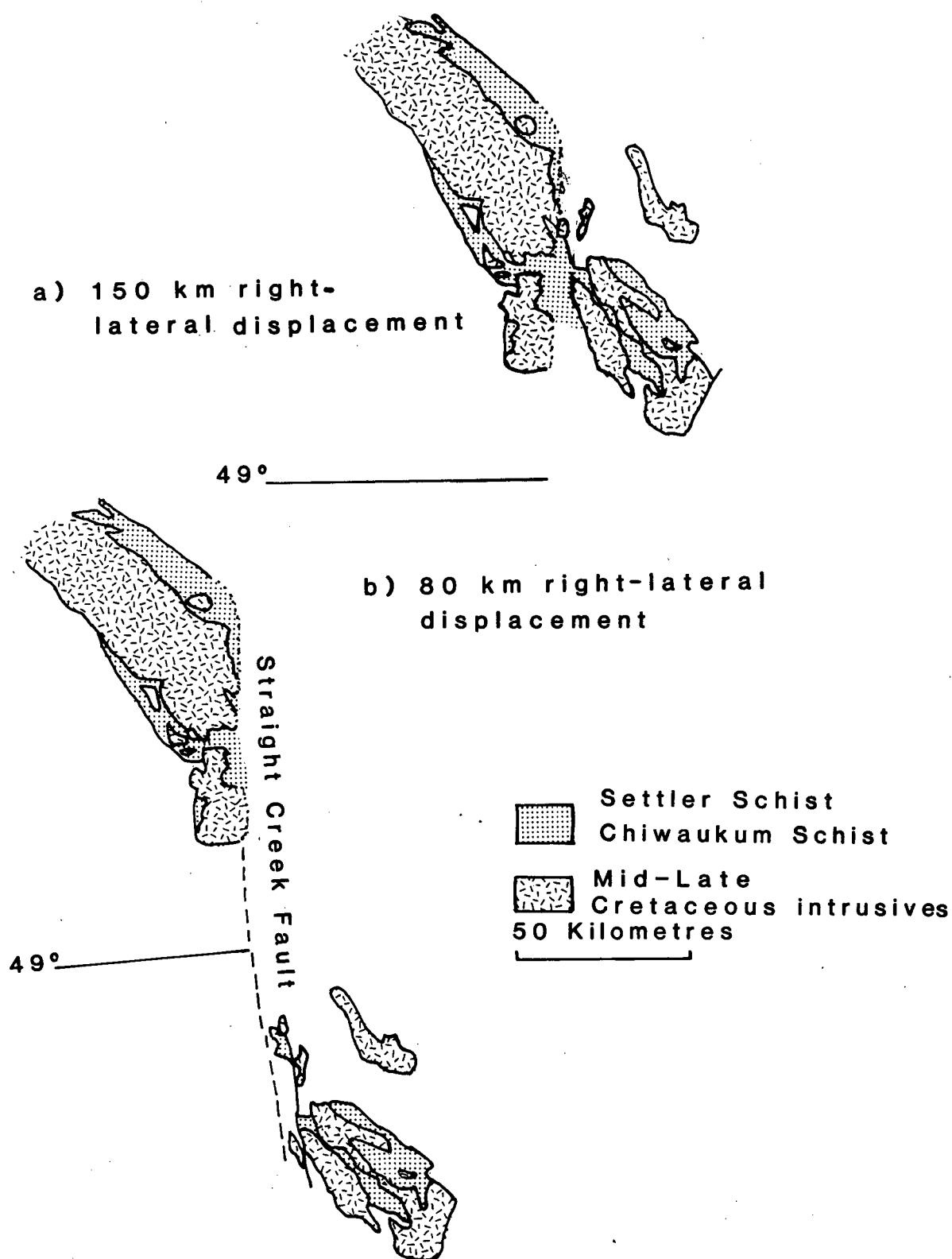


Figure 6.3 Reconstruction of Settler Schist-Chiwaukum Schist using a) Misch (1977); b) Monger (1985). Base map is Figure 1.3.

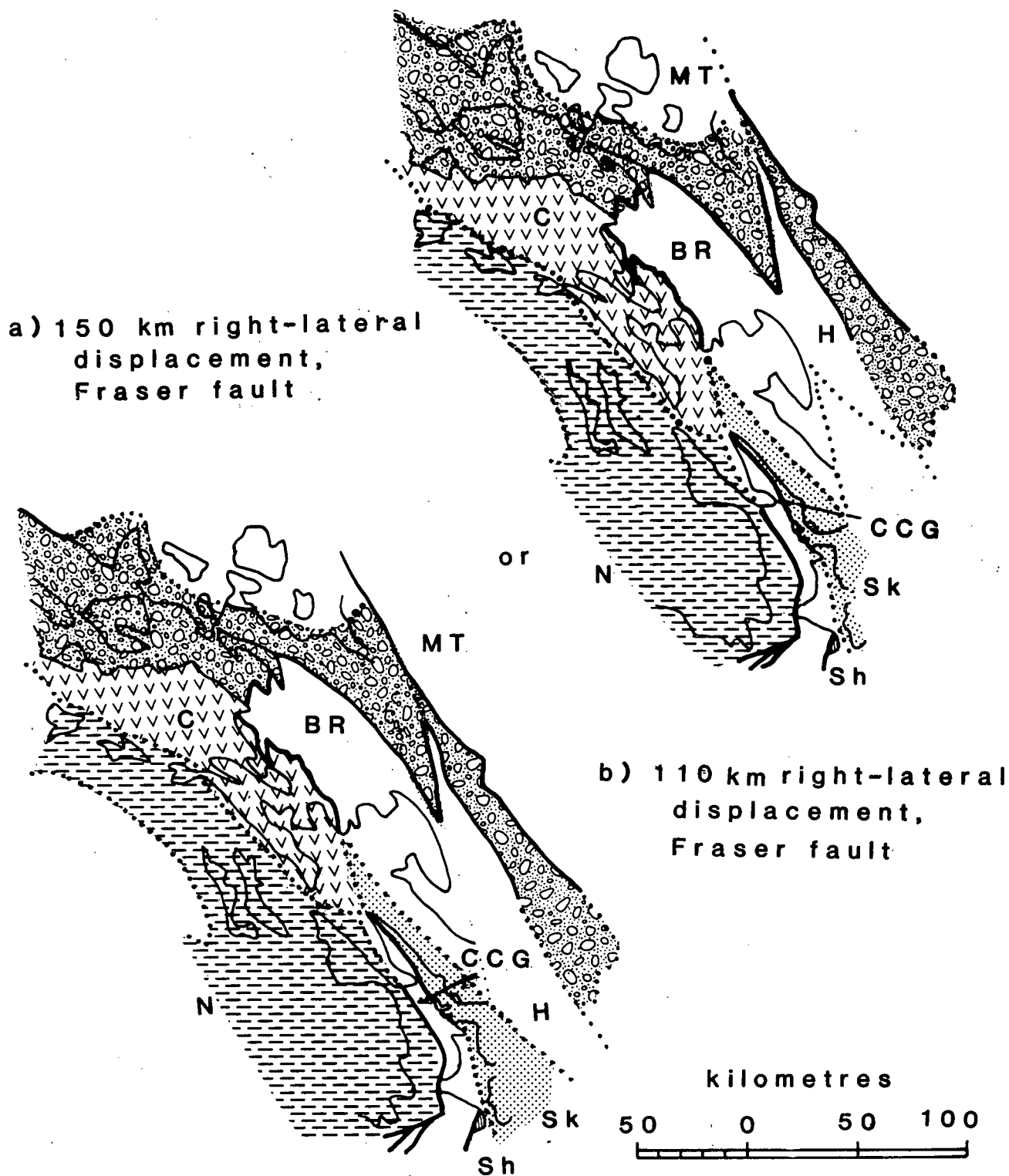


Figure 6.4 Disrupted reconstruction of Bridge River and Methow terranes using a) 150 km displacement, after Misch (1977); b) 110 km displacement, after Kleinspehn (1985).

displacement. By invoking differential movement down through the stack it is possible to reconcile 150 km displacement for the Settler Schist-Chiwaukum Schist with 80 km displacement for the Bridge River-Hozameen Groups.

Monger (1985) notes that post-Cretaceous deformations have masked the boundaries of the small terranes, so that their relationships are not clear. He considers that evolution of the small terranes records closure of oceanic and/or marginal basins between the superterrane. The closure may have been by orthogonal, transcurrent, or transpressive movement.

Isotopic and geological evidence point to correlation of the Cogburn Creek Group with the Bridge River Group and Hozameen Group. Undoing documented fault movements (Figure 6.2 and 4) does not juxtapose them, but there are possible explanations. The first and simplest is that the Cogburn Creek Group never was continuous with the Bridge River Group, but is a sequence of similar sediments and volcanic rocks deposited at the same time from the same source in a nearby basin. The second is that disruption of the Bridge River Group-Cogburn Creek Group Basin by faulting such as the Shuksan thrust, combined with intrusion of voluminous diorite plutons, has separated the two units. The Shuksan thrust has brought in the Settler Schist and imbricate slices of older units and ultramafic rocks from the southeast to overlie the Cogburn Creek Group.

Timing of movement on the Shuksan Thrust is bracketed to Albian by isotopic dating of regional blueschist metamorphism in the Shuksan Metamorphic Suite and intrusion of Spuzzum

batholith. Hence the Shuksan thrust was active before dextral motion on the other faults. Movement on the Shuksan thrust must have died out northwards, ending just north of Cogburn Creek, as Reamsbottom (1971, 1974) did not find a major break between the "Chilliwack" Group (Cogburn Creek Group) and Cairn Needle Formation (Settler Schist). The geometry involved in reconstruction of the Cogburn Creek Group-Bridge River Group as one continuous unit is difficult, because the Cogburn Creek and Bridge River Groups now form parallel belts (Figure 6.1). However, it is not impossible, because they are separated by a wide belt of late Cretaceous and Tertiary intrusive rocks that must have pushed aside the country rock. Not enough evidence is available to choose between the alternate relationships; however, the first (that the two units were never continuous) is simpler. Perhaps the Cogburn Creek Group was deposited in an intermediate position between the Bridge River Group and the Cadwallader terrane, which is a volcanic arc.

The structural position of the Settler Schist, overlying the Shuksan thrust, is similar to that of the Darrington Phyllite. However, the Darrington Phyllite has been dated as 128 ± 6 Ma (Armstrong unpub. data), thus at face value is considerably younger than the Settler Schist. The similarity in structural position may be purely coincidental, as a result of complex movements on various fault systems.



Plate 2.1 Imbricate zone, Shuksan Thrust, shown on saddle east of Settler Lake. Steeply dipping slices of ultramafic rock between Baird Metadiorite (left) and Settler Schist (grassy slope on right).



Plate 2.2 Mafic amphibolite pod in Settler Schist. Dark rim containing large hornblende crystals, surrounding felsic core.

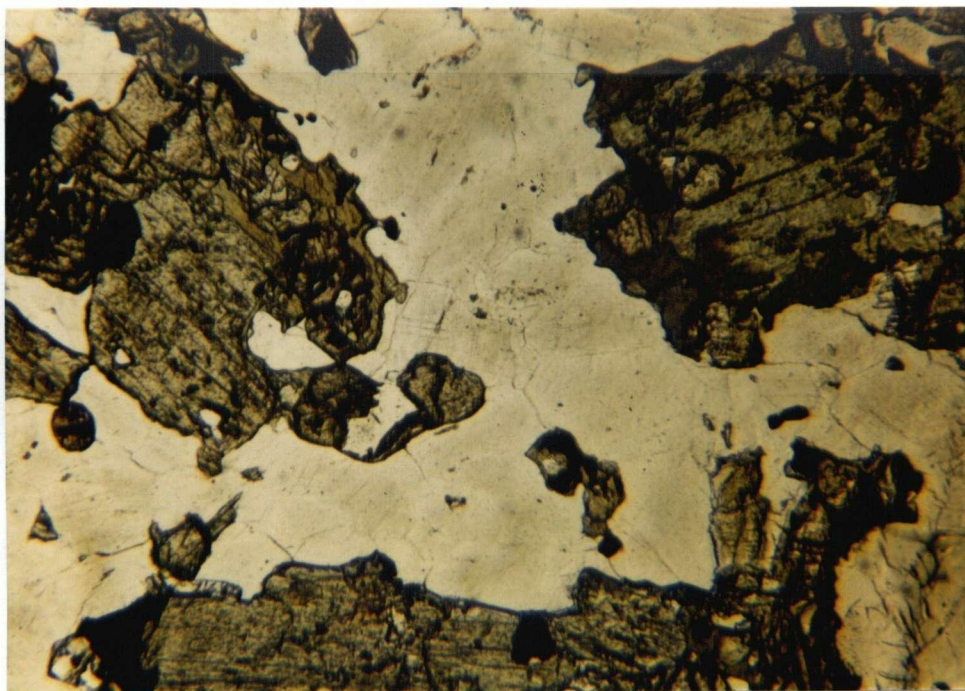


Plate 2.3 Photomicrograph of sample SD101. Photo represents 10 mm in section. Hornblende with brown igneous cores and green metamorphic rims.

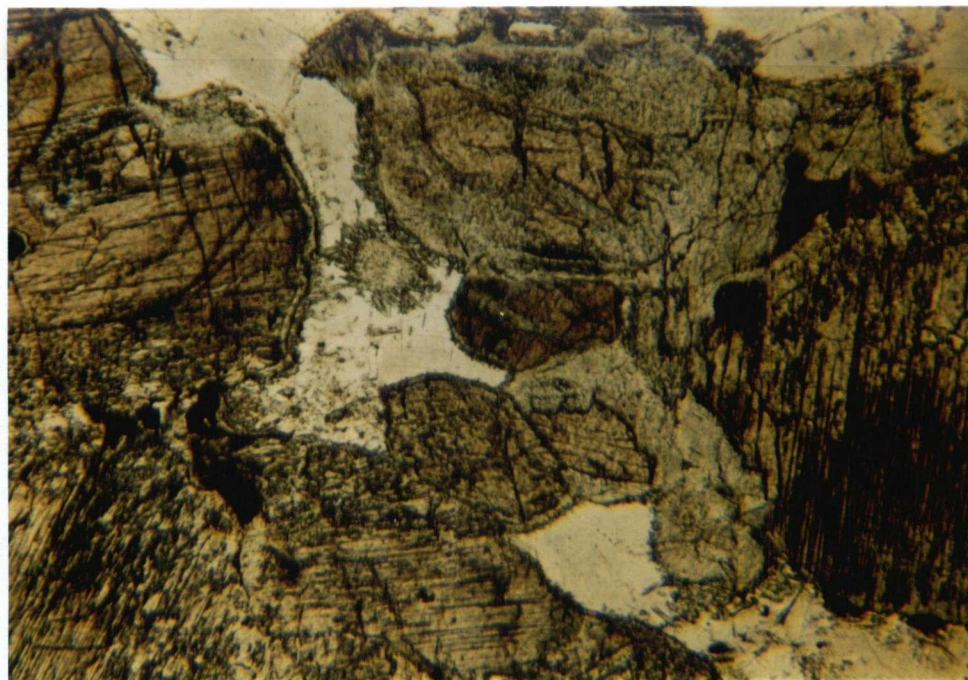


Plate 2.4 Photomicrograph of sample SD66. Photo represents 10 mm in section. Alteration of hornblende during metamorphism, in the hornblende-hypersthene gabbro.

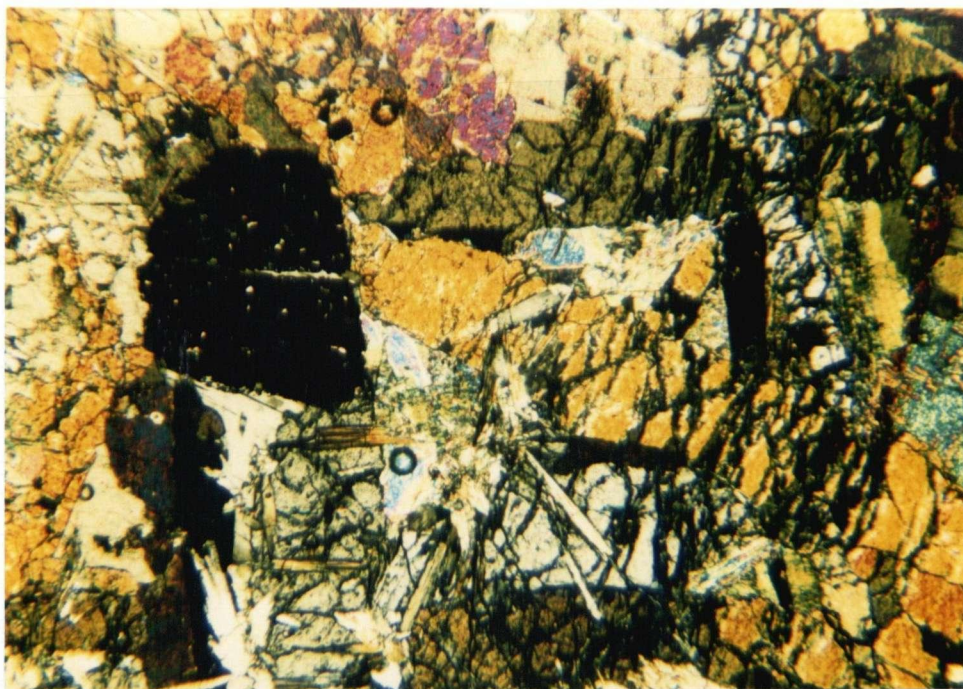


Plate 3.1 Photomicrograph of sample HL30. Photo represents 10 mm in section. Chromite and olivine recrystallised during metamorphism, altered to calcite and tremolite. Crossed nicols.

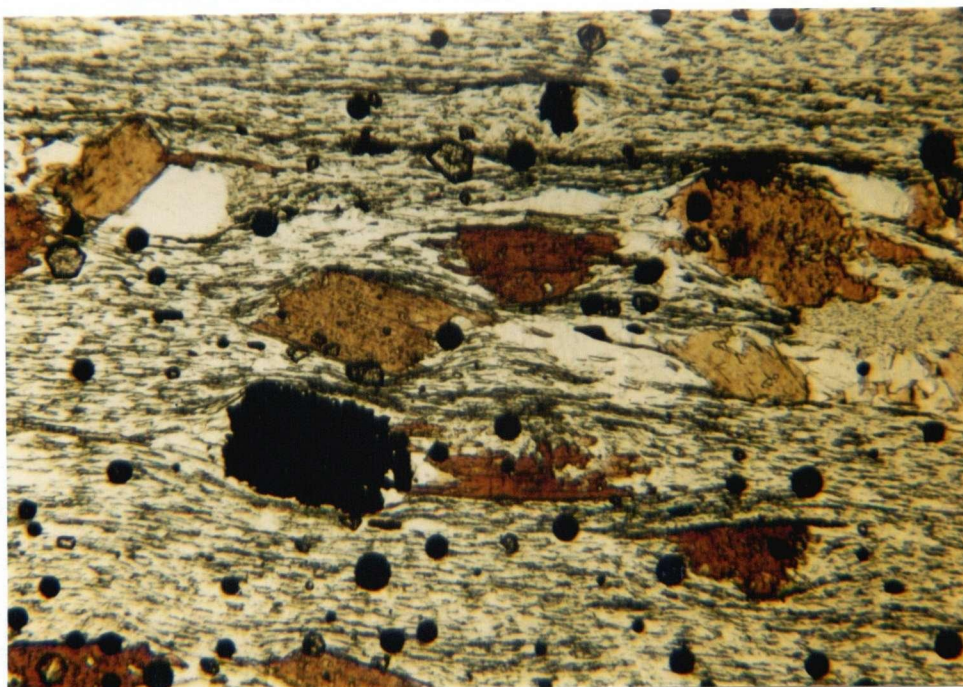


Plate 3.2 Photomicrograph of sample HL16. Photo represents 10 mm in section. Biotite porphyroblasts in quartz biotite schist. Crossed nicols.

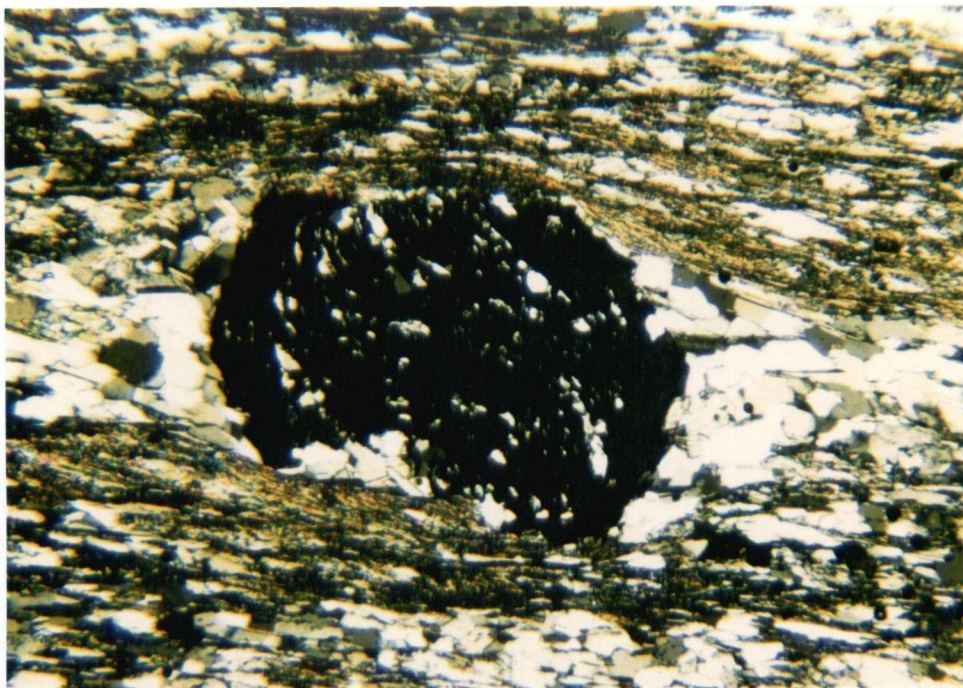


Plate 3.3 Photomicrograph of sample HL15. Photo represents 10 mm in section. Garnet with rotated core and post-tectonic rim. Crossed nicols.

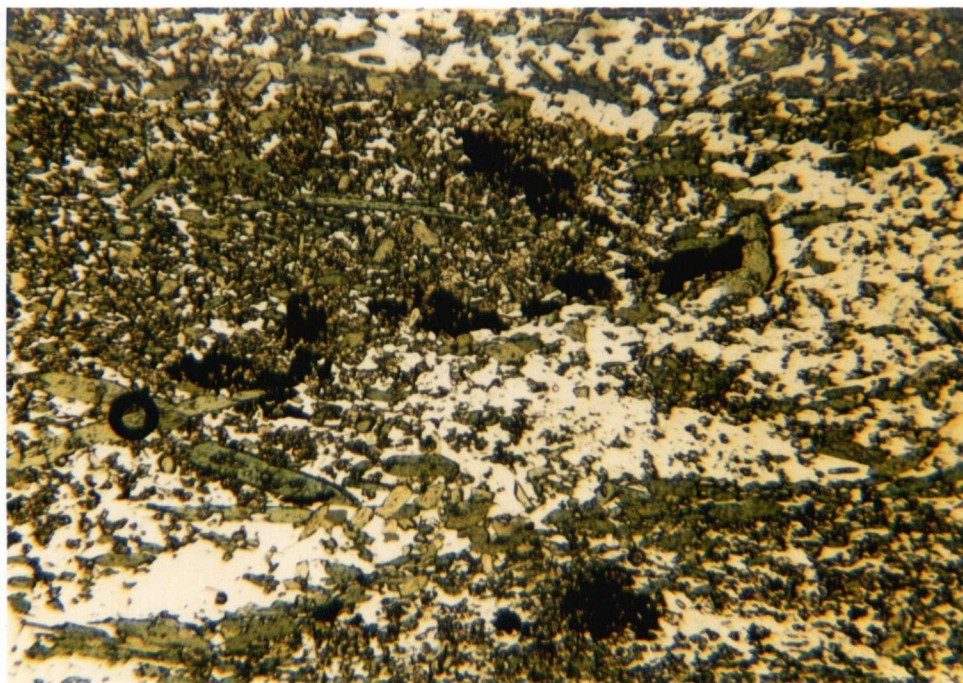


Plate 3.4 Photomicrograph of sample HL80. Photo represents 10 mm in section. Coarse hornblende crystallised along an f_2 fold axis, fine hornblende randomly re-oriented.

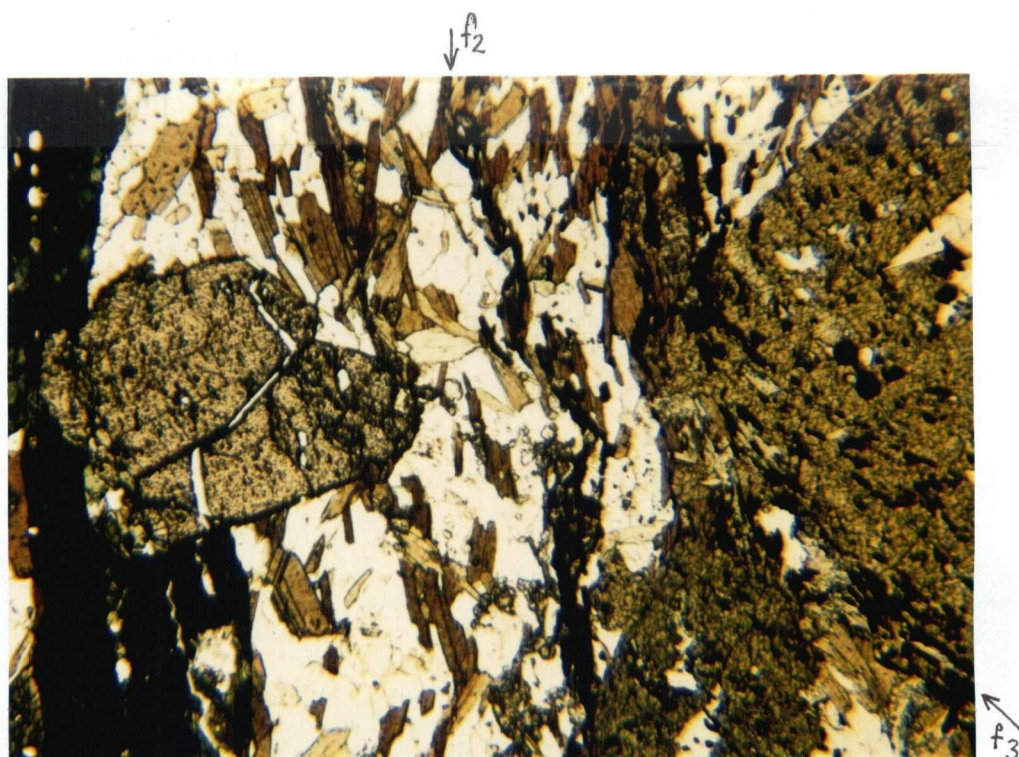


Plate 3.5 Photomicrograph of sample HL142. Photo represents 10 mm in section. Porphyroblastic green hornblende (sides of photo) containing f_2 and f_3 . Staurolite porphyroblasts in centre, epidote with biotite.

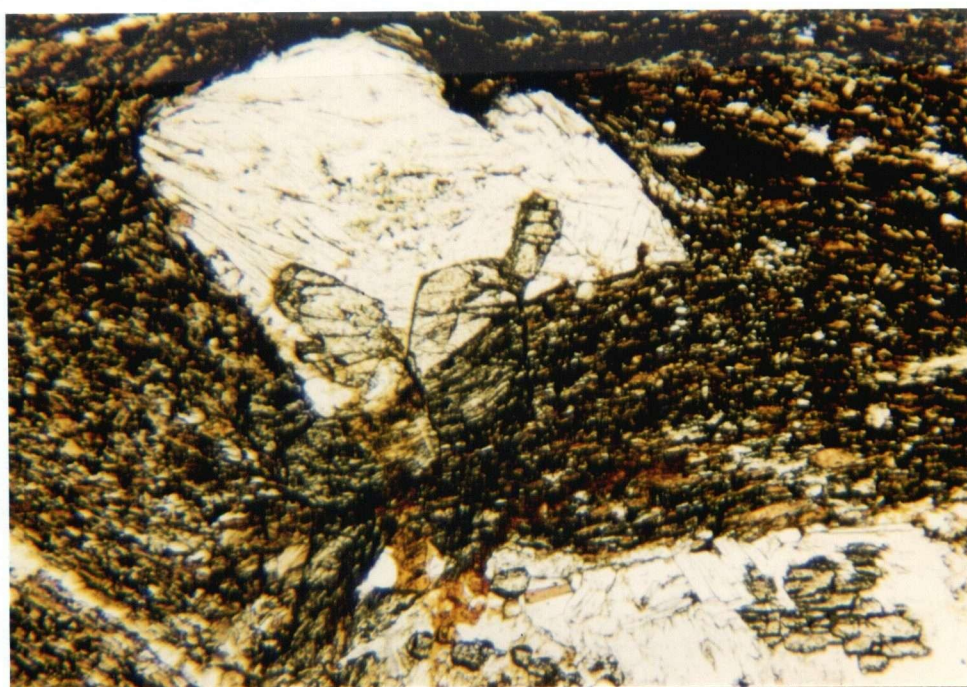


Plate 3.6 Photomicrograph of sample SS110. Photo represents 10 mm in section. Deformed pseudochiastolite with random internal texture and staurolite crossing the boundary. Note sillimanite in lower right corner.

f_2 axis



Plate 3.7

Photomicrograph of sample SS135. Photo represents 10 mm in section. Biotite crystallised along the axial plane of a tight f_2 fold, recrystallised around the f_3 kink fold.

f_3 axis

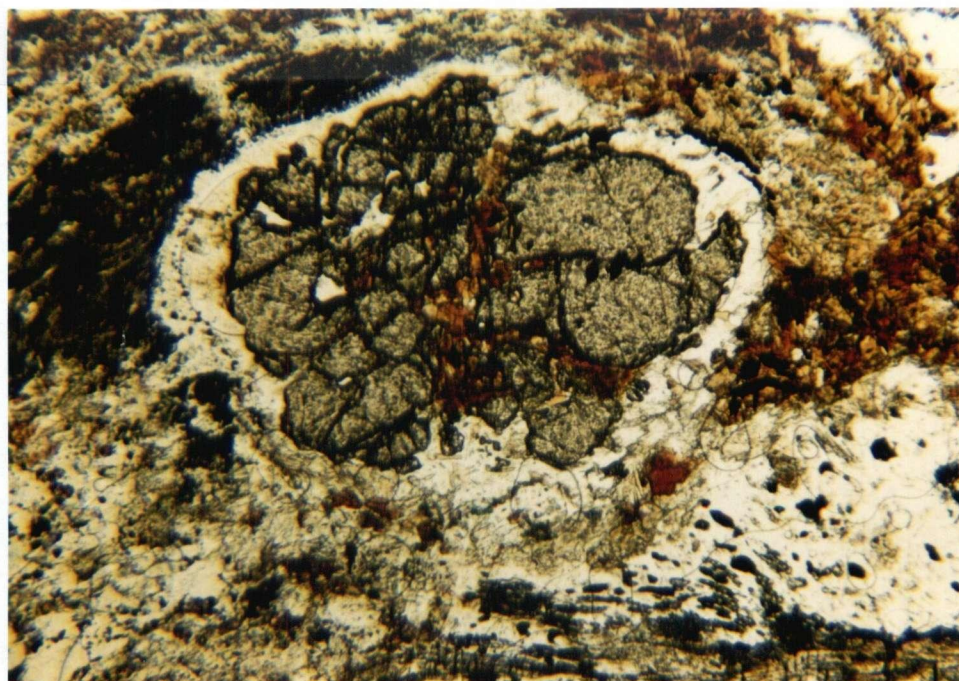


Plate 3.8

Photomicrograph of sample SS66. Photo represents 10 mm in section. Rounded garnet with quartz, muscovite, fibrolite halo, from sillimanite zone. Cracks filled with biotite.



Plate 3.9 Twinned staurolite in sample SS57, Settler Schist. Pencil is 5 cm long. Located at $49^{\circ} 33'N$ $121^{\circ} 37.5'W$. White streaks are sillimanite.



Plate 3.10 Photomicrograph of sample SS114. Photo represents 10 mm in section. Twinned staurolite, zoned with graphite.

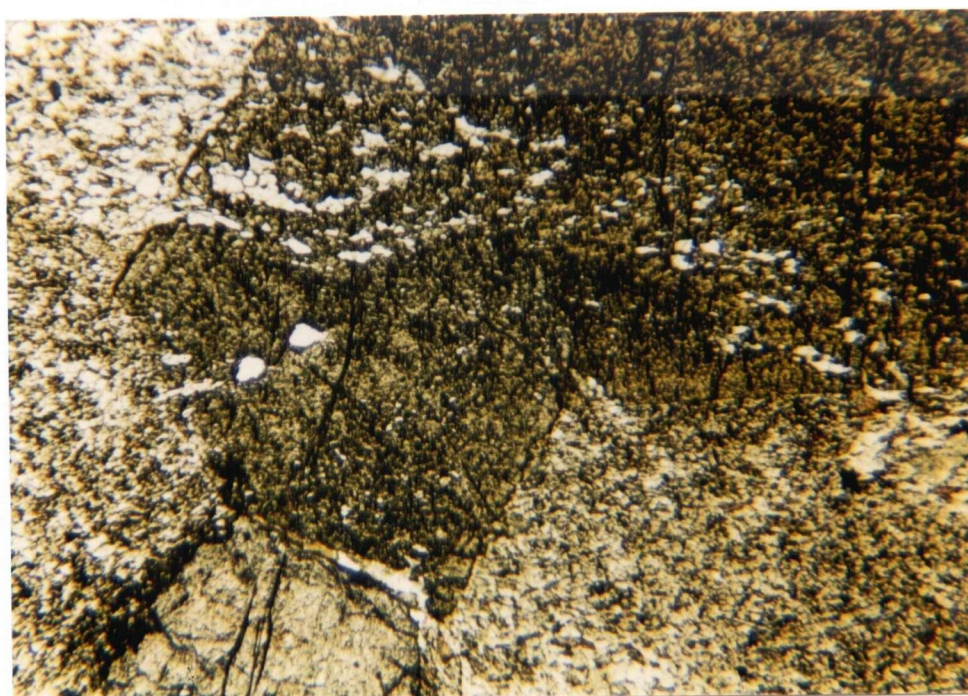


Plate 3.11 Photomicrograph of sample SS53. Photo represents 10 mm in section. Staurolite containing inclusion trail marking f_2 .



Plate 3.12 Sillimanite porphyroblasts from ridge north of Cogburn Creek. Location $49^{\circ} 35.3'N$ $121^{\circ} 39'W$.

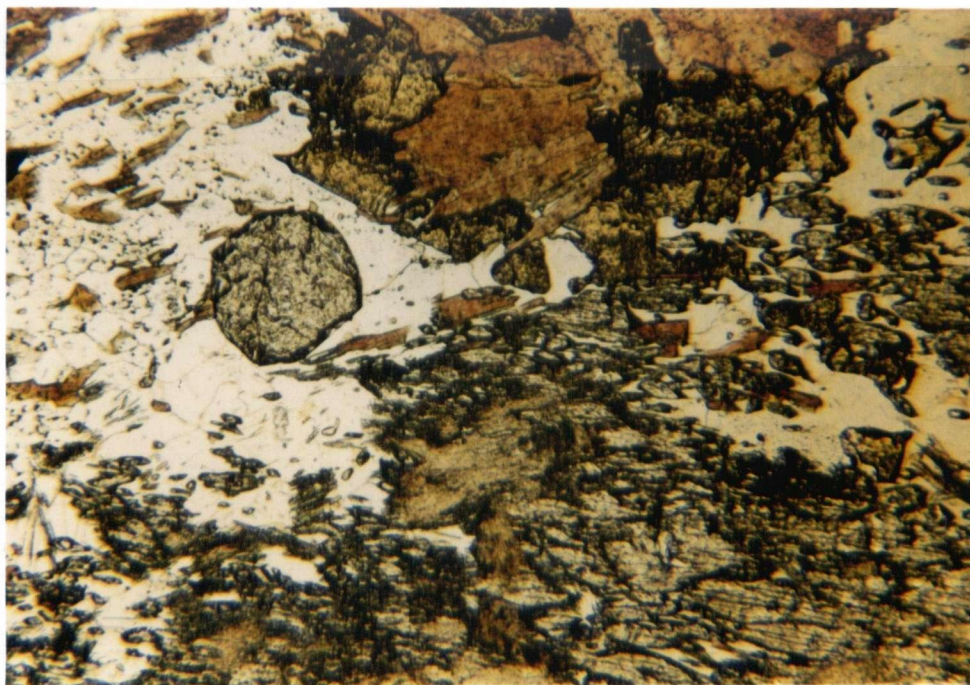


Plate 3.13 Photomicrograph of sillimanite porphyroblast. Photo represents 10 mm in section. Fibrolite patches (fuzzy) and quartz inclusions, rounded garnet in quartz reaction rim.

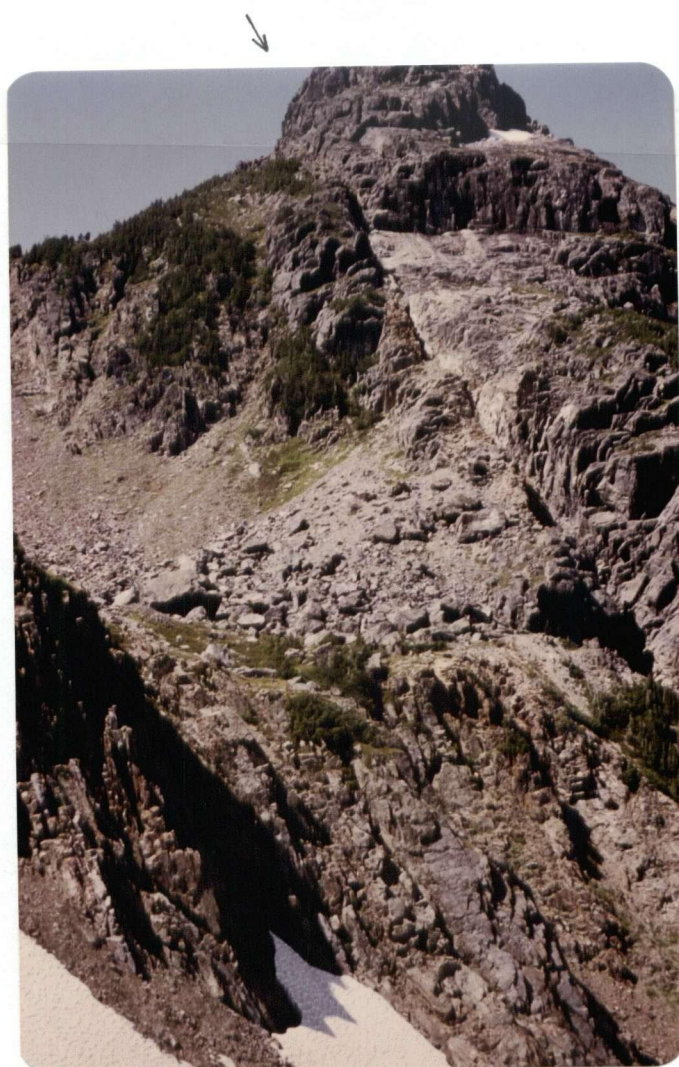


Plate 4.1 Fault contact below the imbricate zone. Looking north, at $49^{\circ} 38.5'N$ $121^{\circ} 31'W$. Cogburn Creek Group chert (left) below Baird Metadiorite (forms peak).

REFERENCES

- Armstrong, R.L. 1980. Geochronometry of the Shuksan Metamorphic Suite, North Cascades, Washington. Geological Society of America, Abstracts with Programs, 12, p. 94.
- Armstrong, R.L., Harakal, J.E., Brown, E.H., Bernardi, M.L. and Rady, P.M. 1983. Late Paleozoic high-pressure metamorphic rocks in northwestern Washington and southwestern British Columbia: The Vedder Complex. Geological Society of America, Bulletin, 94, p. 451-458.
- Babcock, R.S., Armstrong, R.L. and Misch, P. 1985. Isotopic constraints on the age and origin of the Skagit Metamorphic Suite and related rocks. Geological Society of America, Abstracts with Programs, 17, p. 339.
- Bartholomew, P.R. 1979. Geology and metamorphism of the Yale Creek area, B.C. Unpub. M.Sc. thesis, University of British Columbia, Vancouver, 105 p.
- Beck, M.E., Jr., Burmeister, R.F. and Schooner, R. 1981. Paleomagnetism and tectonics of Cretaceous Mount Stuart batholith of Washington: translation or tilt? Earth and Planetary Science Letters, 56, p. 336-342.
- Bremner, T.J. 1973. Metamorphism in the Fraser Canyon, British Columbia. Unpub. M.Sc. thesis, University of British Columbia, Vancouver, 92 p.
- Brown, E.H. and Engebretson, D.C. 1985. Structural history and plate tectonic interpretation of the Easton - Shuksan blueschist, North Cascades, Washington. Geological Society of America Abstracts with Programs, 17, p. 34.

- Brown, E.H., Wilson, D.L., Armstrong, R.L., Harakal, J.E. 1982. Petrologic, structural, and age relations of serpentinite, amphibolite, and blueschist in the Shuksan suite of the Iron Mountain - Gee Point area, North Cascades, Washington. Geological Society of America, Bulletin, 93, p. 1087-1098.
- Chatterjee, N.D. and Johannes, W. 1974. Thermal stability and standard thermodynamic properties of synthetic 2M1-muscovite, $KAl_2(AlSi_3O_{10}(OH)_2)$. Contributions to Mineralogy and Petrology, 48, p. 89-114.
- Crickmay, C.H. 1930. The structural connection between the Coast Range of British Columbia and the Cascade Range of Washington. Geological Magazine, 67, p. 482-491.
- Davis, G.A., Monger, J.W.H. and Burchfiel, B.C. 1978. Mesozoic construction of the Cordilleran "collage", Central British Columbia to Central California. in Howell, D.G. and McDougall, K.A. (eds.). Mesozoic Paleogeography of the Western United States. Society of Economics, Paleogeography and Mineralogy, Pacific Section, p. 1-32.
- Dungan, M.A., Vance, J.A. and Blanchard, D.P. 1981. Retention of primary MORB tholeiite geochemistry by Shuksan greenschists and blueschists, Easton formation, North Cascades, Washington. Geological Society of America, Abstracts with Programs, 13, p. 53.
- Evans, B.W. and Berti, J.W. 1985. A revised metamorphic history for the Chiwaukum Schist, Washington Cascades. Preprint.
- Faure, G. and Powell, J.L. 1972. Strontium Isotope Geology.

Springer-Verlag, New York, 188 p.

Gebauer, D. and Grunenfelder, M. 1979. U-Th-Pb dating of minerals. in Jäger, E. and Hunziker, J.C. (eds.).

Lectures in Isotope Geology. J.C. Springer-Verlag, New York, p. 105-131.

Getsinger, J.S. 1978. A structural and petrologic study of the Chiwaukum Schist northeast of Stevens Pass, North Cascades, Washington. Unpub. M.S. thesis, University of Washington, Seattle, 150 p.

Greenwood, H.J. 1967. Mineral equilibria in the system $\text{MgO-SiO}_2\text{-H}_2\text{O-CO}_2$. in P.H. Abelson (ed.), Researches in Geochemistry, 2. John Wiley and Sons, New York. p. 542-567.

Haugerud, R.A. 1979. Map of the bedrock geology of the North Cascades and surrounding areas.

Haugerud, R.A., Morrison, M.L. and Brown, E.H. 1981. Structural and metamorphic history of the Shuksan Metamorphic Suite in the Mount Watson and Gee Point areas, North Cascades, Washington. Geological Society of America, Bulletin, 92, p. 374-383.

Holdaway, M.J. 1971. Stability of andalusite and the aluminium silicate phase diagram. American Journal of Science, 271, p. 97-131.

Hollister, L.S. 1969a. Contact metamorphism in the Kwoiek area, British Columbia: an end member of the metamorphic process. Geological Society of America, Bulletin, 80, p. 2465-2494.

- Hollister, L.S. 1969b. Metastable paragenetic sequence of andalusite, kyanite and sillimanite in the Kwoiek area, British Columbia. *American Journal of Science*, 267, p. 352-270.
- Hoschek, G. 1969. The stability of staurolite and chloritoid and their significance in metamorphism of pelitic rocks. *Contributions to Mineralogy and Petrology*, 22, p. 208-232.
- Irving, E., Woodsworth, G.J., Wynne, P.J. and Morrison, A. 1985. Paleomagnetic evidence for displacement from the south of the Coast Plutonic Complex, British Columbia. *Canadian Journal of Earth Sciences*, 22, p. 584-598.
- Jäger, E. 1979. Introduction to geochronology; The Rb-Sr method. in Jäger, E. and Hunziker, J.C.(eds.). *Lectures in Isotope Geology*. Springer-Verlag, New York, p. 13-26.
- Johannes, W. 1969. An experimental investigation of the system $MgO-SiO_2-H_2O-CO_2$. *American Journal of Science*, 267, p. 1083-1104.
- Krogh, T.H., 1973. A low contamination method for hydrothermal decomposition of zircon and extraction of uranium and lead for isotopic age determinations. *Geochimica Cosmochimica Acta*, 37, p. 485-494.
- Leiggi, P.A. and Brown, E.H. 1985. Structure of the Shuksan Thrust Fault in the Mount Shuksan area, North Cascades, Washington. *Geological Association of Canada, Program with Abstracts*, 8, p. A42.
- Lowes, B.E. 1972. Metamorphic petrology and structural geology of the area east of Harrison Lake, British Columbia.

- Unpub. Ph.D. thesis, University of Washington, Seattle, 207p.
- Kleinspehn, K.L. 1985. Cretaceous sedimentation and tectonics, Tyaughton - Methow Basin, southwestern British Columbia. Canadian Journal of Earth Sciences, 22, p. 154-174.
- Mattinson J.M. 1972. Ages of zircons from the Northern Cascade Mountains, Washington. Geological Society of America, Bulletin, 83, p. 3769-3784.
- McLeod, J.A. 1975. The Giant Mascot Ultramafite and its related ores. Unpub. M.Sc. thesis, University of British Columbia, Vancouver, 123 p.
- McTaggart, K.C. 1970. Tectonic history of the Northern Cascade Mountains. in Wheeler, J.O. (ed.). Structure of the Southern Canadian Cordillera. Geological Association of Canada Special Paper 6, p. 137-148.
- McTaggart, K.C. and Thompson, R.M. 1967. Geology of part of the Northern Cascades in southern British Columbia. Canadian Journal of Earth Sciences, 4, p. 1199-1228.
- Miller, R.B. and Vance, J.A. 1981. Movement history of the Straight Creek Fault. Geological Society of America, Cordilleran Section Abstracts with Program, p. 97.
- Misch, P. 1966. Tectonic evolution of the Northern Cascades of Washington State. Canadian Institute of Mining and Metallurgy, Special Volume 8, p. 101-148.
- Misch, P. 1977. Dextral displacements at some major strike faults in the North Cascades. Geological Association of Canada, Abstracts with Program, p. 37.

- Monger, J.W.H. 1966. The stratigraphy and structure of the type area of the Chilliwack Group, southwestern B.C.
Unpub. PhD thesis, University of British Columbia, Vancouver, 173 p.
- Monger, J.W.H. 1970. Hope map area, west half, British Columbia. Geological Association of Canada Paper 69-47, 75 p.
- Monger, J.W.H. 1985. Terranes in the southeastern Coast Plutonic complex and Cascade fold belt. Geological Society of America, Abstracts with Programs, 17, p. 371.
- Monger, J.W.H. and Berg, H.C. 1984. Lithotectonic terrane maps of the North American Cordillera. Part B-Lithotectonic terrane map of Western Canada and Southeastern Alaska. U.S. Geological Survey Open File Report 84-523.
- Parrish, R. 1982. U-Pb zircon, common Pb and fission track geochronology: Procedures at the Geochronology Laboratory, UBC. Part 1. U-Pb zircon dating. University of British Columbia, Vancouver, internal report.
- Pigage, L.C. 1973. Metamorphism southwest of Yale, British Columbia. Unpub. M.Sc. thesis, University of British Columbia, Vancouver, 95 p.
- Pigage, L.C. 1976. Metamorphism of the Settler Schist, southwest of Yale, British Columbia. Canadian Journal of Earth Sciences, 13, p. 405-421.
- Pigage, L.C. and Greenwood, H.J. 1982. Internally consistent estimates of pressure and temperature: the staurolite problem. American Journal of Science, 282, p. 943-969.

- Plummer, C.C. 1969. Geology of the crystalline rocks, Chiwaukum Mountains and vicinity. Unpub. M.Sc. thesis, University of Washington, Seattle, 137 p.
- Plummer, C.C. 1980. Dynamothermal contact metamorphism superposed on regional metamorphism in the pelitic rocks of the Chiwaukum Mountains area, Washington Cascades. Geological Society of America, Bulletin, 91, p. 1627-1668.
- Read, P.B. 1960. Geology of the Fraser Valley between Hope and Emory Creek, British Columbia. Unpub. MSc. thesis, University of British Columbia, Vancouver, 145 p.
- Reamsbottom, S.B. 1971. The geology of the Mount Breakenridge area, Harrison Lake, B.C. Unpub. M.Sc. thesis, University of British Columbia, Vancouver, 161 p.
- Reamsbottom, S.B. 1974. Geology and metamorphism of the Mount Breakenridge area, Harrison Lake, B.C. Unpub. PhD. thesis, University of British Columbia, Vancouver, 155 p.
- Richards, T. 1971. Plutonic rocks between Hope, B.C., and the 49th Parallel. Unpub. Ph.D. thesis, University of British Columbia, Vancouver, 178 p.
- Richardson, S.W. 1968. Staurolite stability in a part of the system Fe-Al-Si-O-H. Journal of Petrology, 9, p. 467-488.
- Richardson, S.W., Gilbert, M.C. and Bell, P.M. 1969. Experimental determination of kyanite-andalusite and andalusite-sillimanite equilibria; the aluminium silicate triple point. American Journal of Science, 267, p. 259-272.
- Roddick, J.A. and Hutchison, W.W. 1969. Northwestern part of

the Hope map-area, B.C. (92H W/2): in Report of activities, April to October 1968; Geological Survey of Canada Paper 69-1A, p. 29-38.

Silverberg, D.S. 1985. The Shuksan Fault in the Whitechuck Mountain - Mount Pugh area, North Cascades, Washington. Geological Society of America, Abstracts with Programs, 17, p. 408.

Stacey, S.J. and Kramers, J.D. 1975. Approximation of terrestrial lead isotope evolution by a two-stage model. Earth and Planetary Science Letters, 26, p. 207-221.

Steiger, R.H. and Jäger, E. 1977. Subcommission on geochronology: Convention on the use of decay constants in geo- and cosmochemistry. Earth and Planetary Science Letters, 36, p. 359-362.

Vining, M.R. 1977. The Spuzzum Pluton northwest of Hope, B.C. Unpub. M.Sc. thesis, University of British Columbia, Vancouver, 147 p.

Wanless, R.K., Stevens, R.D., Lachance, G.R. and Delabio, R.N. 1973. Age determinations and geological studies: K-Ar isotopic ages, report 11. Geological Survey of Canada Paper 73-2.

Wasserburg, G.J., Albee, A.L. and Lanphere, M.A. 1964. Migration of radiogenic strontium during metamorphism. Journal of Geophysical Research, 69, p. 4395-4401.

York, D. 1967. The best isochron. Earth and Planetary Science Letters, 2, p. 479-

York, D. 1969. Least squares fitting of a straight line with

correlated errors. Earth and Planetary Science Letters 5,
p. 320-324.

Appendix A. Isotopic Dating: Analytical Methods

Isotopic dating using K-Ar, Rb-Sr and U-Pb zircon methods was carried out at the University of British Columbia, with advice and assistance from R.L. Armstrong, Krista Scott, Joe Harakal, Randy Parrish and Peter Van der Heyden. Analytical techniques are as follows:

K-Ar

Potassium analyses are carried out in duplicate by atomic absorption, using a Techtron AA4 spectrophotometer. Argon is measured by isotopic dilution with a high purity ^{38}Ar spike in an AEI MS-10 mass spectrometer. Reported errors are one standard deviation. The constants are listed in Table B-3.

Rb-Sr

Determination of Rb and Sr concentrations is by replicate analysis of pressed powder pellets using X-Ray fluorescence. Mass absorption coefficients are obtained from Mo K α Compton scattering measurements, and U.S. Geological Survey rock standards are used for calibration. Error on the $^{87}\text{Rb}/^{86}\text{Sr}$ ratios is 2 % (1 σ) where Rb and Sr ppm are >50, and proportional to the reciprocal of the smaller value otherwise.

Sr isotopic composition is measured on unspiked samples prepared using standard ion exchange techniques. The mass spectrometer is a Micromass 54-R. Data acquisition is digitised and automated using a Hewlett Packard HP-85 computer. Experimental data have been normalised to an $^{87}\text{Sr}/^{86}\text{Sr}$ ratio of 0.1194 and adjusted so that the NBS standard SrCO_3 (SRM 987) gives an $^{87}\text{Sr}/^{86}\text{Sr}$ ratio of 0.71020 ± 2 and the Eimer and Amend

Sr a ratio of 0.70800 ± 2 . The precision of a single $^{87}\text{Sr}/^{86}\text{Sr}$ ratio is 0.00010 (1σ). Decay constants for age calculations are in Table B-2. The regressions are calculated according to the technique of York (1967).

U-Pb

Zircon was separated from finely crushed 20 to 40 kg rock samples using wet shaking table, heavy liquid, and a magnetic separator. They were acid washed in strong aqua regia and hand picked as required. Cleaned zircon separate was weighed, dissolved in acid, split for spiked and isotope composition runs, then put through ion exchange columns to separate the lead and uranium, using the procedure of Krogh (1973). We use a mixed ^{208}Pb - ^{235}U spike. Samples were analysed using single Re filaments loaded with and silica gel on a V.G. Isomass 54R mass spectrometer. Data acquisition and reduction are carried out on a Hewlett Packard HP-85 computer. The mass spectrometer is calibrated using the NBS 981 standard. The system blank has composition: 6/4: 17.75, 7/4: 15.57, 8/4: 37.00. U-Pb date errors (1σ) are obtained by individually propagating all calibration and analytical uncertainties through the entire date calculation program and summing all the individual contributions to the total variance.

Appendix B. Isotopic Dating: Analytical data and dates.

Table B-1. Rb-Sr analytical data

Sample Number	Rock Description	Sr ppm	Rb ppm	$\frac{^{87}\text{Rb}}{^{86}\text{Sr}}$	$\frac{^{87}\text{Sr}}{^{86}\text{Sr}}$
<u>Baird Metadiorite</u>					
MD1 WR	highly foliated, green and	493	1.4	0.008	0.7040
MD3 WR	white, metamorphosed	135	0.8	0.016	0.7045
MD6 WR	diorite and gabbro	179	0.3	0.004	0.7043
MD8 WR		145	0.6	0.012	0.7045
MD9 WR		175	0.4	0.006	0.7040
					0.7043
<u>Cogburn Creek Group</u>					
HL37a WR	micaceous recrystallised	18.1	24.6	3.94	0.7135
..... Bi	ribbon chert	16.7	252	43.92	0.7594
					0.7599
HL76 WR	knobbly chloritic green-	349	8.4	0.070	0.7044
					0.7059
.... Pl	schist, coarse metavolc.	268	2.4	0.025	0.7037
.... Hb		55	3.1	0.161	0.7041
HL97 WR	micaceous quartzite	141	58.3	1.20	0.7082
HL103 WR	grey phyllite	386	35.2	0.264	0.7048
HL125 WR	fine grained biotite-	209	41.7	0.578	0.7073
..... Pl	actinolite greenschist	483	1.8	0.011	0.7068
..... Bi		12.5	139	32.37	0.7420
<u>Settler Schist</u>					
Sett1 WR	graphitic phyllite	224	71.3	0.923	0.7074
Sett2 WR	" "	284	70.7	0.720	0.7070
SS82 WR	" "	314	76.3	0.703	0.7071
.... Pl		73.5	4.7	0.185	0.7066

..... Bi		61.2	238	11.26	0.7170
SS109 WR	graphitic phyllite	150	52.8	1.021	0.7072
SS114 WR	" "	164	81.2	1.436	0.7088
SS128 WR	quartz-biotite-garnet	172	73.7	1.24	0.7075
..... Pl	schist, marginal to	285	4.2	0.043	0.7065
..... Bi	Cogburn Granodiorite	23.6	252	30.95	0.7234
SS130 WR	graphitic phyllite/black slate	356	28.9	0.235	0.7065 0.7062
SS132 WR	black slate	157	98.8	1.824	0.7090
SS135 WR	graphitic phyllite	331	65.4	0.571	0.7070
SS143 WR	coarse sandy bi schist	370	30.4	0.24	0.7045
PRB 117	pelitic schist	317	73.5	0.672	0.7065
PRB 173	" "	144	41.2	0.830	0.7064
PRB 72	" "	421	43.8	0.301	0.7055
PRB 172	" "	276	46.6	0.489	0.7054
PRB 122B	quartzofelspathic schist	640	5.3	0.024	0.7038
PRB 90	pelitic schist	204	80.7	1.145	0.7079
PRB 80	" "	213	80.2	1.089	0.7068 0.7066

PRB samples from Bartholomew (1979)

Sills in Schists

HL111 WR	foliated felsic dyke	356	39.3	0.319	0.7040
..... Pl	flecked with biotite, near	352	25.1	0.206	0.7043
..... Bi	contact with Spuzzum D.	22.2	331	43.3	0.7493
SS85 WR	foliated felsic garnet-	368	22.1	0.174	0.7041
..... Pl	cluster dyke intruding	367	2.9	0.023	0.7036
..... Mu	Settler Schist	250	83.0	0.96	0.7051
..... Bi		120	209	5.06	0.7095

Foliated Granodiorite, small body in imbricate zone

SD92 WR	medium grained foliated	390	26.9	0.199	0.7042
.... Pl	granodiorite with biotite,	615	5.0	0.024	0.7040
.... Mu	muscovite, garnets	155	108	2.02	0.7064
.... Bi		94.4	210	6.43	0.7109

Spuzzum Diorite, Hut Creek body

SD36 WR	quartz diorite	724	1.4	0.005	0.7037
.... Pl		1158	0.9	0.002	0.7036
SD66 WR	hornblende-hypersthene gabbro	456	0.4	0.003	0.70365
SD67 WR	"	650	0.8	0.004	0.7038
.... Hb		111	0.9	0.024	0.7040
SD101WR	quartz diorite	691	2.3	0.009	0.7036
SD103 WR	quartz diorite	481	28.5	0.171	0.7039
..... Pl		710	2.4	0.010	0.7036
..... Hb		45.6	4.3	0.272	0.7042
..... Bi		26.4	213	23.35	0.7330
SD110 WR	fine grained diorite	412	5.7	0.040	0.7040
SD117 WR	fine grained hornblende gabbro	668	10.5	0.046	0.7037 0.7035
..... Pl		1415	13.7	0.028	0.7037
..... Hb		104	4.1	0.115	0.7038
SD119 WR	fine grained hornblende gabbro	422	1.8	0.012	0.7036

Spuzzum Diorite, Settler Creek Body

SD71 WR	quartz diorite	385	5.6	0.042	0.7039
.... Pl		1143	17.3	0.044	0.7039
.... Hb		65.3	1.2	0.054	0.7041
SD96 WR	quartz diorite	361	6.6	0.053	0.7039

.... Pl		922	7.5	0.024	0.7038
.... Hb		71.7	2.5	0.101	0.70425
SD97 WR	quartz diorite with	354	16.1	0.132	0.7039
.... Pl	biotite	496	7.3	0.043	0.7038
.... Hb		30.2	2.7	0.256	0.70435
.... Bi		14.9	127	24.71	0.7347
					0.7343
SD98 WR	quartz diorite	358	12.0	0.097	0.7041
.... Pl		1148	29.4	0.074	0.7039
					0.7037
.... Hb		53.3	2.5	0.134	0.7042

Agmatized quartz diorite

SD14 WR	agmatized diorite, near	509	56.0	0.318	0.7053
.... Pl	contact with Cogburn	705	2.11	0.009	0.70445
.... Bi	Granodiorite	15.9	250	45.6	0.7313

Breakenridge Formation

CU1 WR	leucocratic granodioritic	211	33.1	0.452	0.7041
... Pl	gneiss with biotite and	146	2.1	0.042	0.7038
... Mu	muscovite	83.7	95.3	3.30	0.7075
... Bi		50.3	191	10.98	0.7157
CU2 WR	leucocratic granodioritic	207	31.2	0.436	0.7042
... Pl	gneiss with biotite	139	5.0	0.105	0.7038
... Bi		20.7	231	32.4	0.7428

 WR = whole rock, Pl = plagioclase, Hb = hornblende,
 Bi = biotite, Mu = muscovite

Table B-2. Rb-Sr isochron dates

Rock Unit	n	$\frac{^{87}\text{Sr}}{^{86}\text{Sr}}$ Init., σ $\times 10^{-5}$	Date (Ma), σ
Baird Metadiorite	6	0.70383 \pm 32	3.4 \pm 2.4 Ga
Cogburn Creek Group			
1) all data less Bi, chert, HL125 Pl	6	0.70390 \pm 38	296 \pm 58
2) chert HL37a WR-Bi pair	2	0.70896 \pm 40	81 \pm 5
3) metavolc. HL125	3	0.70673 \pm 7	77 \pm 1.6
Settler Schist			
1) all WR data (incl. PRB)	16	0.70429 \pm 32	210 \pm 27
2) phyllite SS82	3	0.70643 \pm 8	66 \pm 1.6
3) schist SS128	3	0.70664 \pm 18	39 \pm 4
Sills in Schists			
1) felsic sill HL111	3	0.70388 \pm 21	74 \pm 10
2) Felsic dyke SS85 less Bi	3	0.70369 \pm 16	105 \pm 20
3) Felsic dyke, SS85	4	0.70381 \pm 15	80 \pm 6
Foliated granodiorite, SD92	4	0.70403 \pm 9	77 \pm 3
Spuzzum Diorite, Hut Creek body			
1) all data less Bi	14	0.70368 \pm 4	127 \pm 41
2) all data	15	0.70370 \pm 4	86 \pm 4
Spuzzum Diorite, Settler Creek body			
a) 1) WR, all less SD97	3	0.70372 \pm 17	274 \pm 179
2) Pl-Hb, all data	8	0.70382 \pm 7	167 \pm 46
3) WR-Pl-Hb, all data	12	0.70368 \pm 6	285 \pm 97
4) all data	13	0.70388 \pm 4	90 \pm 8
b) 1) SD97 WR-Pl-Hb	3	0.70364 \pm 12	186 \pm 49
2) SD97 all data	4	0.70379 \pm 10	89 \pm 7

Agmatite, SD14	3	0.70478 ± 34	42 ± 14
WR-P1	2	0.70448 ± 13	182 ± 33
Breakenridge Fm. gneiss	7	0.70369 ± 6	79 ± 1.6

 Isochron dates calculated using least squares fitting methods of York (1967). Programme written for HP-85 microcomputer by R.L. Armstrong. Error in $^{87}\text{Sr}/^{86}\text{Sr}$ is 0.0001; Rb/Sr ratio assigned 2% error when Rb and Sr concentrations over 50 ppm, otherwise proportional error of ratio divided by lowest ppm. The date for Baird Metadiorite was calculated using 2% error in Rb/Sr because the York least squares calculation would not converge with proportional errors assigned. The slope obtained is close to that obtained using a conventional least squares fit.

Decay constant (Steiger and Jäger 1977):

$$\lambda = 1.42 \times 10^{-11} \text{ yr}^{-1}$$

Errors are 1 σ .

Table B-3. K-Ar analytical data, Spuzzum Diorite

Sample Number	Rock Type	%K	$\frac{^{40}\text{K}}{^{36}\text{Ar}}$ x10 ⁵	$\frac{^{40}\text{Ar}}{^{36}\text{Ar}}$ x10 ³	$\frac{^{40}\text{Ar}(\text{rad.})}{\text{nl/g}}$	% tot	Date Ma \pm σ .
SD66 Hb	hb-hyp gabbro, Hut Creek body	0.046	0.178	0.470	0.310	37.5	162 \pm 7
SD103 Hb	quartz diorite, Hut Creek body	0.462	2.468	1.472	1.49	80.6	80.9 \pm 3
SD117 Hb	hb-hyp gabbro, Hut Creek body	0.391	1.388	0.929	1.20	68.8	77.5 \pm 3
SD71 Hb	hb gabbro, Settler Creek body	0.206	0.754	0.742	0.822	60.6	100 \pm 3
SD97 Hb	quartz diorite, Settler Creek body	0.308	1.025	0.869	1.16	66.5	94.5 \pm 4

Isotope ratio isochron dates (Figure 5.5a)

- 1) Hut Creek body slope 70.1 \pm 5 Ma
 n=3 initial $^{40}\text{Ar}/^{36}\text{Ar}$ 392 \pm 25
- 2) Settler Creek Body slope 78.9 \pm 2 Ma
 n=2 initial $^{40}\text{Ar}/^{36}\text{Ar}$ 388 \pm 88

Concentration isochrons (Figure 5.5b)

- 1) Hut Creek body slope 65.7 \pm 5 Ma
 n=3 initial ^{40}Ar 0.185 \pm 0.016 nl/g
- 2) Settler Creek Body slope 79.7 \pm Ma
 n=2 initial ^{40}Ar 0.139 \pm 0.010 nl/g

 Hb=hornblende, Hyp=hypersthene, rad.=radiogenic
 Decay constants (Steiger and Jäger 1977):
 $\lambda_{\beta} = 4.96 \times 10^{-10} \text{ yr}^{-1}$
 $\lambda_e = 0.581 \times 10^{-10} \text{ yr}^{-1}$
 $^{40}\text{K}/\text{K} = 0.01167 \text{ atom.}\%$
 Errors are 1 σ .

Table B-4. Sample weights for U-Pb analyses

Sample No	Wt spike mg	Wt dissolved zircon mg	Pb blank % tot.Pb	Obs. ratio $\frac{^{206}\text{Pb}}{^{204}\text{Pb}}$
Baird MD	184	0.20	13	60
HL111	22	0.10	4	135
Sett 1	13.3	1.2	1.4	950
Sett 2	12	1.5	2.0	330
Qtz Di HC	26.2	0.010	27	40
Qtz Di SC	21.1	9.2	6	1300
				3560
CU2/1	55.2	9.0	2.5	400
CU2/2	28.5	2.5	4	160

Solution containing zircon was split into 2 aliquots,
one of which was spiked.

Table B-5. U-Pb analytical data including isotope ratios

Sample No	U ppm	Pb ppm	PB r PBc+r	$\frac{^{206}\text{Pb}}{^{238}\text{U}}$	$\frac{^{207}\text{Pb}}{^{235}\text{U}}$	$\frac{^{207}\text{Pb}}{^{206}\text{Pb}}$
Baird MD	356.8	29.3	0.52	0.04258	0.3691	0.06287
		29.9	0.53	0.04253	0.5956	0.10157
HL111	5189	228.2	0.83	0.01729	0.1290	0.05411
		227.3	0.84	0.01741	0.1230	0.05123
Sett 1	1117	53.4	0.95	0.04418	0.4820	0.07913
		53.1	0.97	0.04436	0.4877	0.07973
Sett 2	493.5	27.5	0.88	0.04635	0.5262	0.08233
		27.6	0.88	0.04637	0.5403	0.08450
Qtz Di HC	326.4	24.5	0.40	0.02865	0.2573	0.06512
		24.7	0.39	0.02816	0.3166	0.08154
Qtz Di SC	945.6	13.3	0.99	0.01398	0.1170	0.06071
		944.5	1.03	0.01481	0.1031	0.05048
		14.0	0.96	0.01453	0.1022	0.05103
CU 2/1	218.6	3.9	0.94	0.01654	0.1273	0.05583
		4.0	0.89	0.01645	0.1114	0.04911
		4.0	0.89	0.01649	0.1148	0.05046
CU 2/2	218.6	5.0	0.73	0.01641	0.1173	0.05187
		4.9	0.73	0.01643	0.1119	0.04937

c=common Pb, r=radiogenic Pb.

Isotopic abundance of common Pb based on 200 Ma Pb derived from the growth curve of Stacey and Kramers (1975), except for Baird MD and Settler Schist samples. 2000 Ma Pb was more appropriate for Baird Metadiorite, and 1000 Ma Pb for Settler Schist.

Calculated U-Pb ages are listed in Table B-6.

Rock and zircon descriptions and sample locations are given in Appendix C.

Table B-6. Calculated U-Pb dates

Sample Number	$\frac{^{206}\text{Pb}}{^{238}\text{U}}$ Ma	$\frac{^{207}\text{Pb}}{^{235}\text{U}}$ Ma	$\frac{^{207}\text{Pb}}{^{206}\text{Pb}}$ Ma
Baird MD	269 \pm 10	400 \pm 34	1251 \pm 180
Sett 1	279 \pm 2	401 \pm 3	1183 \pm 12
Sett 2	292 \pm 2	434 \pm 7	1279 \pm 32
HL111	111 \pm 1.5	121 \pm 13	315 \pm 250
Qtz Di HC	181 \pm 7	256 \pm 50	1023 \pm 500
Qtz Di SC	91.8 \pm 0.9	97.0 \pm 8	230 \pm 180
CU 2/1	105 \pm 1	107 \pm 4	153 \pm 87
CU 2/2	105 \pm 1	110 \pm 7	224 \pm 180

 Decay constants (Steiger and Jäger 1977):

$$\lambda^{238} = 1.55125 \times 10^{-10} \text{ yr}^{-1}$$

$$\lambda^{235} = 9.8485 \times 10^{-10} \text{ yr}^{-1}$$

$$\lambda^{232} = 4.9475 \times 10^{-11} \text{ yr}^{-1}$$

$$^{238}\text{U}/^{235}\text{U} = 137.88$$

Errors (1 σ) are derived from spike calibration and fractionation uncertainty and mass spectrometer within-run isotope ratio measurement uncertainties.

Appendix C. Isotopic Dating: Sample descriptions and locations.

Table C-1. Rock descriptions and sample locations

Sample Number	Rock Description	Location	Latitude N Longitude E
<u>Baird Metadiorite</u>			
MD1,3, 6,8,9	highly foliated, green and white, metamorphosed diorite and gabbro	Settler Lake W shore float on beach	49° 31.4' 121° 37.6'
<u>Cogburn Creek Group</u>			
HL37a	recryst. ribbon chert, micaceous partings	Cogburn Creek road, cut above gorge	49° 33.4' 121° 43.2'
HL76	coarse knobbly chloritic metavolcanic greenschist	Cogburn Creek road, cut before 1st tributary	49° 32.85' 121° 44.9'
HL97	grey micaceous quartzite	1510', S side spur betw. Talc & Cogburn Cks	49° 32.45' 121° 43.75'
HL103	grey phyllite	750', S side spur betw. Talc & Cogburn Cks	49° 32.65' 121° 44.3'
HL125	fine grained biotite- actinolite greenschist	On W slope above upper fork in 3-mile Creek	49° 34.6' 121° 44.5'
<u>Settler Schist</u>			
Sett 1	graphitic phyllite	Roadend, S fork Cogburn Creek, at 2500'	49° 31.9' 121° 35.15'
Sett 2	graphitic phyllite	S fork Cogburn Creek, bridge over N trib., W side of valley	49° 33.65' 121° 36.4'
SS82	graphitic phyllite	2995' S side 2nd trib W side S fork Cogburn	49° 32.6' 121° 35.8'
SS109	graphitic phyllite	4150' on ridge E of Settler Creek	49° 32.85' 121° 38.9'
SS114	graphitic phyllite	2300', N of trib, W side Settler Creek	49° 32.75' 121° 39.9'
SS128	qtz-bi-gar schist, near margin of Cogburn Granodiorite	In N fork Cogburn Ck, 0.5km up from junction	49° 34.9' 121° 37.1'
SS130	graphitic phyllite-black slate	Halfway up stream from Cogburn Lake, S fork Cogburn Creek	49° 31.4' 121° 35.72'
SS132	black slate	Halfway up stream from Cogburn Lake, S fork	49° 31.4' 121° 36.0'

SS135	graphitic phyllite	2500' in stream from Cogburn Lake	49° 31.5' 121° 35.3'
SS143	coarse sandy biotite schist	5500', N end ridge N of Old Settler	49° 32.35' 121° 37.6'

Sills in Schists

HL111	foliated felsic sill with bi, nr Spuzzum N Body	Roadcut at 1000', N side Cogburn Creek	49° 33.5' 121° 42.55'
SS85	foliated felsic gar cluster dyke in Settler Schist	W side S fork Cogburn Ck, N of stm, at 3700' from Cogburn Lake	49° 31.95' 121° 35.7'

Foliated granodiorite, small body in imbricate zone

SD92	medium grained granodiorite with bi, mu, garnets	Sidestm W of Settler Creek	49° 32.2' 121° 40.4'
------	---	-------------------------------	-------------------------

Spuzzum Diorite, Hut Creek body

SD36	fine grained leucocratic hb quartz diorite	S side Cogburn Ck, on W rd to Settler Lake	49° 33.45' 121° 41.5'
SD66	fine grained hornblende- hypersthene gabbro	1750' above road on N side Cogburn Creek	49° 33.95' 121° 39.55'
SD67	fine grained hornblende- hypersthene gabbro	Rdcut at 1800' N side Cogburn Creek	49° 34.0' 121° 38.8'
SD101	fine quartz diorite	3600' on W ridge above Hut Ck, N of Cogburn Ck	49° 34.45' 121° 42.25'
SD103	coarse quartz diorite hb+bi	On ridge crest between 3-mi and Hut Cks, 4500'	49° 34.5' 121° 43.2'
SD110	fine quartz diorite hb+bi	In riverbed, forks of Cogburn Ck	49° 34.45' 121° 37.15'
SD117	fine grained hornblende gabbro	At 1850' on N side of Cogburn Ck, at forks	49° 34.5' 121° 38.25'
SD119	fine grained hornblende- hypersthene gabbro	W of SD117, at 1850'	49° 34.6' 121° 38.2'
QtzDiHC	quartz diorite	2100' on N slope above Cogburn Creek	49° 33.93' 121° 42.4'

Spuzzum Diorite, Settler Creek Body

SD71	coarse gabbro	3800', W slopes above S branch Cogburn Creek	49° 32.15' 121° 36.2'
SD96	hb-quartz diorite	E side Settler Creek, roadcut at 2700'	49° 31.85' 121° 39.3'
SD97	fine leucocratic quartz diorite, hb+bi+ gar	E side Settler Creek, roadcut at 2450'	49° 32.5' 121° 39.3'
SD98	coarse quartz diorite	E side Settler Creek, roadcut at 2500'	49° 32.5' 121° 39.3'

QtzDiSC Composite sample of SD71,96,98

Agmatized quartz diorite

SD14	fine foliated quartz diorite bi, garnets	2000' beside N bridge W side S fork Cogburn Creek	49° 33.45' 121° 36.5'
------	---	---	--------------------------

Breakenridge Formation

CU 1	leucocratic granodioritic gneiss with bi and mu	Big Silver River, rd- cut in 1st gorge	49° 38' 121° 49.5'
CU 2	leucocratic granodioritic gneiss with biotite	Big Silver River, rd- cut in 1st gorge	49° 38' 121° 49.5'

Table C-2. Description of zircon samples.

Baird MD	Clear, colourless, broken pieces and complete euhedral grains. 5% contamination.
Sett 1	Zircons are all small and similar in size. Clear and colourless. Fairly rounded, and many contain opaque inclusions. Most probably detrital. Size <325 mesh. Up to 20% contamination, mostly kyanite and graphite.
Sett 2	Similar to Sett 1, but a few about 200 mesh size. 5-10% contamination.
HL111	Zircons mostly long and thin and clear. Size 200-325 mesh, <5% contamination. Some larger grains have opaque inclusions.
Qtz Di NB	Very small sample, 210 handpicked zircons and fragments. Clear and colourless. Size 200-325 mesh.
Qtz Di SC	Zircons clear, colourless, euhedral. Most are long prisms, 200-325 mesh. About 7% contamination, an amber coloured mineral (rutile?).
CU 2	Zircons pink, 200-325 mesh. Clear, euhedral, no inclusions, <5% contamination. Some broken grains. Most are stubby.

Appendix D

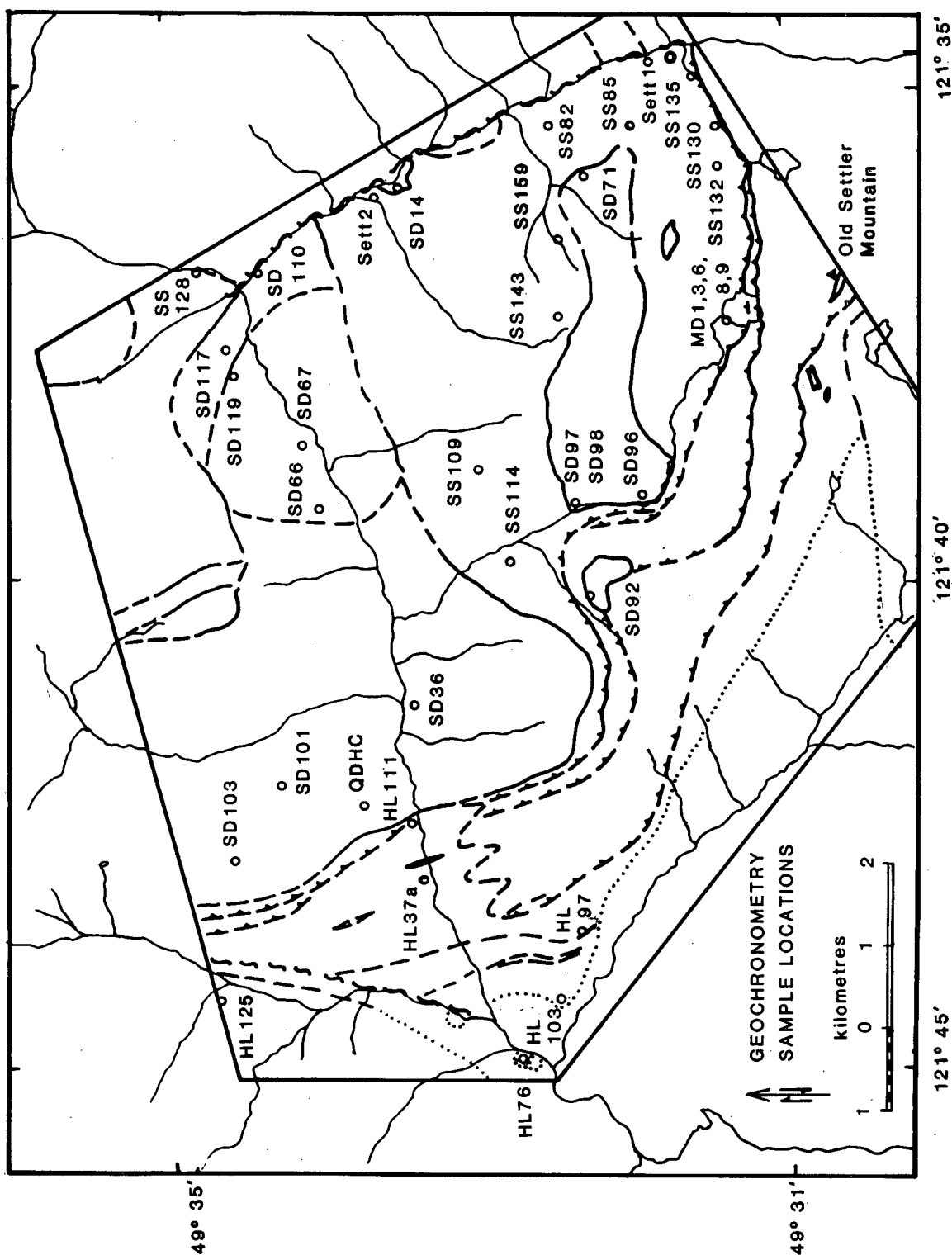


Figure D-2 Map showing locations of geochronometry samples, Cogburn Creek area.

Appendix E. Analytical data for Chilliwack batholith

Table E-1. Rb-Sr analytical data

Sample Number		Sr ppm	Rb ppm	$\frac{^{87}\text{Rb}}{^{86}\text{Sr}}$	$\frac{^{87}\text{Sr}}{^{86}\text{Sr}}$
ChilliWR	main phase diorite	372	33.8	0.263	0.7040
..... Pl		473	4.7	0.029	0.7039
..... Hb		29.0	10.3	1.03	0.7048
..... Bi		14.3	232	47.2	0.7262
					0.7278
JV216 WR	sample from J. Vance	309	57.3	0.537	0.7042
..... Hb	University of Washington,	31.5	51.1	4.70	0.7058
..... Bi	Seattle	29.2	130	12.8	0.7098
					0.7097

 WR = whole rock, Pl = plagioclase, Hb = hornblende,
 Bi = biotite

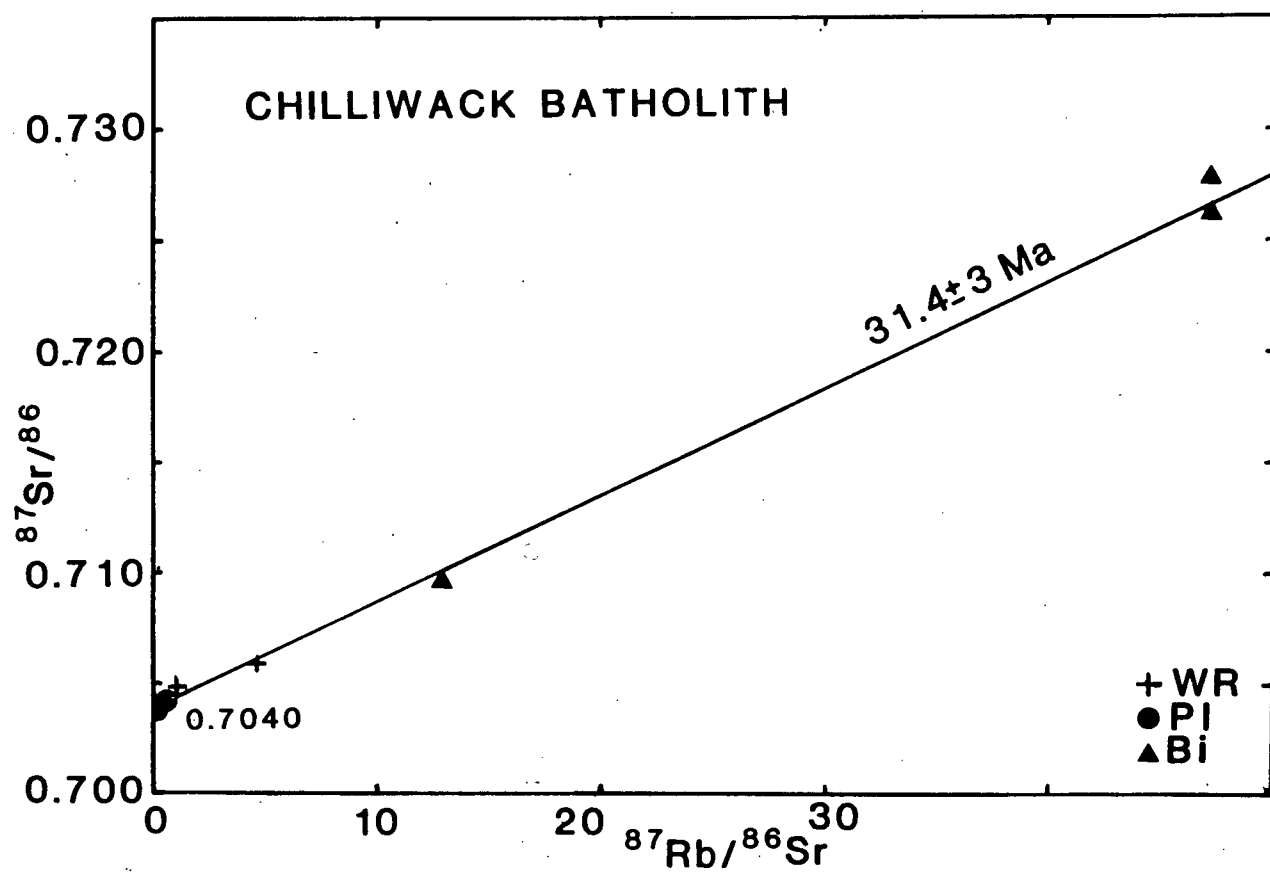


Figure E-1. Rb-Sr isochron plot for Chilliwick batholith, North Cascades Mountains, Washington.